BETTER SHIPS, BLUE OCEANS

163 m WASP container feeder: seakeeping model tests

Volume 1 - Summary, discussion and conclusions

Report No.	:	77001-2-SMB
Date	:	June 2025
Version	:	1.1
		Final Report

163 m WASP container feeder: seakeeping model tests

Volume 1 - Summary, discussion and conclusions

MARIN order No.	:	77001
MARIN Project Manager	:	N/A
Ship model No.	:	M10129
Model scale ratio	:	63.2

Number of pages	:	94

Ordered by	:	Ministerie van Infrastructuur en Waterstaat Rijnstraat 8 2515 XP DEN HAAG The Netherlands

Reference	:	Zeilende vrachtschepen

Reported by	:	N/A
Reviewed by	:	N/A

Version	Date	Version description
1.0	29.04.2025	Draft report
1.1	18.06.2025	Final report

CONTENTS PAGE

REVIEW OF TABLES, FIGURES AND PHOTOGRAPHS

REVIEW OF REPORTS

Table i-1: Deliverables of the current project phase[1]

Deliverable	Contains
MARIN report No. 77001-2-SMB Vol. 1	The present report, delivered in PDF format
MARIN report No. 77001-2-SMB Vol. 2 (Data report seakeeping tests)	All analysis and post-processing of the measured signals, delivered in PDF format
MARIN report No. 77004-1-SMB Vol. 2 (Data report weather criterion tests)	All analysis and post-processing of the measured signals of weather criterion model tests, delivered in PDF format
Digital copy of videos of tests	File share link to copies of the videos

Table i-2: Previously delivered reports for this project[1]

MARIN report No.	Title
77001-1-SEA	Regulatory review: Stability of wind-powered vessels

[1] At the time of writing

MANAGEMENT SUMMARY

The present project was ordered by the Ministry of Infrastructure and Water Management to advance the research on the safety risks associated with wind-propelled ships. This study is part of the 'Onderzoeksprogramma Scheepvaartveiligheid Noordzee 2024'.
It is aimed at investigating the suitability of current stability assessment approaches, exposing potential gaps and exploring alternative assessment options. This study investigated an experimental approach using a wind force setup for a model of a hypothetical, retrofitted container feeder vessel with 6 rotor sails in extreme environmental condition. The goal was to assess the impact of different wind conditions and modelling techniques on the dynamic stability of the investigated vessel. Currently employed empirical and experimental methods were also investigated to provide a baseline for comparisons.

General conclusions on the experimental approach and future work can be summarised as follows:

- Due to the high cost associated with long test durations, it is recommended to determine a baseline of worst case scenario combinations of irregular seas and unsteady wind conditions for experimental assessments of wind propelled vessel dynamic stability.
- A numerical study has been launched to validate the experimental results.
- The numerical study will further address the issue of insufficient test duration in experiments to investigate probabilities of exceedance of peak roll angles in irregular seas with better statistical convergence.
- Numerical studies may also allow the selection of suitable combinations of irregular seas and unsteady wind time traces to obtain worst case roll angles that may lead to capsizing events in rare, but realistic scenarios.

The main goal of the study was to assess whether current regulation is sufficient to assess the stability of wind propelled vessels. It seems justified to conclude that:

- The theoretical assessment of the weather criterion yielded similar or lower values for the stability criteria than the experimental approach using regular waves in the investigated case.
- The probabilities of exceedance of the peak roll angles in irregular seas show highest roll angles for the constant force mode, followed by unsteady and then steady wind modes. However, the results imply that longer test durations are required to assess the probability of exceedance of roll peaks for unsteady wind.
- Results from irregular seas tests in extreme conditions (50.5 kn wind speed) showed that a vessel that complies with existing stability regulation assessment can exceed regulation limits in extreme, but realistic conditions for wind and waves. This case alone shows that regulation without alternative assessment methods may not be sufficient to assure the stability of all wind propelled vessels in extreme conditions.

1 INTRODUCTION

The present project was contracted by the Ministry of Infrastructure and Water Management to advance the research on the safety risk associated with wind-propelled ships. This study is part of the 'Onderzoeksprogramma Scheepvaartveiligheid Noordzee 2024'. The associated literature study to the present experimental work is presented in MARIN report 77001-1-SEA.

Background of the research

The main goal of this study is to assess whether current regulation is sufficient to assess and assure the stability of modern, wind propelled vessels. The present works applies the existing regulation and guidelines to a hypothetical vessels and moves on to test the vessel in relevant scenarios involving realistic irregular seas and wind spectra. Showing that these scenarios lead to situations where the vessel stability is at risk indicates that present regulation is insufficient to assure safety for such a vessel.

Model selection

The intention is to test a realistic, worst case scenario for a vessel with wind propulsion. Based on the literature study outcome, a retrofitted feeder vessel with 6 rotor sails was chosen. It container capacity is roughly equal to 950 TEU. Similar retrofits already exist and are in operation[2]. Figure 1-1 shows a visualisation of the vessel concept. Rotor sails add less damping than wing or soft sails as they are less dependent on the angle of attack. Loading conditions were based on stability calculations fulfilling current regulations with little margin. The basic assumption is that dynamic stability effects that are not addressed sufficiently in current regulations would raise issues in such a vessel under realistic, worst case wind and wave conditions.

Approach

The stability and compliance of the vessel was assessed using the existing regulations. Calculations were done following the current baseline regulation in the IMO IS 2008 code. Weather criterion tests following IMO MSC.1/Circ.1200, which is an alternative assessment to prove stability compliance, were conducted because they are routinely used for this purpose despite not being mandatory. Further tests following the IMO SLF 53/INF.3 were done as they are based on an experimental approach that includes both irregular seas and constant wind force tests, which represents a more realistic scenario than regular waves and calculations, modelling some of the dynamics. IMO SLF 53/INF.3 is not a mandated assessment. These three approaches provide a base line for the stability evaluation vessel and assure compliance with current regulations. In addition, tests in irregular seas and with both steady and unsteady wind were performed to provide a more accurate and realistic modelling approach of the dynamic mechanisms that effect vessel stability. The results of the currently approved methods and the comparison with tests in irregular seas and unsteady and steady wind are used to discuss gaps in current stability regulation concerning wind propelled vessels.

[2] https://zephyretboree.com/en/projects/mervent/ : Zephyr & Boree official website, 'Williwaw : 5 carbon-free container ships', last visited February 2025

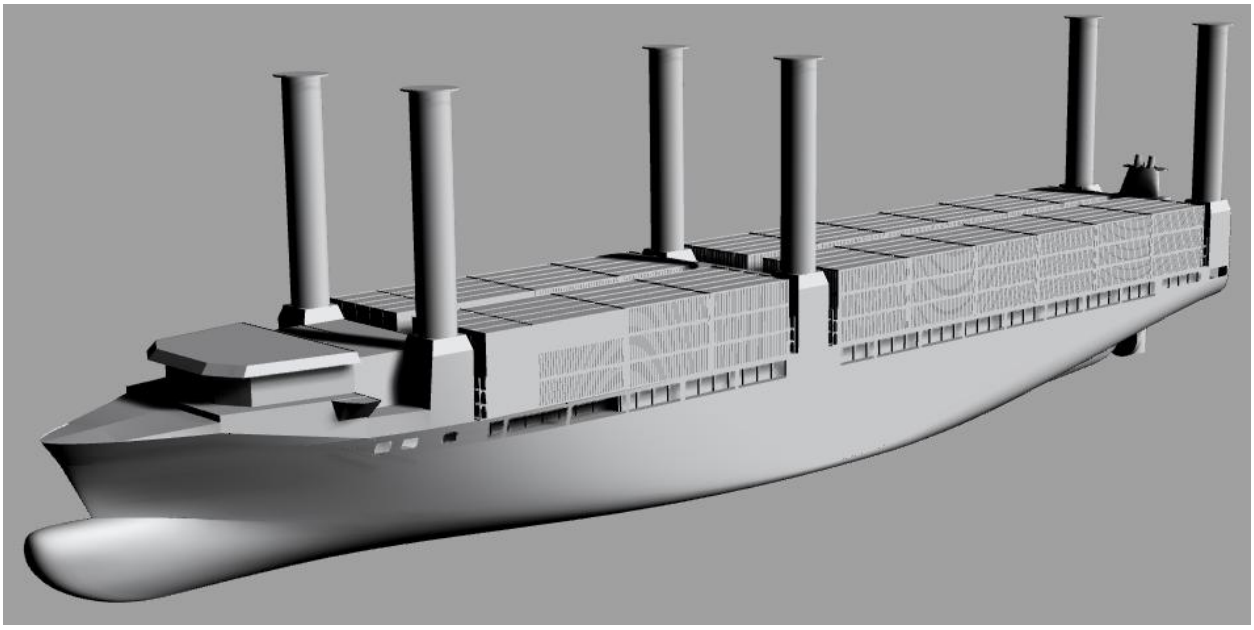

Figure 1-1: Visualisation of the investigated concept vessel.

Structure

Information about the model are given in Chapter 2. Calculation results are presented in Chapter 3. In Chapter 4, the test programme and selected wave conditions are provided. The detailed results of the tests are provided in the data report (Volume 2). Chapter 5 summarises and discusses these results. Chapter 6 gives conclusions and recommendations.

All table, figure and photo numbers with prefix T, F or PH, respectively, refer to the tables, figures and photo sections at the end of the present discussion report.

2 THE MODEL

2.1 General description

For the seakeeping tests, an existing wooden, rigid model of a feeder vessel was modified. A winch system was added to apply the wind forces and moments. Anti-leeway fins were added to emulate likely systems that would be installed in such vessels with wind propulsion. This model, at a geometric scale ratio of 1 to 63.2, was designated model No. M10129. A smaller scale factor is generally desirable for such tests, but the choice was restricted by the availability of suitable stock models. The vessel's main particulars, general arrangement and body plan are provided in Table T1 and Figure F1. An overview of the model is shown in Figure 2-1.

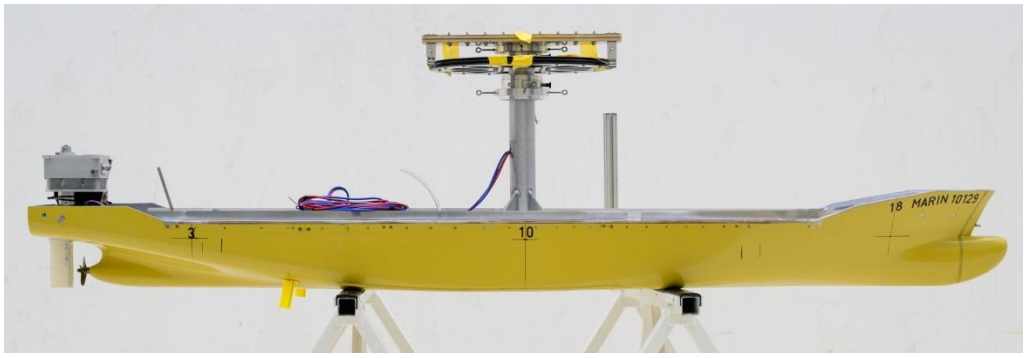

Figure 2-1: Overview of model No. M10129.

2.2 Propulsion and appendages

The model was equipped with a MARIN stock propeller and rudder, bilge keels, as well as the aforementioned anti-leeway fins and winch system. The propeller particulars, propulsion arrangement and appendage details can be found in Table T2 through Table T4 and Figure F2 through Figure F4. Turbulence on the model was triggered using studs at the bow and with sand stripping on the leading edge of all the appendages.

2.3 Weight distribution

The seakeeping tests were performed for one loading condition. The weight distribution was modelled by the following steps.

- Prior to the tests, the weight and weight distribution of the empty model with superstructure were determined on the RESONIC oscillation table.
- Based on the oscillation table measurement, a ballast plan was calculated, and ballast weight were located in the model to match the target mass and radii of inertia.
- The ballasted model was put into the water, the draught marks at stations 3, 10 and 18 were checked. Thereafter the transverse stability (GM) was checked by performing an inclining test. The natural period of roll was measured to determine the radius of inertia. If the results of the tests were not within the desired accuracy, weight were moved or added to more accurately match the specifications. Typically, weight is withing 1% of the specified value, the GM and radii of inertia are within 3% of the desired value.
- Finally, the GM was measured in the basin prior to the tests. In addition the rolling period (T_ϕ) was measured by performing a roll decay test at zero speed in the basin. The initial angle of such a decay is typically below 10 deg and is reached by pushing vertically at the port or starboard side of the model. The roll period was obtained by averaging over the number of analysed oscillations.

Details of the loading condition and hydrostatics can be found in Table T1. Table 2-1 summarises the target and achieved values for the GM, k_{xx}, k_{yy}, k_{zz}, and the measured T_ϕ that followed from this.

Table 2-1: Loading condition

		Target	Realised	*%diff.*
GM	[m]	1.50	1.49	-0.7%
k_{xx}	[m]	9.99	10.27	2.8%
k_{yy}	[m]	42.41	42.24	-0.4%
k_{zz}	[m]	42.41	41.33	-2.5%
T_ϕ	[s]	-	18.43	-

3 CALCULATIONS

Static stability calculations and Frequency domain seakeeping calculations were made before the test to determine the most challenging test conditions based on the hull shape, loading condition and sailing speed of the vessel. Further, hydrostatic information and theoretical considerations were used to estimate the vessel's stability compliance with current regulation.

3.1 Stability calculations

Based on the hull shape of the model and maximum draught, hydrostatic calculations were done to determine loading conditions and a maximum draught that still comply with the current stability regulations.

The limiting criteria are the stability range in roll and the weather criterion stability regulations based on the wind lever, visualised in Figure 3-1. The IMO weather criterion defines wind levers as follows:

$$l_{w1} = \frac{P\,A\,Z}{1000\,g\,\Delta}$$
$$l_{w2} = 1.5\,l_{w1}$$

with:

P = wind pressure of 504 Pa
A = projected lateral area
Z = vertical distance from centre of A to the centre of the underwater lateral area at one-half of the mean draught
Δ = displacement

l_{w2} corresponds to l_{w1} times a gust factor. These levers are interpreted as lines in the GZ curve plot and define the horizontal border line of the areas (a, b). Together with the specified roll angles due to wind action and the angle of down flooding specifying the vertical limits of these areas, they allow a stability evaluation based on energetic considerations. If area b is equal to or larger than area a, the criterion is considered fulfilled.

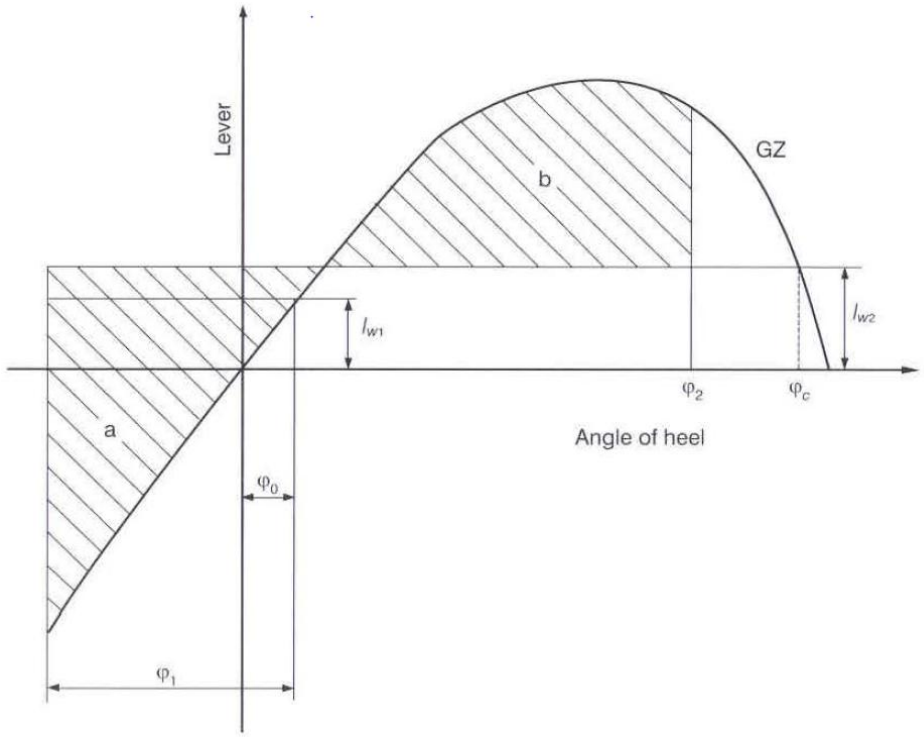

Figure 3-1: GZ curve for severe wind and rolling, taken from IMO IS 2008 (IMO, 2008).

The relevant roll angles were obtained as follows:

f_0 = angle of heel under action of steady wind, corresponding to the intercept between the GZ curve and the line representing l_{w2}, here 4.4 deg.

f_1 = angle of roll to windward due to wave action, calculated according to the IMO intact stability criteria as:

$$\varphi_1 = 109 \cdot k \cdot X_1 \cdot X_2 \cdot \sqrt{r \cdot s}\ [deg]$$

The involved parameters are given in the regulation text for different vessel classes. Here, the following were used to calculate f_1:

k	X_1	X_2	r	s	f_1 [deg]
0.7	0.91	1	0.826	0.044	13.2

f_2 = angle of down-flooding or the second intercept of heeling and righting lever curve, whichever is smaller. The angle of down-flooding was used in the present case and determined assuming the angle from which the coaming is exceeded, here 28 deg. Notably, down-flooding angles of up to 50 deg are mentioned in the IMO intact stability code (IMO 2008, section 2.3.2).

Figure 3-3 shows the GZ curve that was calculated from the hull lines and the limiting roll angles and wind levers used for the investigated vessel. Table 3-1 shows the wind levers, roll angels and areas calculated according to the IMO weather criterion. The vessel was found to comply with the weather criterion stability regulations.

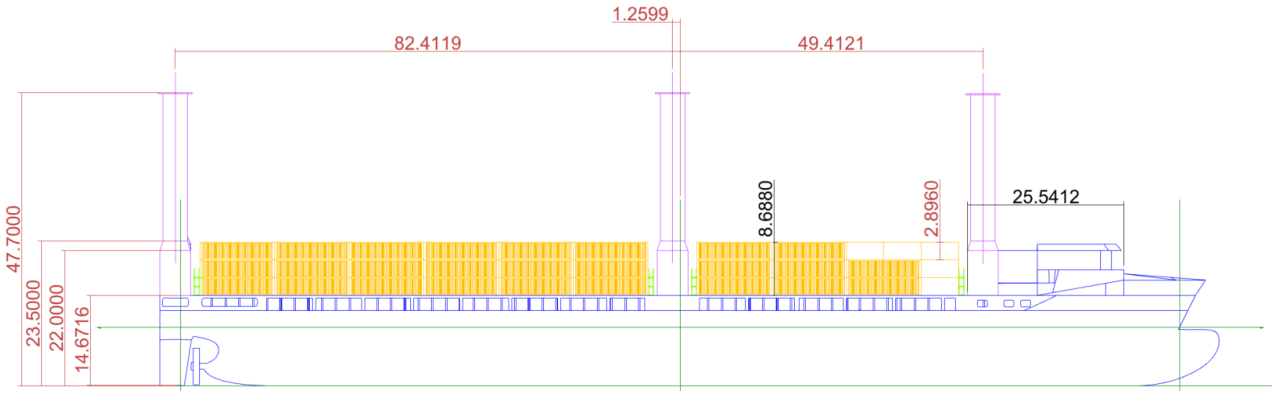

Figure 3-2: Side view of the investigated vessel, lengths given in [m].

Table 3-1: GZ curve and weather criterion parameters.

Item	Description	Value	Unit
T	Average Draught	9.2	[m]
Δ	Displacement	29500	[t]
KG	Vertical Centre Of Gravity	10.7	[m]
GM_{t_dry}	Metacentric height (dry)	1.5	[m]
A	Projected lateral area	2659	[m^2]
Z	Vertical distance from centre of A to the centre of the underwater lateral area at one-half of the mean draught	15.0	[m]
l_{w1}	Wind lever	0.07	[m]
l_{w2}	Wind lever including gust factor	0.10	[m]
f_0	angle of heel under action of steady wind	4.4	[deg]
f_1	angle of roll to windward due to wave action	13.2	[deg]
f_2	angle of down-flooding	28.0	[deg]
a	Area a	2.1	[m*deg]
b	Area b	5.1	[m*deg]
f_c	Capsizing angle	41	[deg]

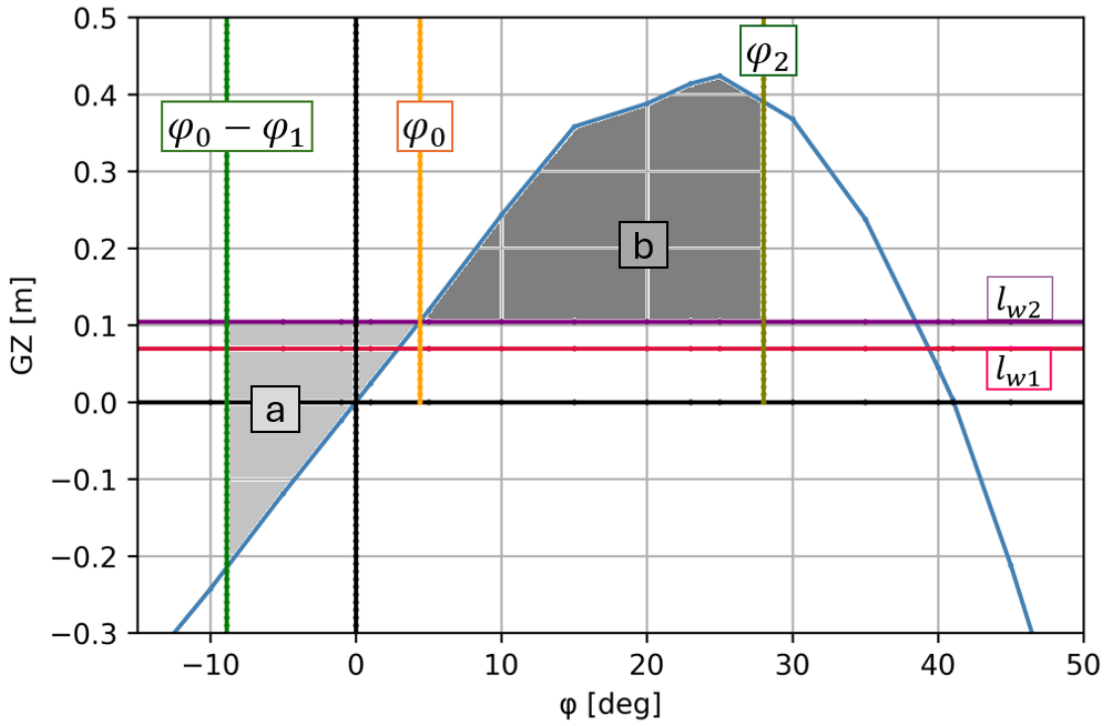

Figure 3-3: GZ curve for severe wind and rolling, calculated from hull shape of the investigated model.

3.2 Seakeeping calculations

Calculations were performed prior to the tests using MARIN's seakeeping code SEACAL. This is a linear frequency-domain code for zero and forward speed, based on 3D diffraction theory Table T14 – Table T16 show the calculation settings, parameters and mesh.

Figure 3-4 and Figure 3-5 show the calculated roll response RMS values for different headings and wave periods at sailing speeds of 0 kn and 12 kn. The results show highest response amplitudes around wave periods of 18 s for headings between 75 deg and 105 deg. For stern-quartering seas at 12 kn, response peaks are also found at Tp of 16 s and 14 s. These wave periods are rare but occur and were therefore chosen as test conditions for the irregular wave tests.

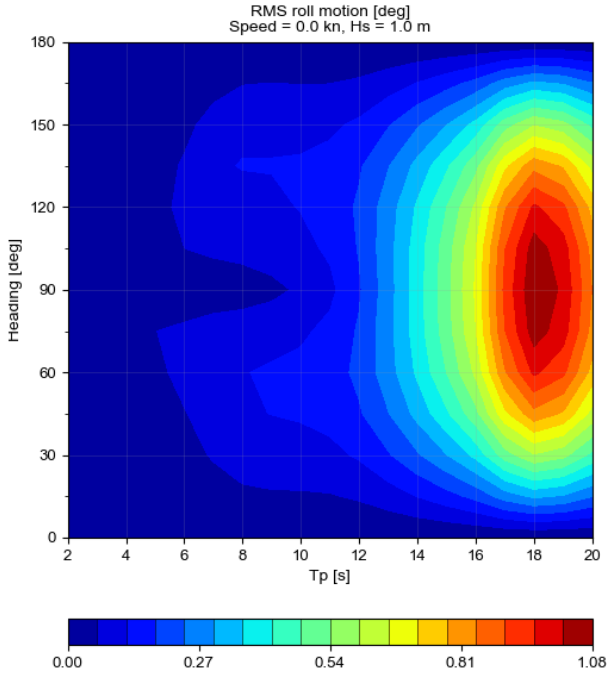

Figure 3-4: Calculated roll response RMS at 0 kn sailing speed.

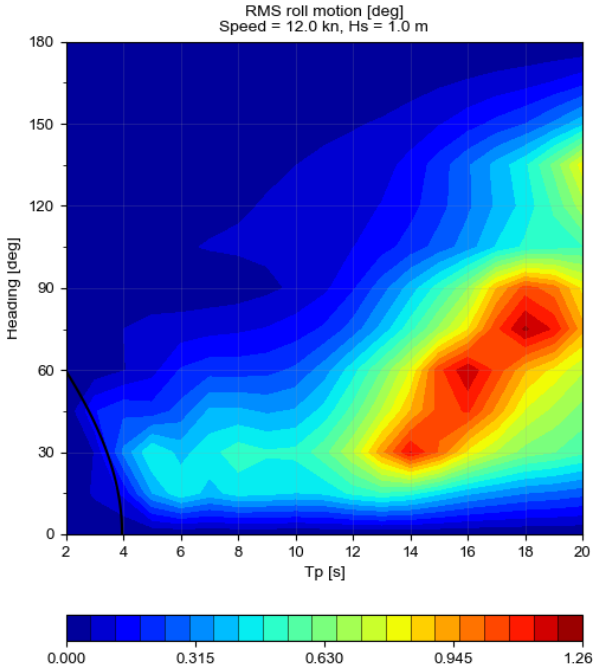

Figure 3-5: Calculated roll response RMS at 12 kn sailing speed.

4 TEST PROGRAMME

4.1 Main targets of the seakeeping investigation

The main objective of the seakeeping tests is to assess the effect of the wind propulsion system on stability. Particularly the modelling approaches using constant wind force, steady and unsteady wind are compared.

4.2 Test conditions

Details on the test conditions are provided in Table T10 through Table T13. Rare but realistic worst case wave and wind conditions for the North Sea spectrum were chosen based on the calculation results. Three wind speed conditions were chosen based on the typical wind speed of the chosen wave condition with gust factor (24.5 kn), the Norsepower maximum operational wind speed recommendation for their rotor sails (35.0 kn) and the dead ship condition (50.5 kn).

Weather criterion tests

To check the compliance of the vessel with existing approved assessments, the regular waves rollback angle according to MSC.1/Circ.1200 was determined in a dedicated test.

Tests in regular waves were performed to obtain the regular waves roll-back angle. The wave height and periods were chosen based on the vessel's natural period of 18.3 s and following IMO MSC.1/Circ.1200. According to Table 4.5.1 in the regulation (shown below as Table 4-1), a wave with steepness (s) of about 0.038 should be selected for the model tests.

Considering that the wave should have the same period as the roll natural period of the ship, then the wave height (H) can be calculated as:

$$H = \frac{s * g * T_{\phi}^2}{2 * \pi}$$

This gives a H of about 19.1 m. Seven wave periods were selected according to the ratios between the roll natural period and wave period of 0.8, 0.9, 0.95, 0.975, 1.0, 1.05 and 1.2.

Table 4-1: Wave steepness as a function of the full scale natural period.

Ship roll period T_{ϕ} [s]	Wave steepness $s = H / \lambda$
<6	0.100
6	0.100
7	0.098
8	0.093
12	0.065
14	0.053
16	0.044
18	0.038
20	0.032
22	0.028
24	0.025
26	0.023
28	0.021
30	0.020
>30	0.020

Table 4-2: Tests in regular waves

#	H [m]	T [s]	Heading [deg]	Vs [kn]
1	19.1	18.3	90	0
2	19.1	17.8	90	0
3	19.1	19.2	90	0
4	19.1	17.4	90	0
5	19.1	22.0	90	0
6	19.1	16.5	90	0
7	19.1	14.6	90	0

Tests in irregular seas

The tests in irregular waves were aimed at assessing the validity of current stability criteria when applied to extreme, but realistic wind and wave scenarios for the chosen vessel. IMO SLF 53-INF.3 was the basis for the selection of the criteria. Constant force tests were done representing SLF 53-INF.3. The wind operating modes using steady and unsteady wind were done to investigate the impact of more realistic dynamical mechanisms on the vessel stability.
Steady wind, unlike constant wind force, considered the changing orientation of the vessel due to motions, especially roll, and thus results in a varying wind force acting on the vessel.
Unsteady wind spectra were generated independently from wave spectra. More tests in bow-quartering seas were originally planned, but only one test was conducted due to time constraints.

Table 4-3: Test in irregular seas.

Mean Speed [kn]	Wave conditions			Wind assistance				Full scale test duration [h:min]
	Mu [deg]	Hs [m]	Tp [s]	TWA [deg]	TWS [kn]	Wind type	Rotor [rps]	
0	90	11.9	19.6	90	50.5	unsteady	0	1:47
0	90	12.6	18.7	-	-	no wind	-	1:05
0	90	12.6	18.7	90	50.5	steady	0	1:05
0	90	12.6	18.7	90	50.5	unsteady	0	1:47
0	90	12.6	18.7	90	50.5	constant force	0	1:05
0	90	13.2	17.8	-	-	no wind	-	1:05
0	90	13.2	17.8	90	50.5	steady	0	0:49
0	90	13.2	17.8	90	50.5	unsteady	0	1:47
0	90	13.2	17.8	90	50.5	constant force	0	1:13

4.3 Selected wave conditions

JONSWAP type spectra with a peak enhancement factor γ of 3.3 were used to represent all wave conditions. The waves were not calibrated prior to the tests, but measured just ahead of the model and beside the model during the test.
Waves were chosen in accordance with SLF 53-INF.3 based on the 20-year return period contour of the DNV worldwide scatter diagram. This way rare, but possible waves around the roll resonance of the vessel were chosen rather than the most common sea states representative of the area. Figure 4-1 shows a summary of the tested wave conditions.

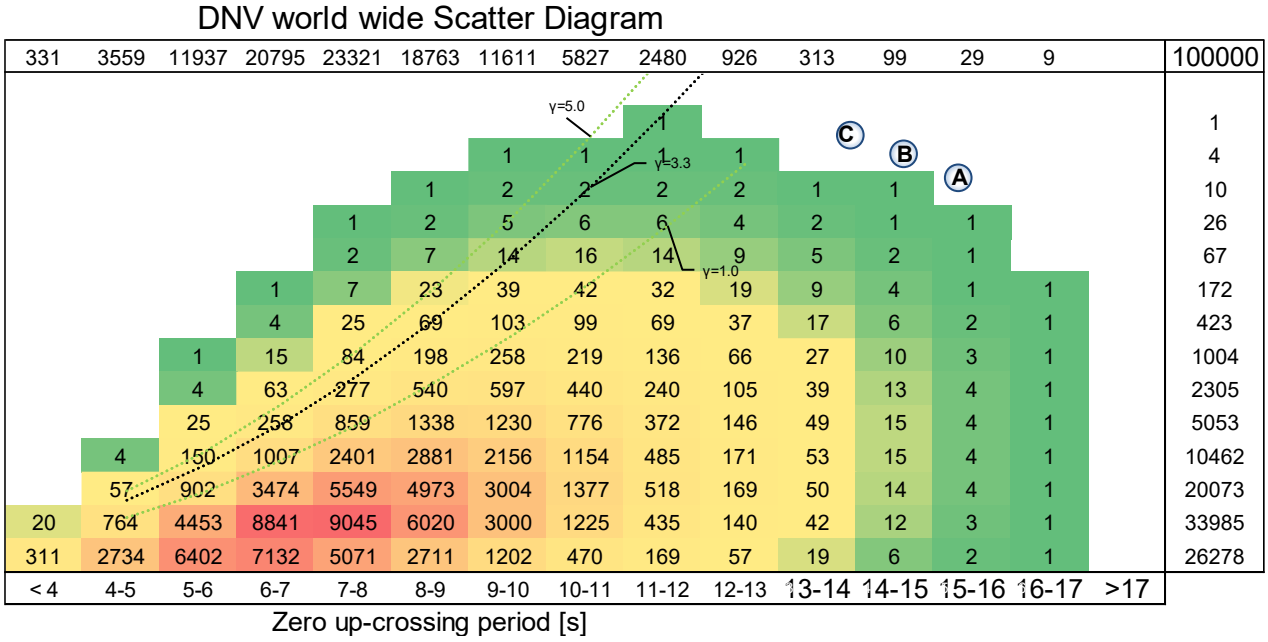

ditions used during study

Hs [m]	Tp [s]	Tz [s]
11.9	19.6	15.24
12.6	18.7	14.54
13.2	17.8	13.84

Figure 4-1: Scatter diagram and chosen wave conditions.

5 RESULTS AND DISCUSSION

The detailed results of the tests are provided in the data report (Volume 2). The following sections provide a summary of the results of weather criterion, roll decay, calm water, regular waves and irregular seas tests.

5.1 Weather criterion tests

To check the compliance of the vessel with existing approved assessments, the regular waves rollback angle according to MSC.1/Circ.1200 was determined in a dedicated test. The full data analysis including time traces can be found in Volume 2 of this report. During these tests, the model was not self-propelled. The wind system was removed, but the same weight distribution was used. Figure 5-1 shows a picture of the model during the weather criterion tests.
Figure 5-2 shows the results of the measurements. The peak roll response which corresponds to the "regular waves roll-back angle" is Φ_{1r} = 19.8 deg and is observed for a wave period of 19.2 s, which corresponds to the vessel's natural roll period. Since the vessel generally starts drifting during wave tests, the maximum response was expected at the natural or a slightly shorter period. The corresponding derived value for the angle of roll to windward due to wave action is φ_1 = 0.7· Φ_{1r} = 13.9 deg.
This is a larger value than the 13.2 deg angle that was calculated for φ_1 in Section 3.1 above. Therefore, the empirical approach described in the IMO 2008 intact stability code yields a slightly lower angle for the given vessel than the experimental assessment following MSC.1/Circ.1200 in the present case.

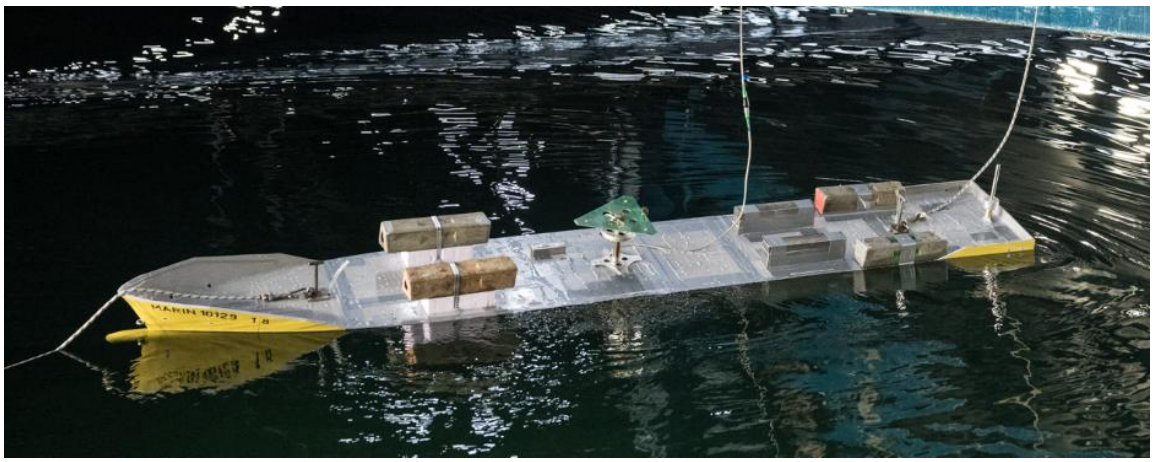

Figure 5-1: Picture of model during weather criterion test.

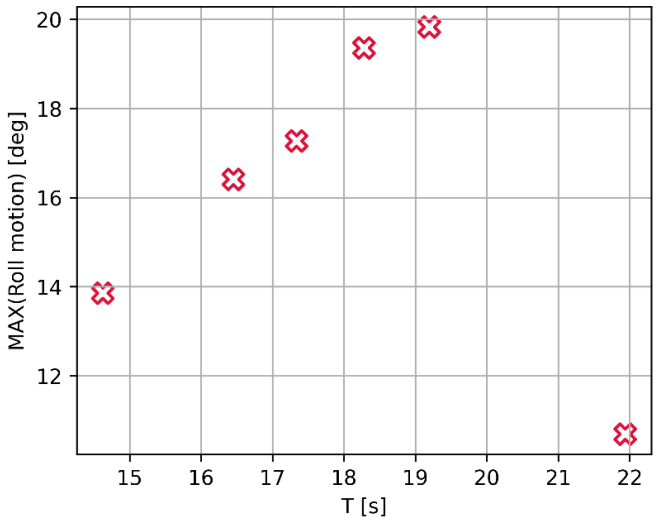

Figure 5-2: Measured maximum roll angles in weather criterion regular wave model tests.

5.2 Irregular wave tests

Figure 5-3 - Figure 5-6 show results for the irregular wave tests per sea state. Tests were done at 0 kn sailing speed, 90 deg heading and 50.5 kn wind speed. Rotor sails were modelled as inactive (not rotating) for the dead ship condition. Mean roll motion results show similar values around 5 deg for all wind modes except for tests without wind. The results without wind show mean roll values in wind direction of 2.5 deg, likely because of a slight shift of a weight in these tests. This was initially not noticed during the tests. The correct maximum and mean values for tests without wind should therefore be considered shifted by 2.5 deg.

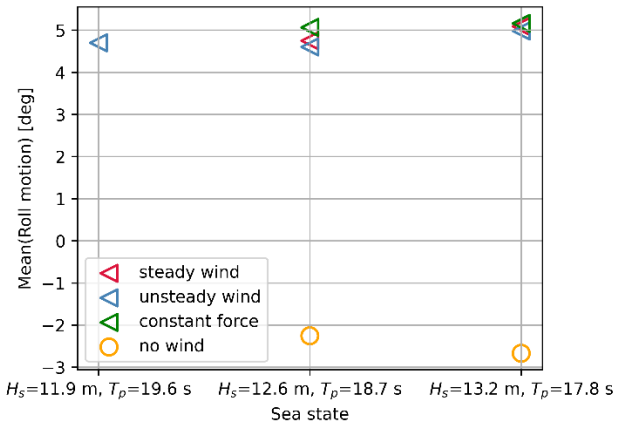

Figure 5-3: Irregular wave test roll mean values in beam seas at 50.5 kn wind speed.

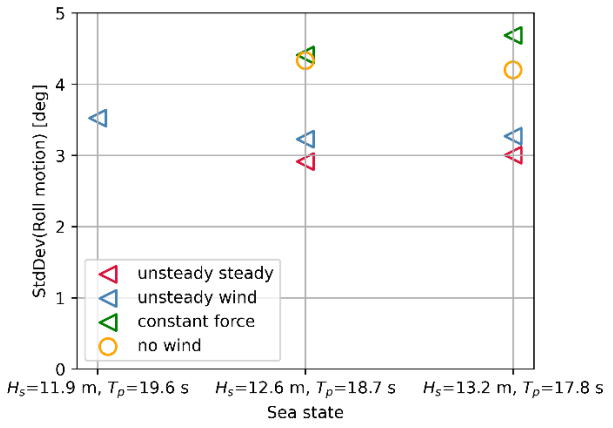

Figure 5-4: Irregular wave test roll standard deviation values in beam seas at 50.5 kn wind speed.

The roll standard deviations show the highest values for the constant wind force and no wind force tests, the lowest values for the unsteady wind tests. For the standard deviations of the Mx moments the opposite is observed, with the unsteady wind case showing the highest values and no wind condition the lowest. This is consistent with the expected added damping due to the aerodynamic forces changing with the exposed area of the vessel as it rolls. Part of the moment generated due to aerodynamic effects works against the moment induced by the waves. The constant force mode is not effected by the change in orientation in the same way and therefore does not introduce additional roll damping due to aerodynamic effects, resulting in the observed higher standard deviations of roll motion.

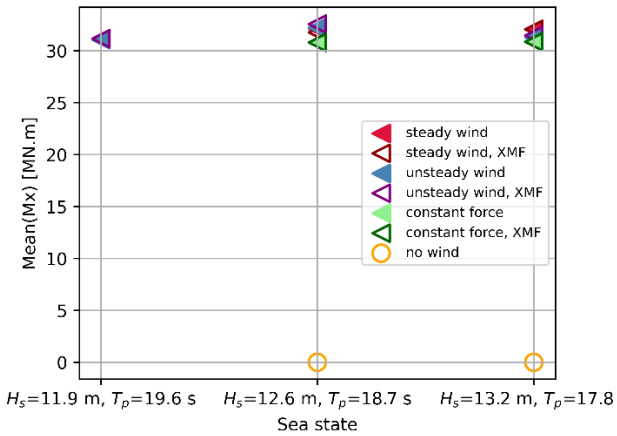

Figure 5-5: Irregular wave test mean values of moment Mx in beam seas at 50.5 kn wind speed.

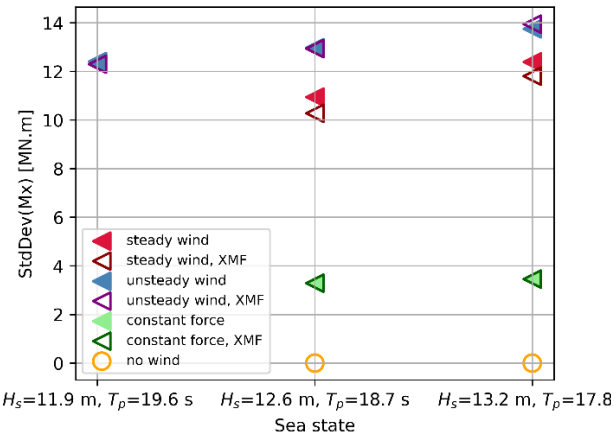

Figure 5-6: Irregular wave test standard deviation values of force Mx in in beam seas at 50.5 kn wind speed.

Figure 5-7 shows the probabilities of exceedance for the roll peak angles measured during the irregular seas tests. The highest roll peak angles were measured in the constant force mode tests, followed by unsteady and then steady wind cases. The lowest peak angles were observed for the no wind case. Largest roll peak angles were expected for the unsteady wind cases because of the gust factor that should result in a larger added moment due to aerodynamic effects. Figure 5-7 shows that some large roll angles were observed for the unsteady wind cases with low probability of exceedance. It is possible that for longer test durations, the largest peak values would occur for unsteady wind. While for the constant force cases, all waves coincide with the maximum 'aerodynamic' loading, it is a challenge to determine the necessary measurement duration to observe an unfavourable combination of irregular wave and wind gust coinciding in the unsteady wind case. However, these combinations of waves and gust are associated with capsizing events of real vessels. Note that the roll peaks of the tests without wind should be considered shifted by 2.5 deg due to the slightly shifted weight distribution, as pointed out above.
To assess the dynamic stability of a vessel, future experimental approaches should therefore aim for either a baseline in terms of measurement time still to be determined or a predetermined combination of representative wave- and wind time trace combinations. The latter would lead to testing conditions that are less representative of common sea states and wind events, but that could represent rare, realistic capsizing scenarios at relatively low experimental cost. Numerical studies may offer an alternative for the assessment of the worst case conditions as they involve much lower cost for long test durations. Detailed numerical studies may also allow an informed choice of the time traces for unsteady wind and irregular seas conditions to employ in experimental work.

For comparison with established approaches for stability assessment, Figure 5-8 shows the peak roll angles measured in irregular seas with wind as well as the angle of roll to windward due to wave action, f_1, determined from the weather criterion tests according to MSC.1/Circ. 1200. When applying the measured values as f_1 to the procedure detailed in Section 3.1, the present vessel would not pass the current criteria for the tested conditions at constant force mode and with unsteady wind mode in H_S = 11.9 m at T_P = 19.6 s.

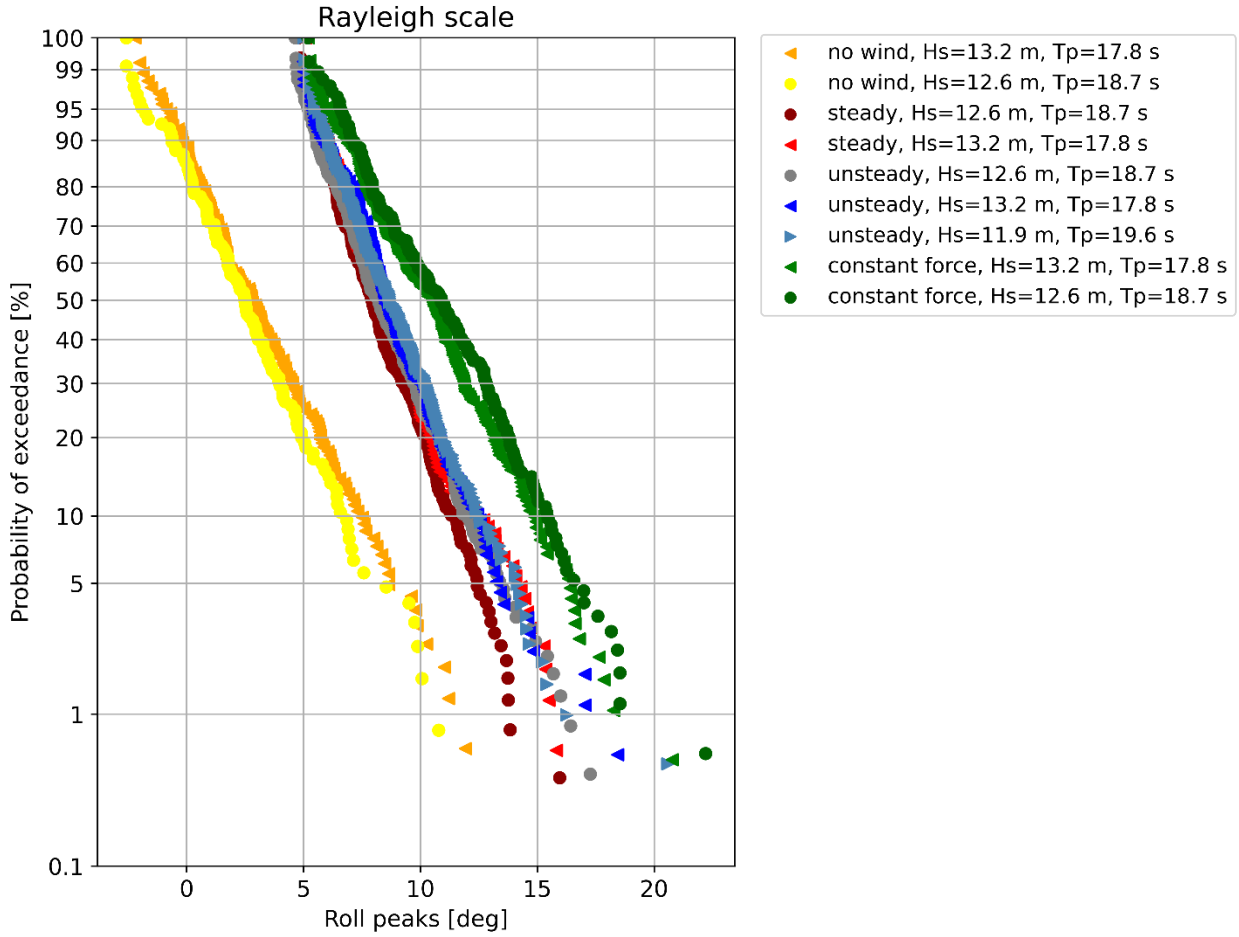

Figure 5-7: Probabilities of exceedance for roll peaks in irregular seas tests.

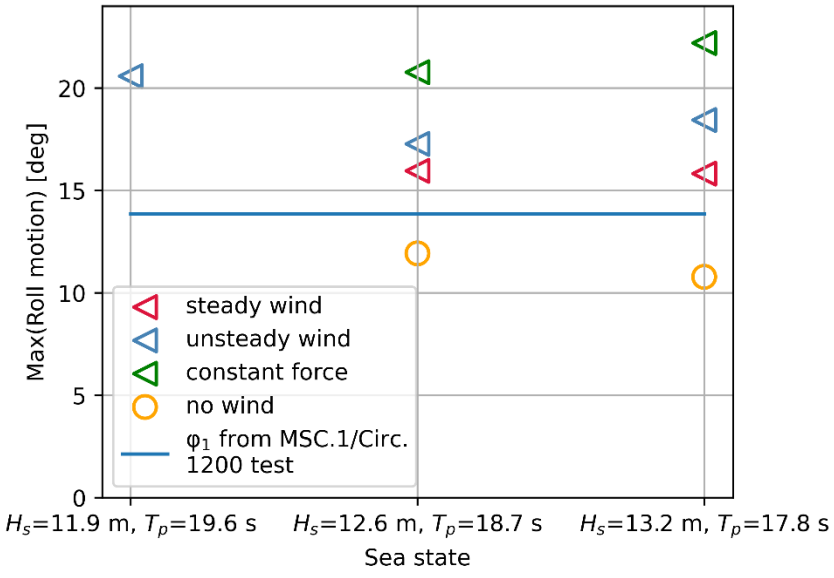

Figure 5-8: Roll peak angles in irregular seas tests and rollback angle due to wave action from MSC.1/Circ. 1200 weather criterion tests.

6 CONCLUSIONS AND RECOMMENDATIONS

Seakeeping model tests were performed for a model of a hypothetical, retrofitted container carrier feeder vessel fitted with six rotor sails in extreme environmental condition. The goal was to assess the impact of different wind and wind modelling techniques on the dynamic stability of such a vessel.

General conclusions on the experimental approach and future work can be summarised as follows:

- Due to the high cost associated with long test durations, it is recommended to determine a baseline of worst case scenario combinations of irregular seas and unsteady wind conditions for experimental assessments of wind propelled vessel dynamic stability.
- A numerical study has been launched to validate the experimental results.
- The numerical study will further address the issue of insufficient test duration in experiments to investigate probabilities of exceedance of peak roll angles in irregular seas with better statistical convergence.
- Numerical studies may also allow the selection of suitable combinations of irregular seas and unsteady wind time traces to obtain worst case roll angles that may lead to capsizing events in rare, but realistic scenarios.

The main goal of the study was to assess whether current regulation is sufficient to assess the stability of wind propelled vessels. Stability regulation from the mandatory IMO IS 2008 code, as well as the alternative, non-mandatory assessments following IMO MSC.1/Circ.1200, and IMO SLF 53/INF.3 were considered in the presented work. It seems justified to conclude that:

- The theoretical assessment of the weather criterion yielded similar or lower values for the stability criteria than the experimental approach using regular waves in the investigated case.
- The probabilities of exceedance of the peak roll angles in irregular seas show highest roll angles for the constant force mode, followed by unsteady and then steady wind modes. However, the results imply that longer test durations are required to assess the probability of exceedance of roll peaks for unsteady wind.
- Results from irregular seas tests in extreme conditions (50.5 kn wind speed) showed that a vessel that complies with existing stability regulation assessment can exceed regulation limits in extreme, but realistic conditions for wind and waves. This case alone shows that regulation without alternative assessment methods may not be sufficient to assure the stability of all wind propelled vessels in extreme conditions.

Wageningen, June 2025
MARITIME RESEARCH INSTITUTE NETHERLANDS

Guilhem Gaillarde
Manager Ships Department

TABLES

Table T1: Main particulars and stability data of the vessel

Model No. M10129 Model scale ratio $\lambda = 63.2$

Designation	Symbol	Magnitude		Unit
		specified	*(realised*)*	
Main particulars				
Length between perpendiculars	L_{PP}	163.00		[m]
Length on waterline	L_{WL}	166.25		[m]
Length overall submerged	L_{OS}	172.86		[m]
Breadth moulded on WL	B_{WL}	27.00		[m]
Draught moulded on FP (relative to baseline)	T_F	9.20		[m]
Draught moulded on AP (relative to baseline)	T_A	9.20		[m]
Displacement volume moulded	∇	28752		[m^3]
Displacement mass in seawater	Δ_1	29,500	*(28,980)*	[t]
Wetted surface area bare hull	S	6084.66		[m^2]
Longitudinal position of centre of gravity				
LCG position from AP	LCG	78.21	*(78.09)*	[m]
Vertical position of cog and stability				
Transverse metacentric height (incl. free surface correction) without wind	GMt_{WET}	1.50	*(1.49)*	[m]
Transverse metacentric height (incl. free surface correction) with active wind system	GMt_{WET}	1.50	*(1.58)*	[m]
Vertical position centre of gravity (dry)	KG	10.74	*(11.05)*	[m]
Vertical position centre of buoyancy	KB	4.98		[m]
Transverse metacentre above base	KM	12.25		[m]
Mass radius of gyration around X-axis	k_{XX}	9.99	*(10.27)*	[m]
Mass radius of gyration around Y-axis	k_{YY}	42.41	*(42.24)*	[m]
Mass radius of gyration around Z-axis	k_{ZZ}	42.41	*(41.33)*	[m]
Natural period of roll (incl. added mass, target value provided by calculations) without wind	$T\phi$	-	*(18.40)*	[s]
Natural period of roll (incl. added mass, target value provided by calculations) witch active wind system	$T\phi$	-	*(18.43)*	[s]
Coefficients				
Block coefficient	C_B	0.71		-
Amidships section coefficient	C_M	1.00		-
Prismatic coefficient	C_P	0.71		-
Water plane coefficient	C_{WP}	6.04		-
Length-Breadth ratio	L_{PP}/B_{WL}	2.94		-
Breadth-Draught ratio	B_{WL}/T	17.72		-
Length-Draught ratio	L_{PP}/T	0.71		-

**: when measurable*

Table T2: Main particulars of propellers

Designation	Symbol	Magnitude	Unit
Propeller model No. S612 Centre			
Diameter	D	5.58	[m]
Pitch ratio at 0.7R	$P_{0.7}/D$	1.00	-
Boss- diameter ratio	d/D	0.18	-
Expanded blade area ratio	A_E/A_0	0.45	-
Number of blades	z	4	-
Direction of rotation	clockwise looking ahead		

Table T3: Main particulars of rudders and control settings

Height, chord, thickness and area are given for the movable part of the rudder.

Designation	Symbol	Magnitude	Unit
***Rudder particulars** (see also **Figure F2**)*			
Number of rudders	-	1	-
Average height	b_R	7.71	[m]
Average chord	c_R	4.08	[m]
Geometric aspect ratio (b_R/c_R)	λ	1.89	-
Maximum thickness	T	0.74	[m]
Max thickness / chord	T / c_R	18.12	[%]
Projected area	A_R	31.46	[m^2]
Longitudinal position of rudder axis from AP	x_R	-1.11	[m]
Offset of rudder axis from centreline	y_R	0.00	[m]
Angle of the rudder in yz-plane with horizontal	β_R	90	[deg]
Total rudder area ratio, $A_R / (L_{PP}*T_{mean})$	-	2.10	[%]
Rudder settings for autopilot			
max rudder angle	δ_{MAX}	35	[deg]
rudder angle per deg course deviation	C_Ψ	3.00	[deg/deg]
rudder angle per deg/s rate of turn	B_Ψ	7.95	[deg/(deg/s)]
rudder angle per m transverse course deviation	C_Y	0.00	[deg/m]
rudder rate of application	$\dot{\delta}$	4.00	[deg/s]

Table T4: Main particulars of bilge keels

Designation	Symbol	Magnitude	Unit
***Bilge keels** (see also **Figure F3**)*			
Total length	L_{BK}	48.69	[m]
Height	H_{BK}	0.40	[m]
Location: between station 6 and station 13 (29.9% of Lpp)			

Table T5: Designation, notation, sign convention and measuring devices of measured quantities

Sample frequency 50 Hz.

Designation	Notation	Positive for	Measured by
Wave elevation:		**WAVE 4: 398 m forward of station 10, at CL WAVE 2: Next to station 10 and 309 m to port side**	
Incident wave elevation	WAVE 2 WAVE 4	Wave elevation upwards	Acoustic type wave probe

Sample frequency 100 Hz.

Motions of ship at COG:			
Surge (*with respect to carriage*) Sway (*with respect to carriage*) Heave Roll Pitch Yaw	SURGE SWAY HEAVE ROLL PITCH YAW	Ship forwards Ship to port side Ship upwards Starboard down Bow down Bow to port side	Optical tracking system
Propeller revolutions:			
Propeller revolutions	RPM	Sailing ahead	Digital encoder
Permillage winches wind system:			
Permillage winch fore Permillage winch aft Permillage winch port side Permillage winch starboard fore Permillage winch starboard aft	FX PROM F FX PROM A FY PROM PS FY PROM SBF FY PROM SBA	Pulling	From software based on winch encoder

Sample frequency 200 Hz.

Designation	Notation	Positive for	Measured by
Position and velocity of carriage:			
X position on north rail	C.AbsEnN	Carriage moving east	SSI encoder
X position on south rail	C.AbsEnS		
Speed on north rail	C.SpeedN		Velocity measuring wheel
Speed on south rail	C.SpeedS		
Y position of sub carriage	C.AbsEnMC	Carriage moving north	SSI encoder
Speed of sub carriage	C.SpeedMC		Velocity measuring wheel
Rudder angles:			
Rudder angle	RUD ANG	Rudder nose to port side	Set point

Table T6: Designation, notation, sign convention of XMF signals

Designation	Notation	Positive for
Wind parameters:		
True wind speed (unsteady wind)	XMF TWS_EF	Always positive
True wind speed (setpoint)	WIND TWS*	Always positive
True wind angle (setpoint)	WIND TWA*	180 is wind from the bow
Apparent wind speed	WIND AWS*	Always positive
Apparent wind angle	XMF AWA_deg	180 is wind from the bow
Fletner rotation	ROTATION*	Always positive
Forces and moments superstructure (earth fixed):		
Longitudinal force	XMF Fx_superstr	Ship forwards
Transversal force	XMF Fy_superstr	Ship to port side
Vertical force	XMF Fz_superstr	Ship upwards
Roll moment	XMF Mx_superstr	Starboard down
Pitch moment	XMF My_superstr	Bow down
Yaw moment	XMF Mz_superstr	Bow to port side
Forces and moments at wind propulsion (earth fixed):		
Longitudinal force	XMF Fx_WindProp	Ship forwards
Transversal force	XMF Fy_WindProp	Ship to port side
Vertical force	XMF Fz_WindProp	Ship upwards
Roll moment	XMF Mx_WindProp	Starboard down
Pitch moment	XMF My_WindProp	Bow down
Yaw moment	XMF Mz_WindProp	Bow to port side

* from XMF via Marin measurement system

Table T7: Attachment point of wind forces

Name	Location		
	x [m] w.r.t. AP	y [m] w.r.t. CL	z [m] w.r.t. BL
FX LINE F	81.50	0.00	34.63
FX LINE A	81.50	0.00	34.63
FY LINE PS	81.50	0.00	34.63
FY LINE SBF	97.30	0.00	39.37
FY LINE SBA	65.70	0.00	40.01

Table T8: Designation, notation and sign convention of calculated quantities

Sample frequency 200 Hz.

Designation	Notation	Positive for
Motions at COG:		
Longitudinal motion	SURGE	Ship forwards
Transverse motion	SWAY	Ship to port side
Speed of ship at COG:		
Longitudinal speed Transversal speed	VX SHIP VY SHIP	Sailing ahead
Winch forces in wind system:		
Longitudinal force fore Longitudinal force aft Transversal force port side Transversal force starboard fore Transversal force starboard aft	FX WINCH F FX WINCH A FY WINCH PS FY WINCH SBF FY WINCH SBA	Pulling
Wind forces and moment at COG based on winches (earth fixed):		
Longitudinal force Transversal force Roll moment Yaw moment	FX WINCH FY WINCH MX WINCH MZ WINCH	Ship forwards Ship to port side Starboard down Bow to port side

Table T9: Filter frequencies of measured and calculated quantities – specified by test condition

Signal type	Filter frequencies
	Low-pass filter upper limit [rad/s]
Motions, ship speed and wave elevation	8.0
XMF output	1.0

Table T10: Overview of tests in transit in calm water

MARIN test ID 77001_01SMB_	Mean Speed [kn]	Wind assistance				Remarks
		TWA [deg]	TWS [kn]	type	Rotor [rps]	
04_001_001_01	0	270	50.5	steady	0.00	
04_002_001_01	0	270		spectrum	0.00	
01_003_002_02	12	-	-	no wind	-	
03_001_006_02	12	220	24.5	steady	1.78	
03_001_005_02		225		steady	1.92	no xmf data
03_001_004_02		270		steady	1.90	
03_001_003_03		300		steady	2.22	
03_001_002_01		315		steady	1.15	
03_001_012_01	12	220	35.0	steady	1.32	xmf data not complete
03_001_011_01		225		steady	1.43	
03_001_009_02		300		steady	1.65	
03_001_008_03		315		steady	1.15	
03_001_007_01		330		steady	1.10	xmf data not complete
03_002_006_01	12	220	24.5	spectrum	1.78	
03_002_005_01		240		spectrum	2.22	
03_002_004_01		270		spectrum	1.90	
03_002_002_01		315		spectrum	1.15	

Table T11: Overview of decay tests in calm water

MARIN test ID 77001_01SMB_	Mean Speed [kn]	Wind assistance				Remarks
		TWA [deg]	TWS [kn]	type	Rotor [rps]	
03_003_005_01	0	-	-	no wind	-	
03_003_004_01	12	-	-		-	
03_003_006_01	16	-	-		-	
03_003_001_01	0	0	0	steady	0	
03_003_002_01	12	0	0	steady	0	
03_003_003_01	16	0	0	steady	0	

Table T12: Overview of tests in transit in regular waves

MARIN test ID 77001_01SMB_	Wave conditions			Mean Speed [kn]	Wind assistance				Remarks
	Mu [deg]	H [m]	T [s]		TWA [deg]	TWS [kn]	type	Rotor [rps]	
03_004_003_01	220	5	10	0	-	-	no wind	-	
03_003_006_02	220	5	10	12	220	0.0	steady	0	
03_005_005_01	220	5	10	12	220	24.5	steady	1.78	
03_005_007_02	220	5	10	12	220	24.5	spectrum	1.78	
03_005_008_01	220	5	10	12	220	35.0	spectrum	1.32	
03_004_002_01	315	5	10	0	-	-	no wind	-	
03_003_005_01	315	5	10	12	315	0.0	steady	0	
03_005_001_02	315	5	10	12	315	24.5	steady	1.15	
03_005_003_01	315	5	10	12	315	24.5	spectrum	1.15	
03_005_004_01	315	5	10	12	315	35.0	spectrum	1.15	
03_004_001_01	330	5	10	0	-	-	no wind	-	
03_003_004_01	330	5	10	12	-	-	no wind	-	
03_005_009_02	330	5	10	12	330	24.5	steady	1.87	
03_005_010_01	330	5	10	12	330	35.0	steady	1.1	
03_005_011_01	330	5	10	12	330	24.5	spectrum	1.87	
03_005_012_01	330	5	10	12	330	35.0	spectrum	1.1	

Table T13: Overview of tests in transit in irregular waves

JONSWAP wave spectrum (gamma = 3.3)

MARIN test ID 77001_01SMB_	Test duration [s]	Wave conditions			Mean Speed [kn]	Wind assistance				Remarks
		Mu [deg]	Hs [m]	Tp [s]		TWA [deg]	TWS [kn]	type	Rotor [rps]	
03_007	6402	220	5.0	10.0	12	220	24.5	spectrum	1.78	
04_009	6402	270	11.9	19.6	0	270	50.5	spectrum	0	
04_010	6402	270	12.6	18.7	0	-	-	no wind	-	
04_003	6402	270	12.6	18.7	0	270	50.5	steady	0	
04_004	3915	270	12.6	18.7	0	270	50.5	spectrum	0	
04_007	3915	270	12.6	18.7	0	270	0.0	constant force	0	
04_011	3915	270	13.2	17.8	0	-	-	no wind	-	
04_005	2934	270	13.2	17.8	0	270	50.5	steady	0	xmf data not complete
04_006	4427	270	13.2	17.8	0	270	50.5	spectrum	0	
04_008	4427	270	13.2	17.8	0	270	0.0	constant force	0	

Table T14: Calculation parameters.

Item	Value	Unit
speed	(0.0 to 16.0 step 4.0)	[kn]
heading	(0.0 to 180.0 step 15.0)	[deg]
frequency	(0.05 to 2.0 step 0.05)	[rad/s]
rollb44	(0.5) (5.0) (10.0) (20.0)	[deg]
depth	Deep	[m]

Table T15: Natural frequencies and damping used in calculation.

Item	Description	Value	Unit
T_z	Natural Period of Heave	7.964, 7.956, 7.947, 7.938, 7.93	[s]
B_33_crit	Critical Heave Damping	98582.95, 98481.45, 98374.29, 98267.05, 98159.12	[kN.s/m]
T_phi	Natural Period of Roll	18.608, 18.608, 18.608, 18.608, 18.608	[s]
B_44_crit	Critical Roll Damping	2554060.0, 2554020.0, 2554019.0, 2554019.0, 2554018.0	[kN.m.s/rad]
T_theta	Natural Period of Pitch	7.7, 7.652, 7.623, 7.608, 7.608	[s]
B_55_crit	Critical Pitch Damping	172769300.0, 171706800.0, 171054100.0, 170719300.0, 170706400.0	[kN.m.s/rad]

Table T16: Damping methods used in calculation.

Item	Description	Value	Unit
methodEqvLinRollDampCoef		IKEDA	
methodPotRollDampCoef		POT	
methodRatioRollDampCoef		None	
methodEddyRollDampCoef		IKEDA	
methodLiftRollDampCoef		IKEDA	
methodFrictRollDampCoef		IKEDA	
methodWaveRollDampCoef		IKEDA	
methodLinQuaRollDampCoef		None	
methodLinQuaRollDampCoef		None	
methodLinQuaRollDampCoef		None	
methodLinQuaRollDampCoef		None	

Table T17: Hull shape used in SEACAL calculations. Total number of panels: 2591.

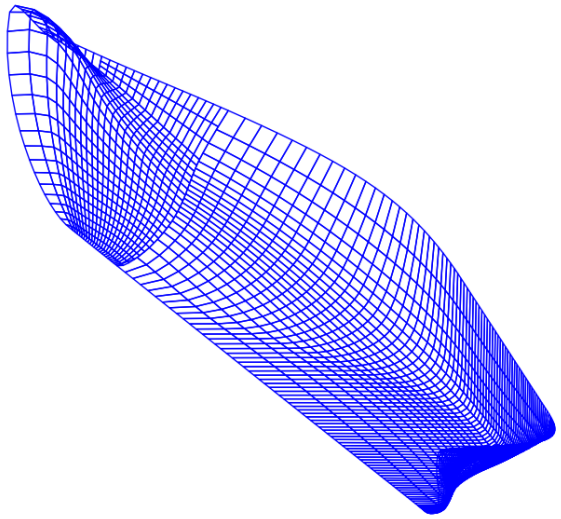 looking from xyz: 300_ 40_ -40	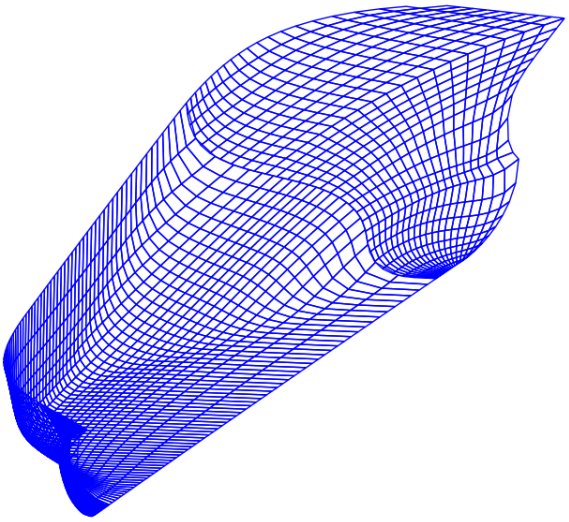 looking from xyz: -150_ 40_ -40

FIGURES

Figure F1: General arrangement and small scale body plan

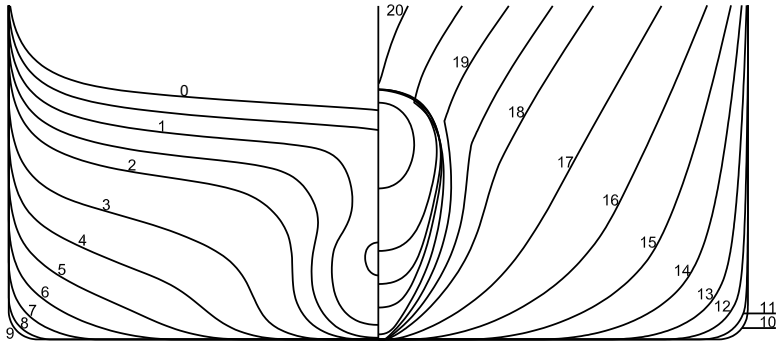

OVERVIEW OF SHIP MODEL No. 10129
DIMENSIONS ARE GIVEN IN mm FOR SHIP

Figure F2: Rudder and propeller arrangement

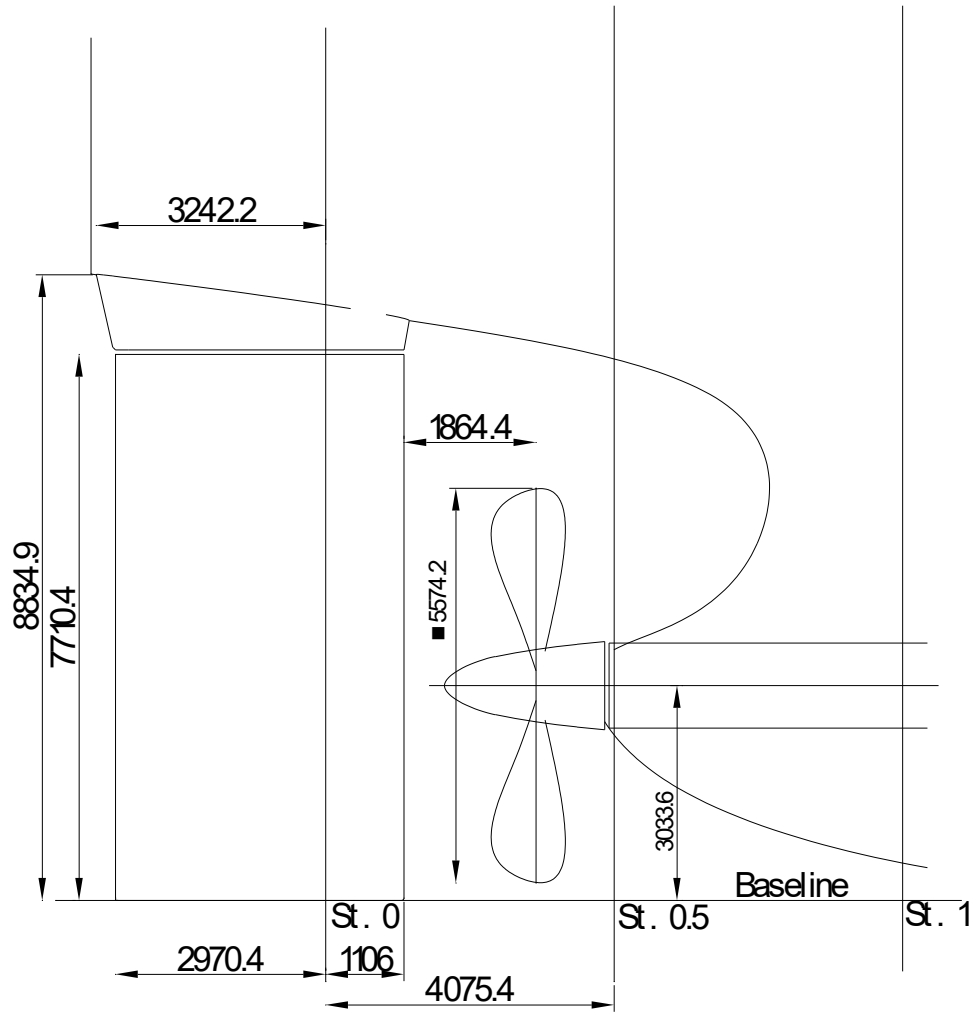

SKEG I, 1 HEADBOX I, 1 RUDDER I, AND PROPELLER MODEL No. S612 FOR SHIP MODEL No. 10129

DIMENSIONS ARE GIVEN IN mm FOR SHIP

Figure F3: Particulars and location of the bilge keels

Station	Distance
End BK	12265
7	12753
8	13114
9	13260
10	13268
11	13172
12	13016
Start BK	12999

DISTANCES ARE MEASURED ALONG THE STATIONS FROM CENTRELINE OF SHIP TO STREAMLINE BILGE KEEL

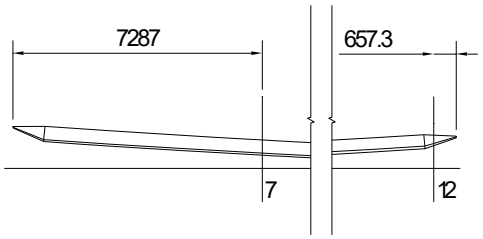

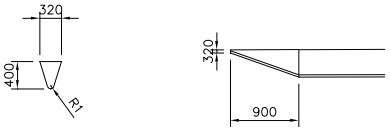

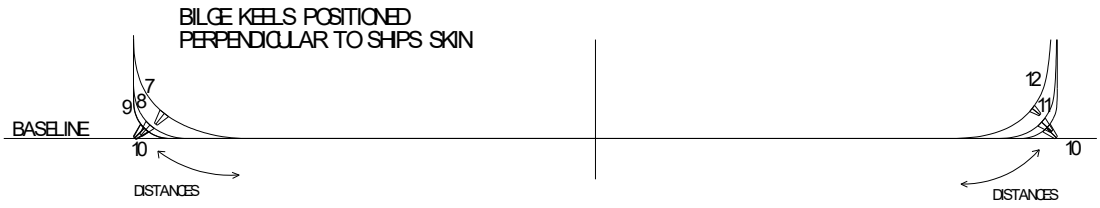

2 BILGE KEELS FOR SHIP MODEL No.10129

DIMENSIONS ARE GIVEN IN mm FOR SHIP

Figure F4: Particulars and location of dagger boards

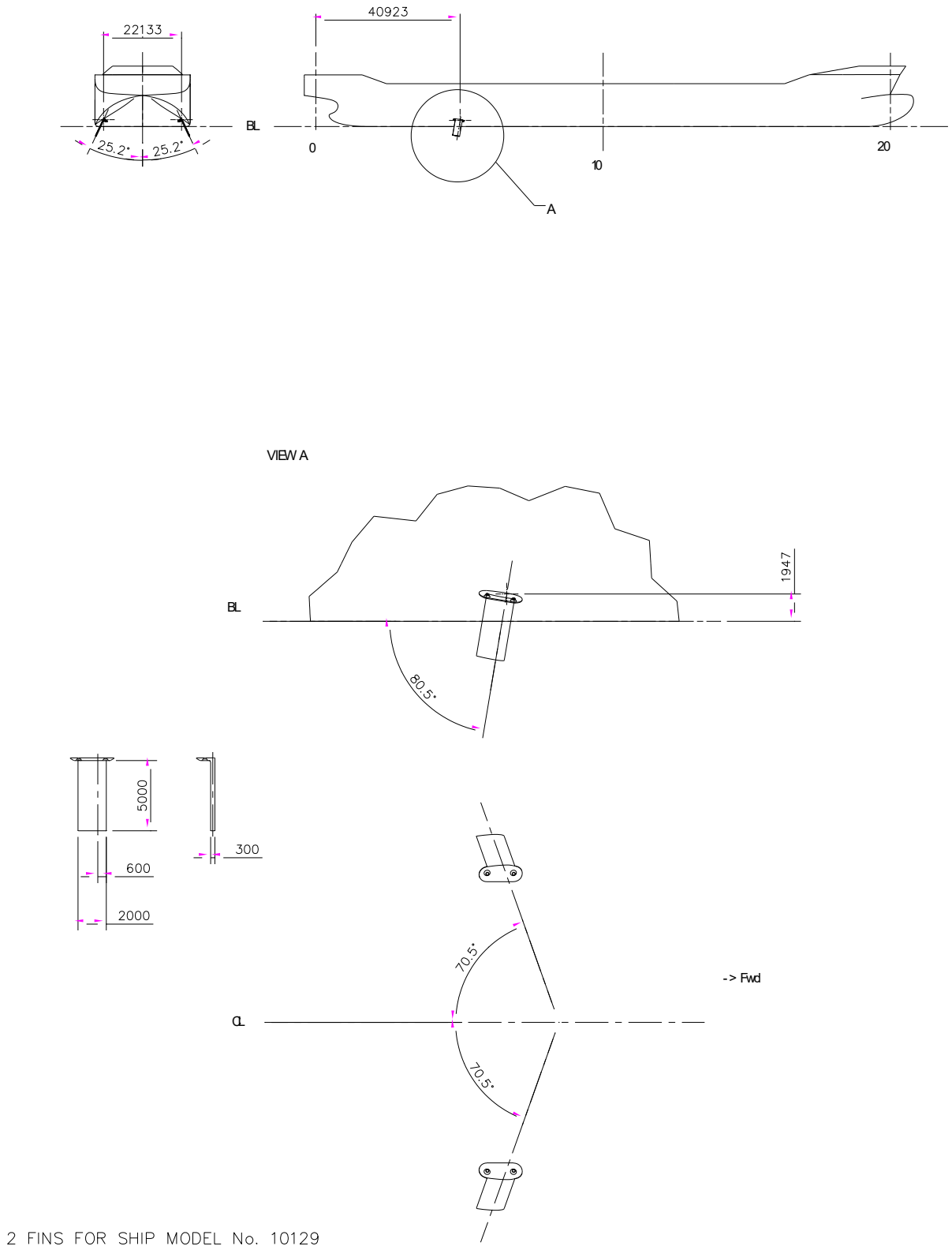

PHOTO PAGES

Photo PH1: Side view of the model

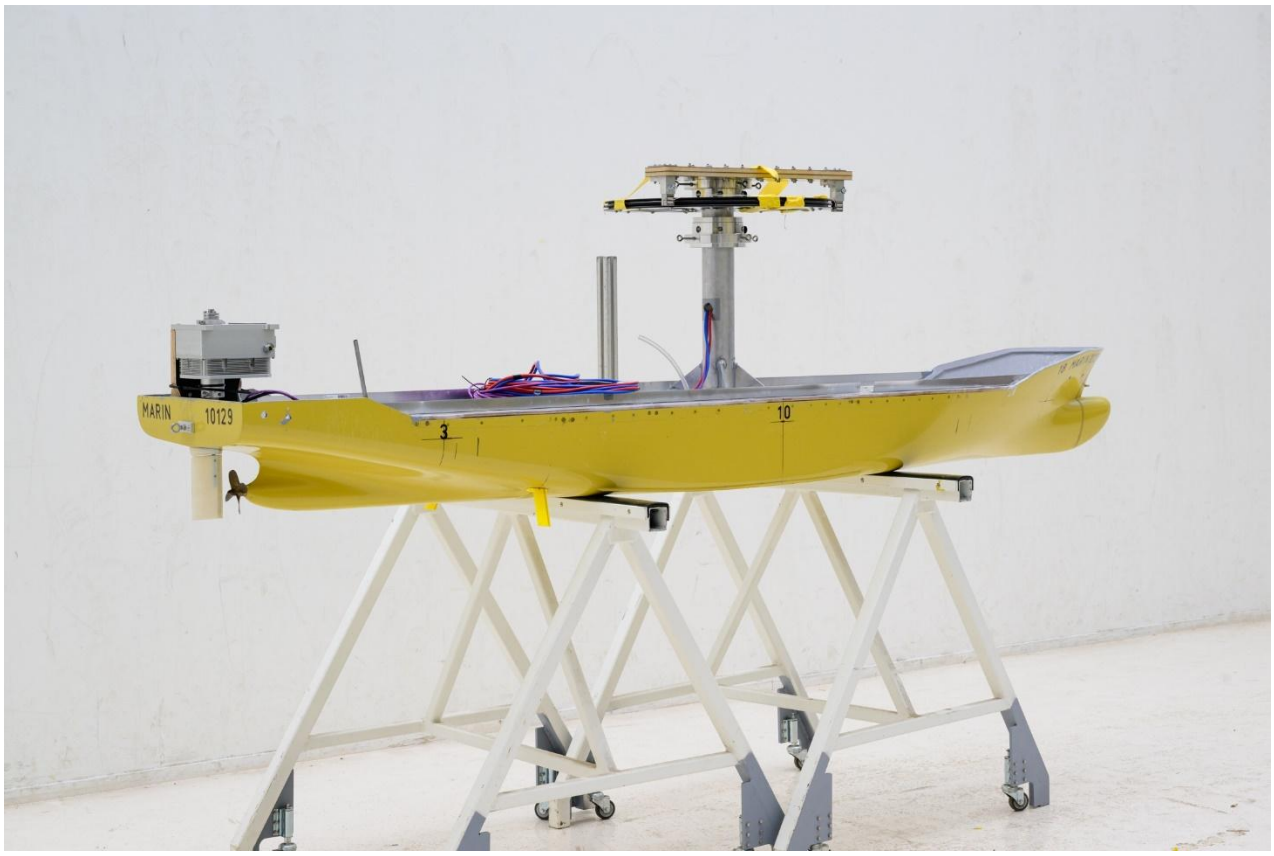

Photo PH2: Side view of the model

Photo PH3: Bow view of the model

Photo PH4: Bow view of the model

Photo PH5: Aft view of the model

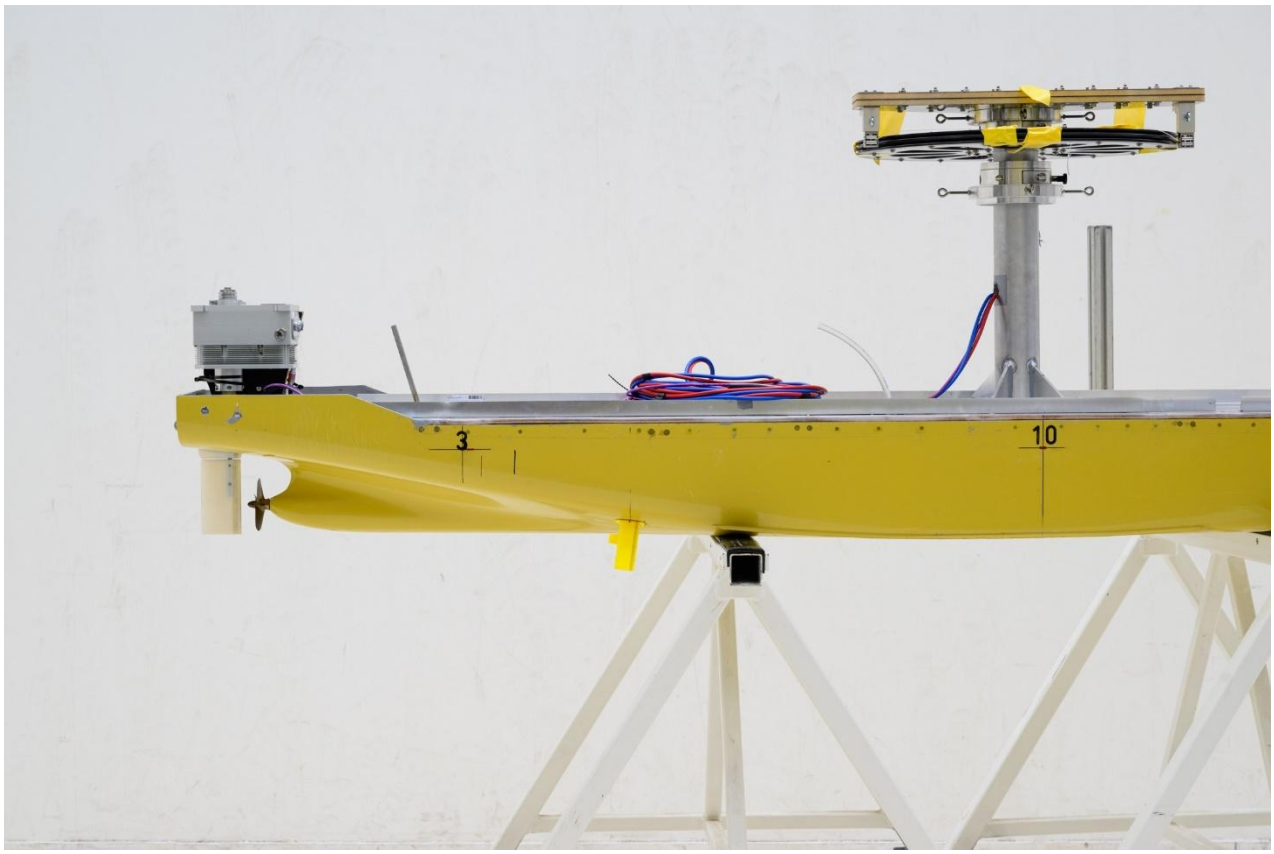

Photo PH6: Aft view of the model

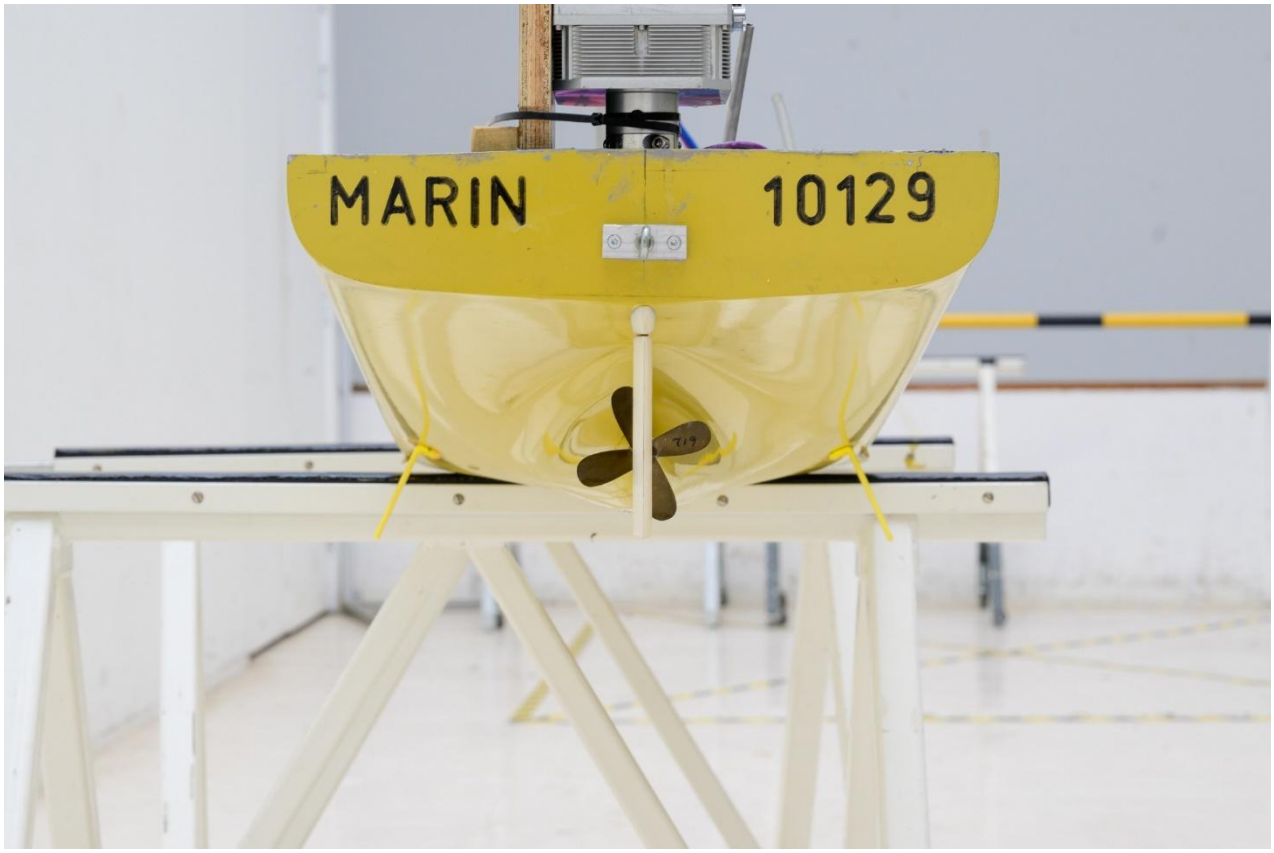

Photo PH7: Details of the rudders and propellers

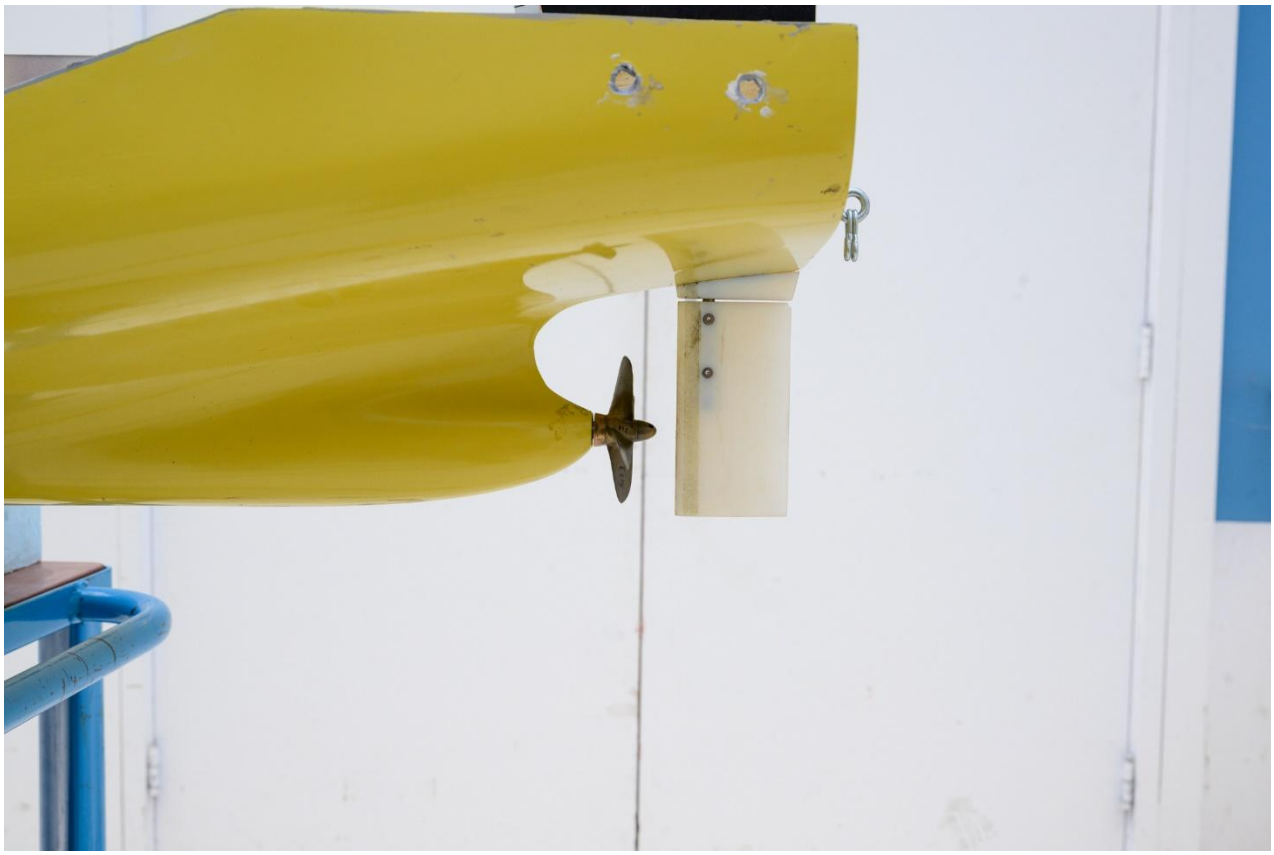

Photo PH8: Details of the rudders and propellers

Photo PH9: Details of the wind mast

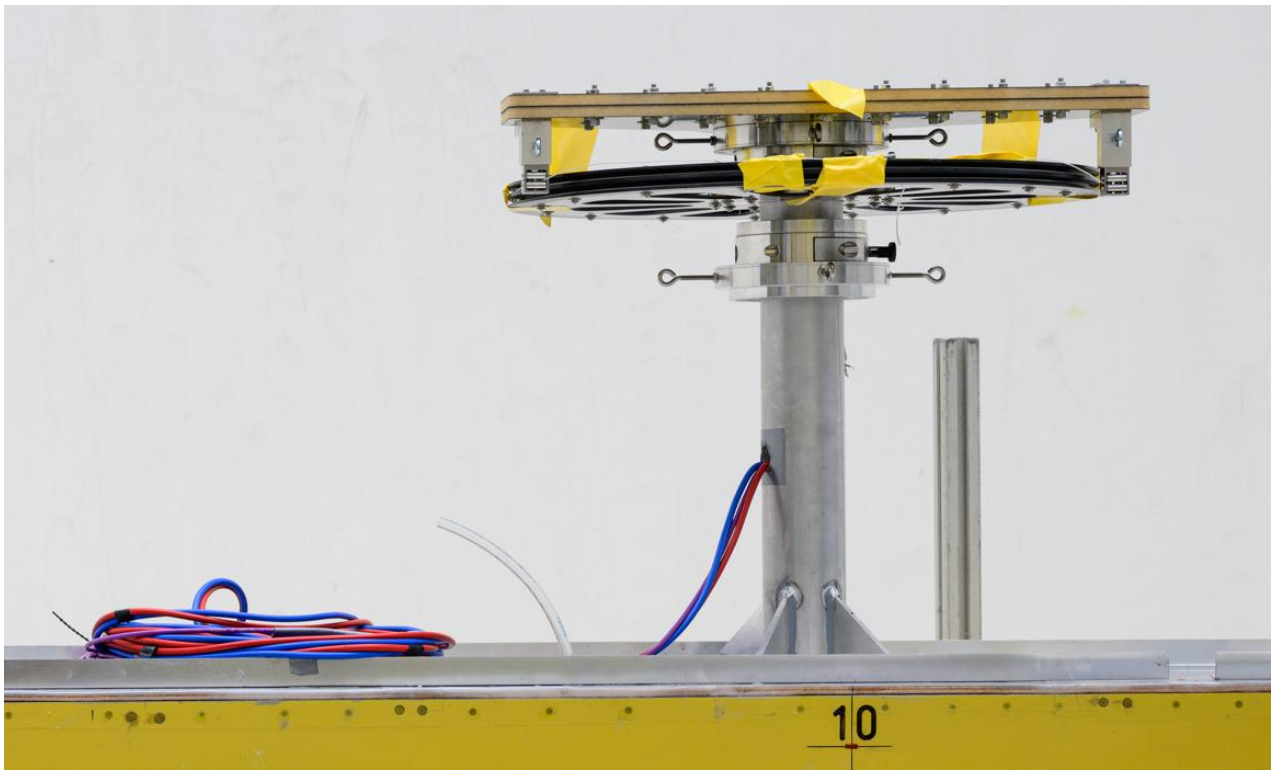

Photo PH10: Details of the dagger boards

APPENDICES

APPENDIX I

WIND-WAVE CLIMATOLOGY AND AREA OF OPERATIONS

Wind statistics

The oldest and simplest way to characterise an offshore environment is to characterise the wind climate, for instance in terms of the frequency of occurrence of various Beaufort numbers. These wind classes are related to area dependent "average" wave conditions. The tables below summarises some commonly used relations.

Example of wave conditions as function of Beaufort number

Beaufort number	Wind velocity		Observed average significant wave height					
	Range	Mean	North Atlantic ocean (Roll[3])		North sea Petri[4])		Fully arisen sea, Bhattacharyya[5] and Komen	
[-]	$U_{\underline{wind}}$ [kn]	U_{wind} [kn]	H_s [m]	T_2 [s]	H_s [m]	T_2 [s]	H_s [m]	H_s [m]
1	1 - 3	2.0						
2	4 - 6	5.0			0.9	5.9	0.15	0.2
3	7 - 10	8.5	1.4	6.3	0.9	4.4	0.40	0.5
4	11 - 16	13.5	1.7	5.8	1.3	4.7	1.00	1.2
5	17 - 21	19.0	2.15	5.8	1.9	5.3	2.01	2.4
6	22 - 27	24.5	2.9	6.4	2.9	6.4	3.20	3.9
7	28 - 33	30.5	3.75	6.9	3.7	6.9	5.15	6.0
8	34 - 40	37.0	4.85	7.6	5.2	8	7.58	8.8
9	41 - 47	44.0	6.2	8.3			10.73	12.6
10	48 - 55	51.5	7.45	8.8			14.73	17.3
11	56 - 63	59.5	8.4	9			19.63	22.9
12	>64							

[3] Roll, H. U., *"Height, length and steepness of Sea waves in the North Atlantic and dimensions of sea waves as functions of wind force"*, Special Publication No. 1 of the Office of Sea-Weather Service, 1953, Translation by Manley St. Denis, Tech. Res. Bull. No. 1-19, The Society of Naval Architects and Marine Engineers, 98 pp, Dec. 1958.

[4] Petri, O, "Statistik der Meereswellen in der Nordsee (auf Grund von Beobachtungen der Bordwetterwarten des Deutschen Wetterdienstes)", Deutscher Wetterdienst Seewetteramt, Einzelvoröff. Nr. 17, Hamburg.1956.

[5] Bhattacharyya R., *"Dynamics of marine vehicles"*, ISBN 0-471-07206-0, 1978.

Sea state definition according to NATO Stanag 4194 Annex D

Sea state Number	Probability	Wind speed		Significant wave height		Peak wave period	
		Range	Mean	Range	Mean	Range	Most probable
[-]	[%]	U_{wind} [kn]	U_{wind} [kn]	H_s [m]	H_s [m]	T_p [s]	T_p [s]
1	0	0 - 6	3.0	0 - 0.1	0.05		
2	7.2	7 - 10	8.5	0.1 - 0.5	0.30	3.3 - 12.8	7.5
3	22.4	11 - 16	13.5	0.5 - 1.25	0.88	5 - 14.8	7.5
4	28.7	17 - 21	19.0	1.25 - 2.5	1.88	6.1 - 15.2	8.8
5	15.5	22 - 27	24.5	2.5 – 4.0	3.25	8.3 - 15.5	9.7
6	18.7	28 - 47	37.5	4. - 6	5.00	9.8 - 16.2	12.4
7	6.1	48 - 55	51.5	6 - 9	7.50	11.8 - 18.5	15
8		56 - 63	59.5	9 - 14	11.50	14.2 - 18.6	16.4
9		>63	>63	>14		15.7 - 23.7	20

Although often used in ship operations this approach fails to recognise the fact that one wind speed can come with a wide range of wave heights and periods, strongly depending on the fetch and duration (or more generally the history) of the wind. Since wind speed and direction are highly variable this means that in practice, the waves are never in equilibrium with the wind.

In the situation of a relatively high wind speed (a “young”, growing wave) most of the energy input will take place at the high frequency tail of the wave spectrum. The result is a short, steep wave.
If the wind speed drops relatively quickly the continuing non-linear transfer of wave energy from shorter to longer wave components as well as frequency segregation (long waves travel faster than short waves) yields swell type wave conditions.

The fact that one wave height can show very different period characteristics has serious consequences because, as will be shown in the following, the motion characteristics of ships strongly depend on the wave period. This implies that wave height statistics only provide a rather narrow basis for design.

Wave scatter diagrams

In the offshore industry, the availability of wave measurements has led to the introduction of so-called scatter diagrams, reflecting the joint statistics of significant wave height and average zero-upcrossing period. Work by BMT (Hogben[6] and BMT[7]) has provided a practical basis for the design of ships.

[6] Hogben, N., Dacuhna, N.M.C. and Olliver, G.F.; “Global Wave Statistics”, BMT, London, 1986.
[7] BMT; PC Global Wave Statistics - User Manual.

Wind speed

The added resistance and total mean environmental loads are the sum of a wind- and a wave- (or motion-) induced component. This means that the joint statistics of wind and waves are of interest. Empirical information used in earlier wave models (Janssen *et al.*[8]), which relates a peak period T_p to the wave height and wind speed v_w at 10 m height, was therefore used to describe average non-stationary wind-wave relations. Their work can be expressed as:

$$T_p = \frac{9.25 \cdot {H_{1/3}}^{0.688}}{{v_w}^{0.376}}$$

Systematic calculations based on this work (accounting for the varying spectral shape) suggest for the zero-upcrossing period the following relation with wind speed:

$$v_w = A \cdot {T_2}^{B} \cdot {H_{1/3}}^{C \cdot {T_2}^{D}}, \text{with: } A = 80.443;\ \mathrm{B} = -1.8421;\ \mathrm{C} = 1.6012 \text{ and } \mathrm{D} = -0.0474$$

v_w in this formulation is the wind speed at 10 m height in m/s, T_2 is the average zero-upcrossing period in seconds as defined in Appendix 3 and $H_{1/3}$ is the significant wave height in metres. The values of the coefficients A to D depend on atmospheric conditions (like stability), where the field data suggest the values given above. Results from these formulations show that high wind speeds occur in combination with short, steep waves.

Although no wind is modelled during the tests in the SMB, the above relation is used in the post-processing to predict the sustained speed including wind added resistance.

Wave spectra

A wave spectrum is characterised by the significant wave height, peak enhancement factor and information on the wave period. The latter can refer to the peak of the spectrum (T_p), the average value from the spectrum (T_1) and the average time between two zero-upcrossings (T_2). Their mutual relations are indicated in the table below for two types of wave spectrum. Details of the statistical description of an irregular sea can be found in Appendix III.

Wave spectral parameters

	JONSWAP	Pierson-Moskowitz / Bretschneider
T_p / T_2	1.287	1.405
T_p / T_1	1.198	1.296
T_1 / T_2	1.072	1.086

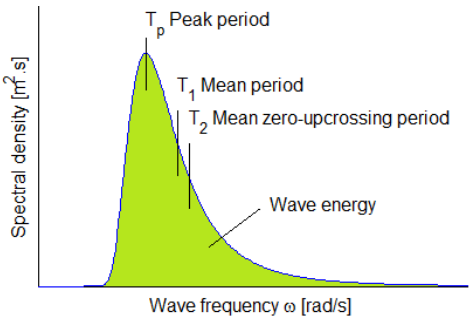

[8] Janssen, P.A.E.M., Komen, G.J. and Voogt, W.J.P.; "An Operational Coupled Hybrid Wave Prediction Model", Journal of Geophysical Research, Vol. 89, pp. 3635-3684, 1984.

APPENDIX II

DATA ANALYSIS

Data scaling

The results of the measurements have been scaled up to full size values according to Froude's law of similitude. In the table below the scaling factors as applied are shown.

Table A2-1: Data scaling table

Quantity	Scaling factor	Model	Prototype
Linear dimensions	λ = 63.2	1 m	63.20 m
Volumes	λ^3 = 252,436	1 dm³	252.44 m³
Mass	$\lambda^3\gamma$ = 258,747	1 kg	259.00 t
Forces	$\lambda^3\gamma$ = 258,747	1 N	2540.8 kN
Angles	1 = 1.00	1 deg	1 deg
Linear velocities	$\lambda^{0.5}$ = 7.95	1 m/s	7.95 m/s
Angular velocities	$\lambda^{-0.5}$ = 0.126	1 deg/s	0.126 deg/s
Linear accelerations	1 = 1.00	1 m/s²	1 m/s²
Angular accelerations	λ^{-1} = 0.016	1 deg/s²	0.016 deg/s²
Time	$\lambda^{0.5}$ = 7.95	1 s	7.95 s

Note: γ is the ratio of the specific mass of seawater to that of the fresh water in the basin, with γ = 1.026. All measured pressures and loads refer to seawater conditions; in fresh water the loads reduce by 2.6%.

Statistical analysis

The statistical analysis performed on the various motions, relative motions, forces and accelerations, and on the wave elevation, is as given on below, based on the following general picture of a record.

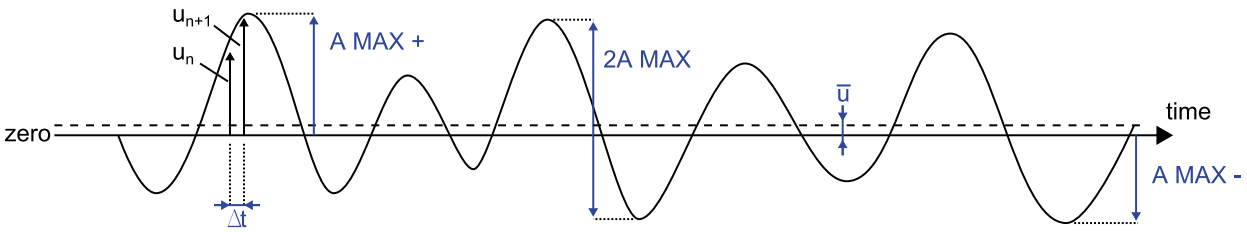

Example of signal record

For the wave elevation the mean equals zero.

1. *Mean value*: $\bar{u}$ (MEAN)

   $\bar{u} = \frac{1}{N}\sum_{n=1}^{N} u_n$ (N is number of samples)

2. *Standard deviation*: σ_u (ST.DEV.)

   $\sigma_u = \sqrt{\frac{1}{N}\sum_{n=1}^{N}(u_n - \bar{u})^2}$

3. *Maximum value*: A MAX +
   Highest crest value, positive unless stated otherwise.

4. *Maximum value*: A MAX -
   Highest trough value, negative unless stated otherwise.

5. *Maximum double amplitude*: 2A MAX
   This is the maximum crest to trough value.

6. *Significant peak value*: A 1/3 +
   This is the mean of the one-third highest zero to crest values, positive unless stated otherwise.

7. *Significant trough value*: A 1/3 -
   This is the mean of the one-third highest zero to trough values, negative unless stated otherwise.

8. *Significant double amplitude*: 2A 1/3
   This is the mean of the one-third highest crest to trough values.

9. *Number of oscillations*: NO
   This is the total number of oscillations in the record.

Response functions in irregular seas

Apart from the statistical analysis, another result of the tests in irregular seas is the spectral density of a signal. The response functions are calculated from the spectral densities in the following way:

$$H_u = \frac{u_a(\omega_e)}{\zeta_a(\omega_e)} = \sqrt{\frac{S_{uu}(\omega_e)}{S_{\zeta\zeta}(\omega_e)}}$$

in which:

H_u	=	response function of a signal u
$u_a(\omega_e)$	=	amplitude at frequency (ω_e) of signal u
$\zeta_a(\omega_e)$	=	amplitude at frequency (ω_e) of wave elevation ζ
$S_{uu}(\omega_e)$	=	spectral density of signal u
$S_{\zeta\zeta}(\omega_e)$	=	spectral density of wave elevation ζ

The frequency ω_e at which these spectral densities and response functions are calculated represents the true frequency of the ship motions. Transformation of ω_e to ω takes place according to:

$$\omega_e = \omega - kV\cos\mu$$

or for deep water:

$$\omega_e = \omega - \frac{\omega^2}{g} V\cos\mu$$

or:

$$\omega = \frac{1 - \sqrt{1 - 4\omega_e \frac{V\cos\mu}{g}}}{2\frac{V\cos\mu}{g}}$$

in which:

ω	=	wave frequency	in rad/s
ω_e	=	frequency of wave encounter	in rad/s
k	=	wave number = $2\pi/\lambda$	in m^{-1}
λ	=	wave length	in m
V	=	speed of ship (to be taken negative when sailing astern)	in m/s
μ	=	heading of the ship	(defined in Section 0)
g	=	acceleration due to gravity	in m/s^2.

After these manipulations, the results are plotted on base of ω, the wave frequency.

Response functions in regular waves

From the tests in regular waves the amplitude of the first harmonic component, the mean value and phase angles were derived. The phase relationship was determined with respect to the wave height at a location in a transverse plane through the CoG. From the amplitudes, RAOs are derived by dividing the motion amplitude by the wave amplitude:

$$\frac{u_a}{\zeta_a} = \frac{\text{motion amplitude}}{\text{wave amplitude}}$$

From the thrust increase as given in the tables, the thrust response function is derived by dividing this thrust increase by the squared wave amplitude:

$$\frac{\Delta T}{\zeta_a^2} = \frac{\text{thrust increase}}{\text{squared wave amplitude}}$$

Natural periods and motion decay tests

Motion decay tests are performed to determine the damping coefficients, damped period and natural period of a vessel or system. Decaying signals are characterised by a decaying oscillation around a mean value, with an approximately constant period. An example of a decaying signal is shown in the figure on the right. It is assumed that the decaying system can be accurately described by the following equation:

$$a\ddot{x} + b(\dot{x}) + cx = 0$$

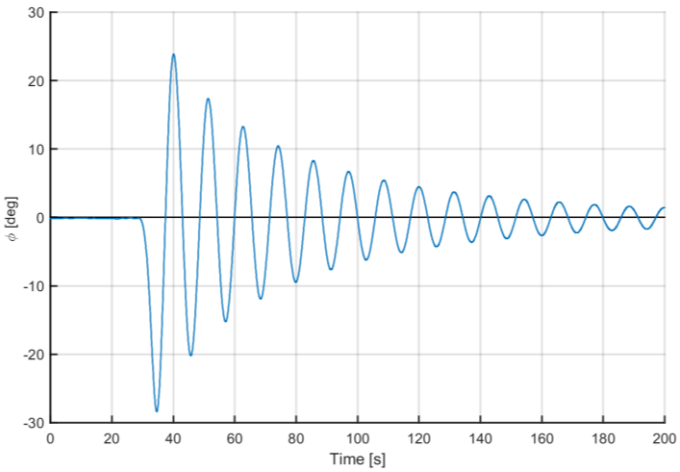

Example time series of decaying roll signal

Where:

x	=	a motion signal (e.g. roll, pitch or heave)
$\dot{x}$	=	the first derivative of the motion signal (e.g. roll velocity)
$\ddot{x}$	=	the second derivative (e.g. roll acceleration)
a	=	the mass or inertia of the vessel (including added mass or added inertia)
c	=	the restoring term of the vessel
b	=	the damping term

The damping is assumed to consist of various terms. The following terms are implemented for analysis at MARIN:

$$b(\dot{x}) = B_1\dot{x} + B_2\dot{x}|\dot{x}| + B_3\dot{x}^3$$

Where:

B_1	=	the linear damping coefficient
B_2	=	the quadratic damping coefficient
B_3	=	the cubic damping coefficient (disregarded within this project)

The system damping can be analysed by three methods. First, it can be solved by inserting the measured motion, velocity and acceleration and solving in a least squared sense. This is called the “least squares fit”. Secondly, a classic “PQ analysis” can be performed. PQ analysis sets out all individual crests and troughs as a function of amplitude and fits a polynomial. The polynomial coefficients are denoted by P and Q (and R in the cubic damping case). Lastly, the motion signal itself can be fit in an optimal sense by varying the relative damping and natural period of the system until an optimum is found. This is called “motion optimised”.

All three methods determine the same damping values, but with different approaches to what is optimal. The classic PQ analysis works very well for lightly damped systems, but has difficulties to provide accurate values for highly damped systems (e.g. ships sailing at speed). The least squares fit and motion optimised methods are closely related. The motion optimised method actually removes the need for fitting velocity and acceleration in the system of equations, which sometimes causes irregularities in the fitting.

In the present report, the damping values resulting from a motion optimised fitting are provided and the cubic damping coefficient is disregarded. From the P and Q polynomial coefficients, the equivalent damping is obtained as:

$$B_{eq} = \frac{P + Q \cdot \phi_{amp}}{2\pi} B_{crit} \qquad \text{With:} \qquad B_{crit} = \frac{2g\Delta GM}{2\pi / T_{\phi}}$$

Where ϕ_{amp} is the roll amplitude for which B_{eq} is linearised, g is the gravity constant, Δ is the ship mass and T_{ϕ} the ship natural period.

More details regarding the analysis of motion decay tests can be found in Appendix IV.

APPENDIX III

MATHEMATICAL DESCRIPTION OF IRREGULAR PHENOMENA

General

A quantity x, varying irregularly in time or space, is called a stochastic variable. The stochastic variables that are most interesting in the field of seakeeping vary in time and can each be described by a distribution function of the probability that x fulfils a certain condition. Examples of such distribution functions are (see Figure A):

1. The probability distribution for the period of time that the value x lies between a and b.
2. The probability distribution of amplitudes of x lying between a and b.

Figure A

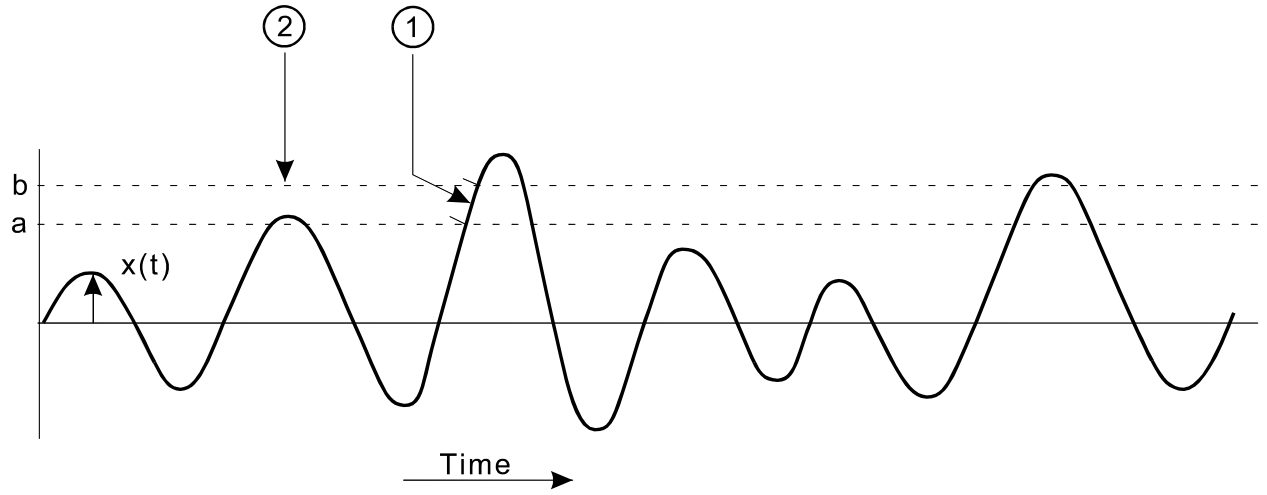

These various descriptions are discussed under the following subheadings. Before doing so, it is necessary to mention a few characteristics to classify random processes.

A process, described by a stochastic variable x, is completely defined if all statistical properties are known, or to be precise, when the expectation values E[x], E[x^2], E[x^3], ... are all known. In general this is not the case.

Processes can be classified by certain properties of their statistics. If for a process all statistical properties are invariant with respect to time shifts, the process is called ***stationary***. This means, for example, that:

$$E[x(t)] = E[x(t+\tau)] \qquad -\infty < \tau < \infty \tag{1}$$

E[x] is the ***mean value*** of x, also denoted by $\bar{x}$.

The statistical properties of a random process can be measured in several ways, depending on the character of the process. For instance, assume a sea with a large number of wave height measuring buoys of the same type, measuring simultaneously. The mean value of the wave elevations is established as the average of the registration of all buoys at time t = t_m. Now, the actual waves at sea are a weakly stationary process.

In the case of long periods of time the expectation values are not time invariant, but for practical purposes the wave elevation (and as a result: ship motions) can be considered as stationary processes.

A stationary process is called ergodic when it is allowed to replace the averaging over space by an averaging over time and to use the registration of one single buoy for the characterisation of the sea state, as described above, or to use one ship model to measure its motions.

Probability distribution of x(t)

The wave elevations are a continuous function of time (see Figure A) and the probability that $a \le x \le b$ is given by the probability density function $p_x(y)$ in such a way that:

$$P[a \le x \le b] = \int_a^b p_x(y)\,dy$$

where:

$$\int_{-\infty}^{\infty} p_x(y)\,dy = 1 \qquad (2)$$

If the process has a normal (Gaussian) distribution the probability density function is:

$$p(x) = \frac{1}{\sigma_x \sqrt{2\pi}} . \exp\left[- \frac{(x - \bar{x})^2}{2\sigma_x^2} \right] \qquad (3)$$

in which:

$\bar{x}$ = E[x], the mean value, and

σ_x = the standard deviation of the process.

The standard deviation is defined as the root of the variance and:

$$\sigma_x^2 = \text{VAR.} = E[x - E[x]]^2 = E[x^2] - (E[x])^2 \qquad (4)$$

Now it is possible to calculate for a normal distributed stochastic variable x the probability that, for instance, $(\bar{x} + \frac{n}{2}\sigma_x) \le x \le (\bar{x} + \frac{n+1}{2}\sigma_x)$ for several values of n. The result is shown in the histogram in Figure B on the next page. Note that the mean value does not necessarily coincide with the point of reference in the measuring system, so in the above definition of a Gaussian distribution x is given relative to $\bar{x}$.

Figure B: Normalised Gaussian distribution

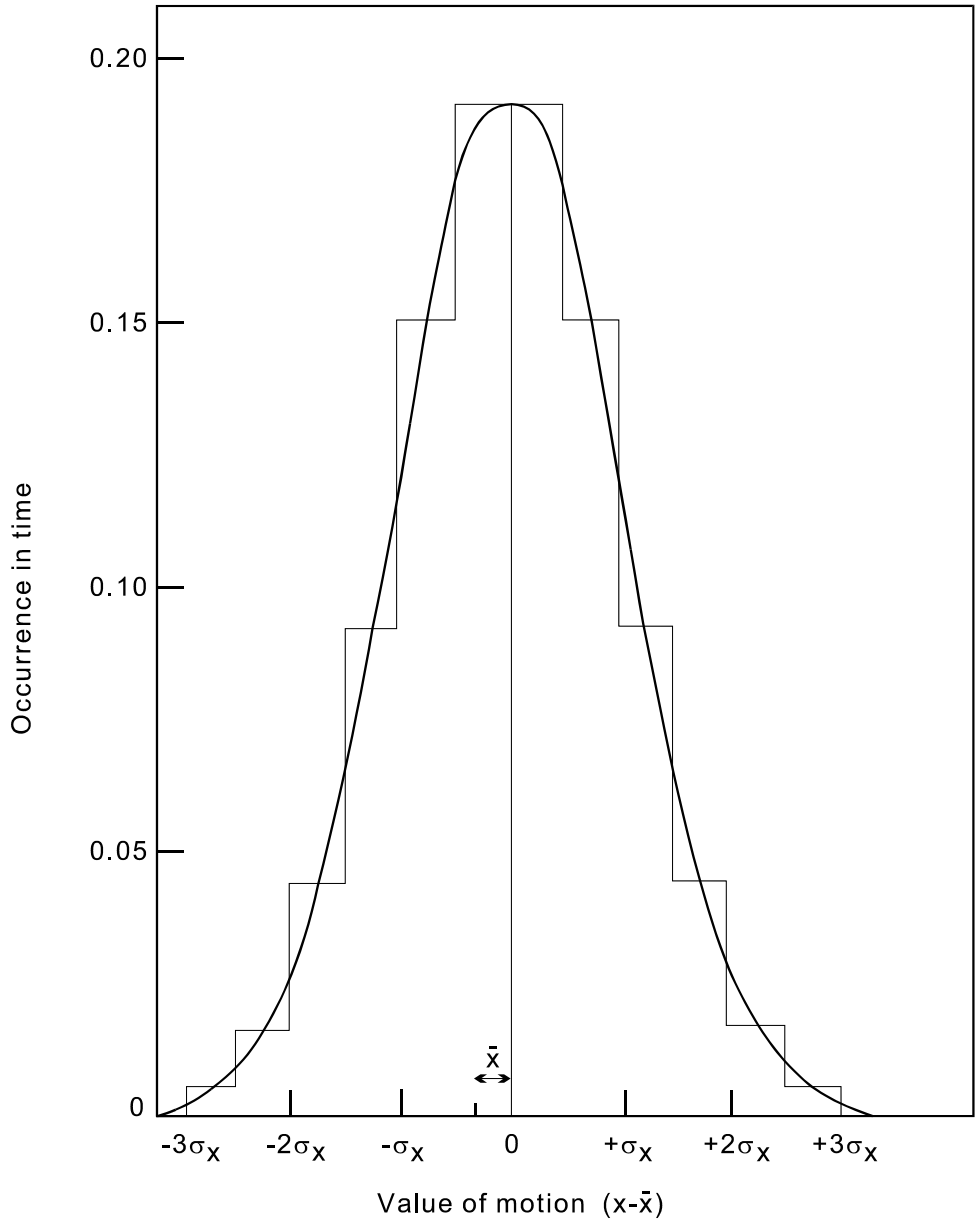

NOTE: width of the columns in the histogram = ½σ_x

σ_x = standard deviation of the variable x

The probability that the value for $(x - \bar{x})$ exceeds a certain level x_m can be expressed as:

$$P[x_m \leq (x - \bar{x}) < \infty] = \int_{x_m + \bar{x}}^{\infty} p_x(y)\, dy \tag{5}$$

Using (3), (4) and (5) the following table gives results for several values of x_m.

x_m	Probability percentage $P[x_m \leq x < \infty]$	Probability percentage $P[-\infty < x \leq x_m]$
$\bar{x} - 3\sigma_x$	99.87	0.13
$\bar{x} - 2\sigma_x$	97.72	2.28
$\bar{x} - 1\sigma_x$	84.10	15.90
$\bar{x} + 1\sigma_x$	15.90	84.10
$\bar{x} + 2\sigma_x$	2.28	97.72
$\bar{x} + 3\sigma_x$	0.13	99.87

Probability distribution of amplitudes of x(t)

Additionally, the stochastic variable x can be described by the distribution of the amplitudes (= peak values) of x. When x has a normal distribution, the amplitudes follow a Rayleigh distribution. As regards these amplitudes, which are the most interesting quantities in the measurement of ship motions, several stochastic quantities can be defined:

when:

xa ≡ the amplitude of $[x - \bar{x}]$, then:

$x_{a1/3}$ ≡ the mean of the highest one-third of the amplitudes of xa, or as it is often called: the significant single amplitude of x;

$2x_{a1/3}$ ≡ mean of the highest one-third of the maximum to minimum values of xa, often called: the significant double amplitude of x.

The most probable maximum value 2xa max. (double amplitude) of the variable x depends on the number of oscillations No, as calculated by Longuet-Higgins[9]).

$$2x_{amax} = 2\sigma_x \sqrt{2\theta} \tag{6}$$

with:

$$\theta = \ln N_o - \ln\left[1 - \frac{1}{2\theta}(1 - e^{-\theta})\right] \tag{7}$$

9) Longuet-Higgins, M.S.; “On the Statistical Distribution of the Heights of Sea Waves”, Journal of Marine Research 1952, Number 3.

For large values of No it can be shown that:

$$2x_{amax.} = 2\sigma_x \sqrt{2 \ln N_o} \tag{8}$$

In actual measurements, the registration of x over a period of time is used. This period of time has to be long enough to give a reliable estimate of the statistical properties of the variable x as well as for the above introduced stochastic variables $xa_{1/3}$ and $2ax_{1/3}$. It is generally accepted to be sufficient when this period corresponds to half an hour real time or includes at least 180 oscillations. Then, the mean value is given by:

$$E[x] = \bar{x} = \frac{1}{T} \int_{t_1}^{t_2} x(t)\, dt \qquad \text{with} \qquad T = t_2 - t_1$$

and the standard deviation is:

$$\sigma_x = \sqrt{\frac{1}{T} \int_{t_1}^{t_2} [x(t) - \bar{x}]^2 \, dt}$$

The observed processes are stationary - or at least weakly stationary - and ergodic. So the above described simplifications for the establishment of $\bar{x}$ and σ_x are allowed. When the duration of the measurement is sufficiently long, the difference between the standard deviation of the sample and the standard deviation of the actual density function can be neglected. The probability functions actually found from sampling an experiment generally conform very well with the theoretical distributions for x-values in the vicinity of $\bar{x}$. Due to the limited sample size the agreement at x-values far from $\bar{x}$ is hard to prove.

Spectral density of x

When the stochastic quantity x, varying irregularly in time t ($0 \leq t < T$ with $T \rightarrow \infty$), is plotted as a function of time and its variations between t and $t + \Delta t$ are bounded for $\Delta t \rightarrow 0$, then x(t) can be represented by an infinite number of harmonic components with arbitrary phase angles:

$$x(t) = x_0 + \sum_{n=1}^{\infty} x_n \cos(\omega_n t + \varepsilon_n) \qquad \text{(Fourier series)} \tag{9}$$

in which:

x_n = the amplitude of harmonic component n
ε_n = phase angle of the n-th component
ω_n = $n\omega_1$ = angular frequency of the n-th harmonic component
ω_1 = $2\pi/T$ (T = measuring time)

and so: $x_o = \bar{x}$ the mean value of x.

Now, suppose there is a stationary, ergodic process, described by the stochastic variable $x_T(t)$ of which the observation takes place over a time interval ($-T < t < T$, $T \rightarrow \infty$), as shown in Figure C.

Figure C

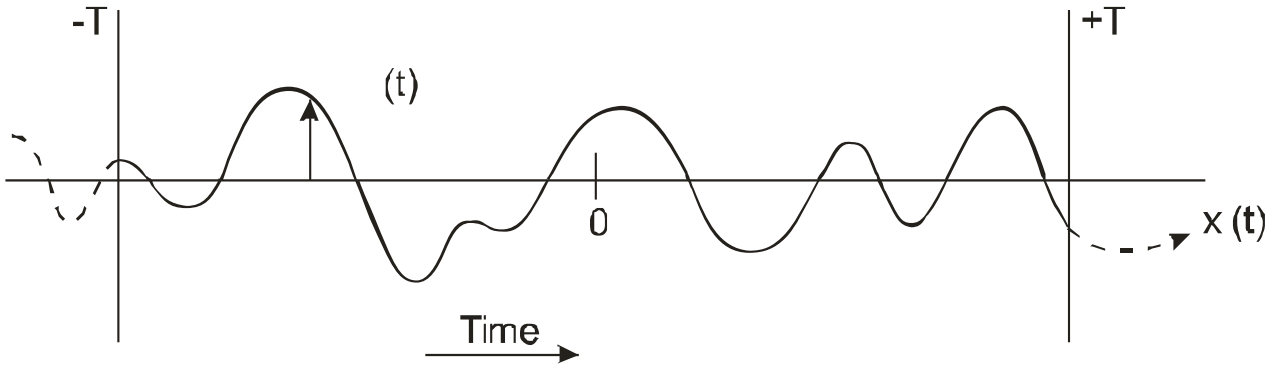

Then the Fourier series can be replaced by the Fourier transformation and the following relations result:

$$X_T(\omega) = \int_{-\infty}^{\infty} x_T(t)\, e^{-i\omega t}\, dt = \int_{-T}^{T} x(t)\, e^{-i\omega t}\, dt \tag{10}$$

$$x_T(t) = \frac{1}{2\pi} \int_{-\infty}^{\infty} X_T(\omega)\, e^{+i\omega t}\, d\omega \quad \text{(inverse Fourier transformation)}$$

The mean value and mean square value (= standard deviation when $\bar{x} = 0$) are defined as follows:

$$\bar{x} = \lim_{T\to\infty} \frac{1}{2T} \int_{-\infty}^{\infty} x_T(t)\, dt = \lim_{T\to\infty} \frac{1}{2T} \int_{-T}^{T} x(t)\, dt \tag{11}$$

$$\bar{M}_x = \lim_{T\to\infty} \frac{1}{2T} \int_{-\infty}^{\infty} \{x_T(t)\}^2\, dt = \lim_{T\to\infty} \frac{1}{2T} \int_{-T}^{T} \{x(t)\}^2\, dt \tag{12}$$

The spectral density function $S_{xx}(\omega)$ of the random process $x_T(t)$ can be proven to be[10]:

$$S_{xx}(\omega) = \lim_{T\to\infty} \frac{1}{2\pi T} |X_T(\omega)|^2 \tag{13}$$

---

10) Therefore use is made of the auto-covariance function $R_{xx}(\tau)$, defined as:
$R_{xx}(\tau) = E[\{x(t) - E[x(t)]\} . \{x(s) - E[x(s)]\}]$

with $\tau = s - t$. In the representation of this section, with $\bar{x} = 0$, is:

$$R_{xx}(\tau) = \lim_{T\to\infty} \frac{1}{2T} \int_{-\infty}^{\infty} x_T(t)\, x_T(t+\tau)\, dt$$

Now, $S_{xx}(\omega)$ is defined as the Fourier transformation of the auto-covariance function:

$$S_{xx}(\omega) = \frac{1}{\pi} \int_{-\infty}^{\infty} R_{xx}(\tau)\, e^{-i\omega\tau}\, dt$$

Using Parceval's theorem on Fourier transformations[11], the mean square can be expressed in terms of frequency:

$$\overline{M}_x = \lim_{T\to\infty} \frac{1}{2T}\left\{\frac{1}{2\pi}\int_{-\infty}^{\infty} |X_T(\omega)|^2 d\omega\right\} = \frac{1}{2}\int_{-\infty}^{\infty} S_{xx}(\omega)\, d\omega \qquad (14)$$

The spectral density function can be related to the energy W which will be clarified in the following discussion. The Fourier transformation $X_T(\omega)$ is the continuous representation of the amplitudes x_n in the Fourier series of $x_T(t)$. Now, the potential energy E_n of the component with frequency ω_n is proportional to $(x_n)^2$ and analogously the potential energy in the frequency range of $\omega_i \le \omega \le \omega_j$ is:

$$W(\omega_i \le \omega \le \omega_j) \_ \int_{\omega_i}^{\omega_j} |X_T(\omega)|^2 d\omega$$

and the average potential energy over a period of time is, using (13):

$$W \sim \lim_{T\to\infty} \frac{1}{T}[W(\omega_i \le \omega \le \omega_j)] = \int_{\omega_i}^{\omega_j} S_{xx}(\omega)\, d\omega \qquad (15)$$

So, the average potential energy of $x_T(t)$, associated with the frequency band $\omega_i \le \omega \le \omega_j$, is given by the integral of $S_{xx}(\omega)$ over the frequency interval and hence $S_{xx}(\omega)$ may be called the ***energy spectral density function.***

The concept of response

Mechanical and physical systems may be interpreted as a transducer transmitting energy from the input x(t) towards the output or response y(t). Suppose the output is uniquely determined in terms of the input: y(t) = L[x(t)], then the system is completely defined if the nature of the operator L is known. The spectral density representation of a stochastic variable allows an output density function $S_{yy}(\omega)$ to the input density $S_{xx}(\omega)$ by means of a frequency response function, provided that the observed system is linear[12].

---

11) This theorem states that:

$$\int_{-\infty}^{\infty} \{x(t)\}^2 dt = \frac{1}{2\pi}\int_{-\infty}^{\infty} |X(\omega)|^2 d\omega$$

12) A system is linear if the response characteristics are additive and homogeneous:
$L[x_1(t) + x_2(t)] = L[x_1(t)] + L[x_2(t)] = y_1(t) + y_2(t)$
$L[ax(t)] = aL[x(t)] = ay(t)$ (a = constant).

Consider the situation where the unit impulse, described by the Dirac delta function[13] $\delta(t - t_0)$, is applied at time $t = t_0$ to a linear system and let $h(t - t_0)$ be the response of the system: $L[\delta(t - t_0)] = h(t - t_0)$. Because such an input-output system is causal, $h(t - t_0)$ does not exist for $t_0 > t$. Now, an arbitrary input $x(t)$ can be expressed as a sum of impulses, that is:

$$x(t) = \int_{-\infty}^{t} x(t_0)\,\delta(t - t_0)\,dt_0 \qquad (16)$$

in which case, assuming that L is time-invariant:

$$y(t) = L[x(t)] = \int_{-\infty}^{t} x(t_0)\,L[\delta(t - t_0)]\,dt_0 = \int_{-\infty}^{t} x(t_0)\,h(t - t_0)\,dt_0 =$$

$$= \int_{0}^{\infty} x(t - \tau)\,h(\tau)\,d\tau$$

where: $t - t_0 = \tau$ was substituted.

For the truncated variables $x_T(t)$ and $y_T(t)$ as used before, with their Fourier transformations $X_T(\omega)$ and $Y_T(\omega)$, it is thus found that:

$$y_T(t) = \int_{0}^{\infty} x_T(t - \tau)\,h(\tau)\,d\tau \qquad (17)$$

and:

$$Y_T(\omega) = \int_{-\infty}^{\infty} e^{-i\omega t}\left[\int_{0}^{\infty} x_T(t - \tau)\,h(\tau)\,d\tau\right]dt$$

$$= \int_{0}^{\infty} h(\tau)\left[\int_{-\infty}^{\infty} e^{-i\omega t}\,x_T(t - \tau)\,dt\right]d\tau$$

---

[13] The Dirac function or “unit impulse function” is an infinitely sharp peak function with the following character:

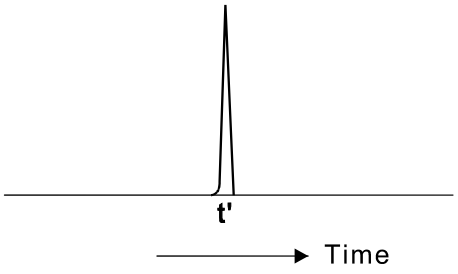

$\delta(t - t') = 0$ for $t \neq t'$

and:

$$\int_{t'-\varepsilon}^{t'+\varepsilon} \delta(t - t')\,dt = 1 \quad \text{for } \varepsilon \to +0$$

and:

$$\int_{-\infty}^{\infty} x(t)\,\delta(t - t')\,dt = x(t').$$

$$= \int_0^\infty h(\tau) \left[\int_{-\infty}^{\infty} x_T(u)\, e^{-i\omega u} du \right] e^{-i\omega\tau}\, d\tau \qquad (18)$$

$$= X_T(\omega) \int_0^\infty h(\tau)\, e^{-i\omega\tau}\, d\tau$$

$$\equiv X_T(\omega)\, H(\omega)$$

in which $u = t - \tau$.

$H(\omega)$ is the Fourier transformation of $h(t)$ and is called the frequency response function. Using the definition for the spectral density function (13), it follows that for real processes $x_T(t)$ and $y_T(t)$:

$$S_{yy}(\omega) = \lim_{T\to\infty} \frac{1}{2\pi T} |Y_T(\omega)|^2 = \lim_{T\to\infty} \frac{1}{2\pi T} |X_T(\omega)|^2 |H(\omega)|^2$$

and thus:

$$S_{yy}(\omega) = S_{xx}(\omega) |H(\omega)|^2 \qquad (19)$$

So, the relation is derived that the output spectral density function is equal to the product of the input spectral density function and the square of the frequency response function.

In a graphic representation:

Figure D

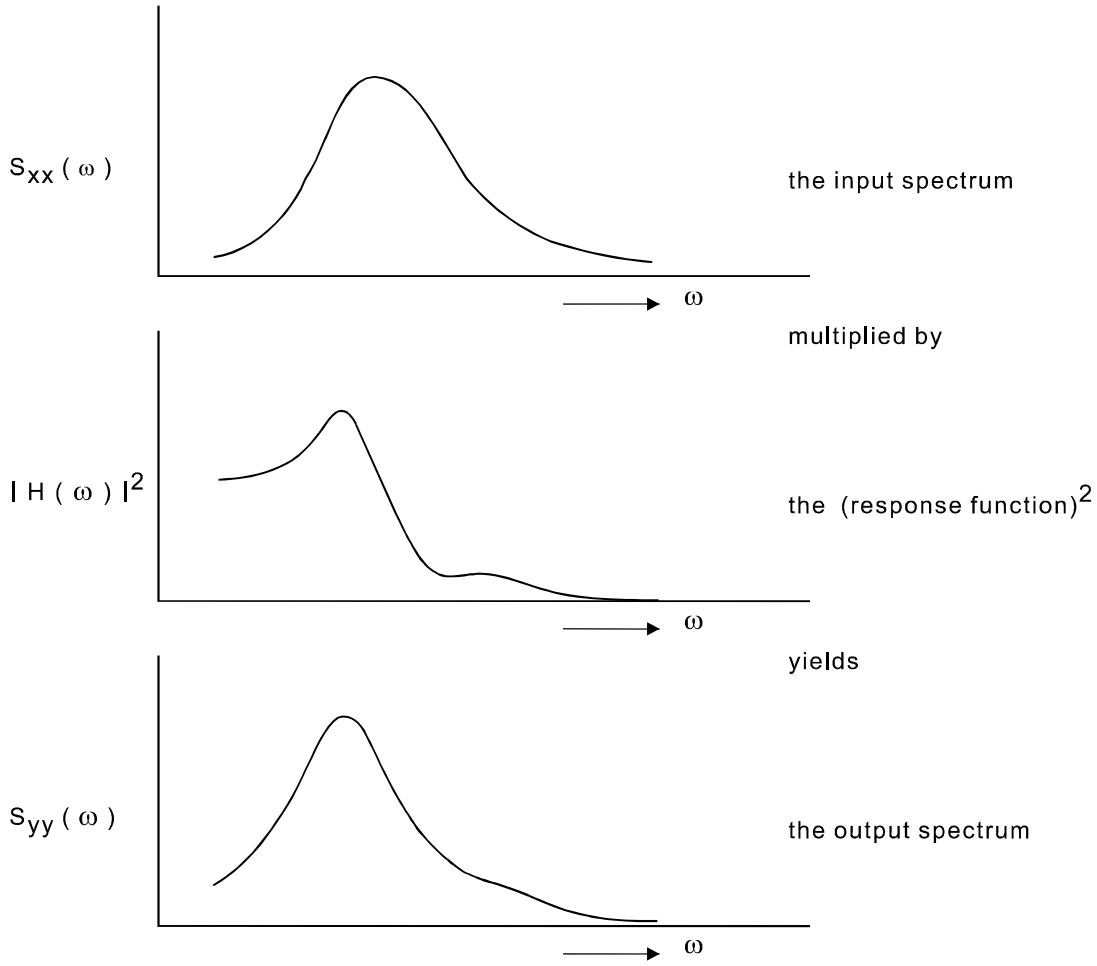

Some relations

The following quantities can now be calculated with use of the spectral density function:

$$m_{x0} = \int_0^\infty S_{xx}(\omega)\, d\omega \tag{20}$$

and

$$m_{x1} = \int_0^\infty S_{xx}(\omega)\, \omega\, d\omega \tag{21}$$

For a stochastic variable x, describing a stationary ergodic process, is:

$$\overline{M}_x = \frac{1}{2} \int_{-\infty}^{\infty} S_{xx}(\omega)\, d\omega \tag{14}$$

When $S_{xx}(\omega)$ is an even, real function and x has a narrow spectrum and zero mean value, it follows that:

$$\bar{M}_x = \int_0^\infty S_{xx}(\omega)\, d\omega = m_{x0}$$ (= area under the spectrum)

and:

$$\sigma_x = \sqrt{\bar{M}_x} = \sqrt{m_{x0}} \qquad (22)$$

$$T_1 = 2\pi \frac{m_{x0}}{m_{x1}} \qquad (23)$$

When x follows a normal distribution, then it can be calculated that:

$$4\sigma_x = 2x_{a1/3} \quad \text{(significant double amplitude)} \qquad (24)$$

Irregularity of waves

Since it is known that the distributions of the wave elevations at sea are approximately normal, all formulae mentioned earlier are valid to describe irregular sea conditions. To judge the behaviour of vessels at sea, irregular seas are assumed to have energy spectral density functions, or power spectra, that can be described by:

$$S_{\zeta\zeta}(\omega) = A \cdot \omega^{-r} \cdot e^{-B \cdot \omega^{-s}} \qquad (25)$$

Formula (25) represents the hypothetical spectra, similar to the Pierson-Moskowitz[14] spectra for fully developed seas, when:

r = 5
s = 4
A = $172.8\ (\zeta_{w1/3})^2\ (T_1)^{-4}$
B = $691.0\ (T_1)^{-4}$

Assuming that the wave height is a random variable with a narrow band normal distribution and zero mean value one arrives at (see also (24) and (23)):

$$\zeta_{w1/3} \simeq 4\sqrt{m_{\zeta 0}}$$

$$T_1 \simeq 2\pi \frac{m_{\zeta 0}}{m_{\zeta 1}}$$

where $\zeta_{w1/3}$ is the significant wave height and T_1 the average wave period.

[14] Pierson, W.J. and Moskowitz, L.; “A proposed Spectral Form for Fully Developed Wind Seas Based on Similarity Theory of S.A. Kitaigorodskii”, Journal of Geophysical Research, Vol. 69, December 1964.

In relating the spectra (25) to observations, the average observed wave height ζ_w is assumed to coincide with the significant wave height $\zeta_{w1/3}$. The average observed period T is assumed to coincide with the average calculated period T_1. So, observed sea conditions can be represented by means of a spectrum, as shown in Figure E, where the observations of H.U. Roll on the North Atlantic Ocean are represented in Pierson-Moskowitz spectra.

Figure E

PIERSON-MOSKOWITZ SPECTRA
(s = 4) and (r = 5)
Significant wave height $\zeta_{w1/3}$ and average period T_1
according to Roll for the North Atlantic Ocean
$T_1 = 2\pi\ (m_{\zeta 0}/m_{\zeta 1})$

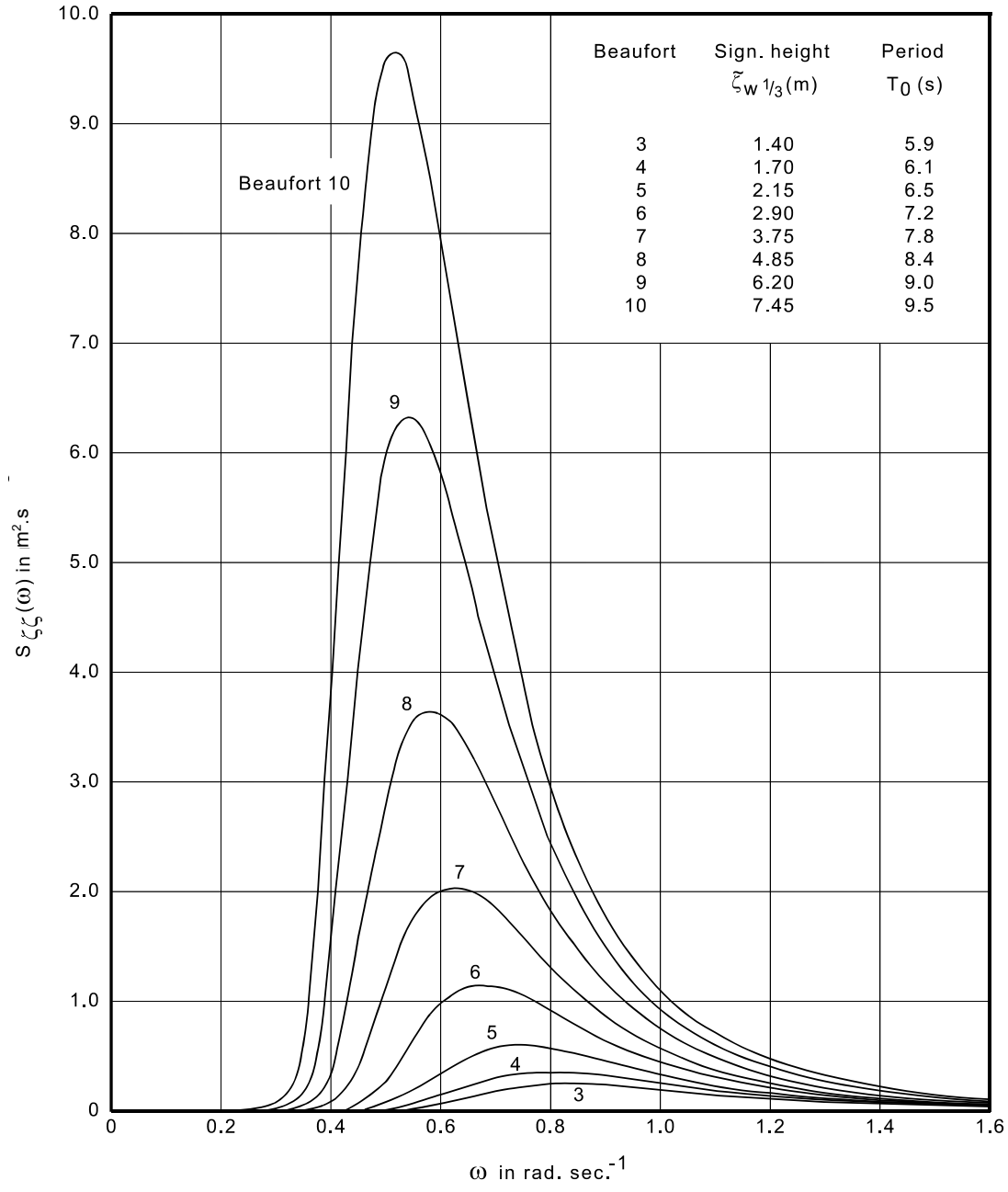

Irregularity of waves

Since it is known that the distributions of the wave elevations at sea are approximately normal, all formulae mentioned earlier are valid to describe irregular sea conditions. To judge the behaviour of vessels at sea, irregular seas are assumed to have energy spectral density functions, or power spectra, that can be described by the JONSWAP[15] formula:

$$S_{\zeta\zeta}(\omega) = \alpha . g^2 . \omega^{-5} . \exp\left[-1.25(\omega/\omega_0)^{-4}\right] . \gamma^{\exp\left[-(\omega-\omega_0)^2/(2\sigma^2.\omega_0^2)\right]} \qquad (26)$$

$$\sigma = \begin{cases} \sigma_a \text{ for } \omega \leq \omega_0 \\ \sigma_b \text{ for } \omega > \omega_0 \end{cases}$$

in which:

ω	=	circular frequency
ω_0	=	spectral peak frequency
g	=	acceleration due to gravity

The dimensionless shape parameters α, γ, σ_a and σ_b are generally taken as:

$\alpha = 0.0989$; $\gamma = 3.3$; $\sigma_a = 0.07$; $\sigma_b = 0.09$

Assuming that the wave height is a random variable with a narrow band normal distribution and zero mean value one arrives at (see also (24) and (23)):

$$\zeta_{w1/3} \simeq 4\sqrt{m_{\zeta 0}}$$

$$T_1 \simeq 2\pi \frac{m_{\zeta 0}}{m_{\zeta 1}}$$

where $\zeta_{w1/3}$ is the significant wave height and T_1 the average wave period.

In relating the spectra (26) to observations, the average observed wave height ζ_w is assumed to coincide with the significant wave height $\zeta_{w1/3}$. The average observed period T is assumed to coincide with the average calculated period T_1. So, observed sea conditions can be represented by means of a spectrum, as shown in Figure F, for a range of Beaufort numbers.

[15] Hasselman, K. et al.; “Measurement of Wind-Wave Growth and Swell Decay During the Joint North Sea Wave Project (JONSWAP)”, Deutsches Hydrographisches Institut Hamburg, 1973.

NOTE: The relation between the average period T_1 and the peak period T_0 for the JONSWAP type spectra is $T_0/T_1 = 1.20$.

Figure F

JONSWAP SPECTRA

Significant wave height $\zeta_{w1/3}$ and peak period T_0
according to Roll for the North Atlantic Ocean

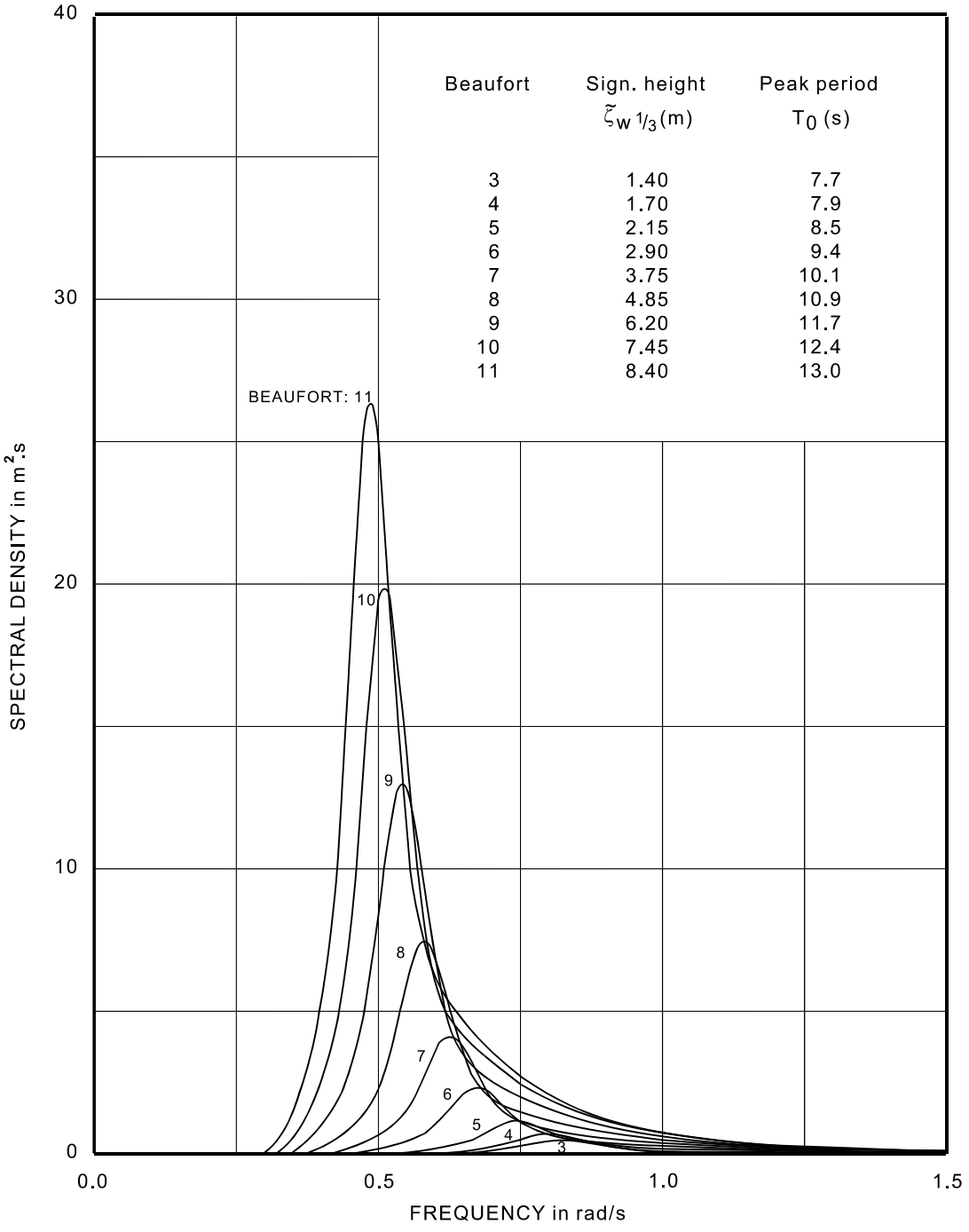

APPENDIX IV

DECAY TESTS, DETERMINING DAMPING AND PERIODICITY

Decay/free extinction tests are performed to determine the damping coefficients, damped period and natural period of a vessel or system. Decaying signals are characterised by a decaying oscillation around a mean value, with an approximately constant period. An example of a decaying signal is shown below:

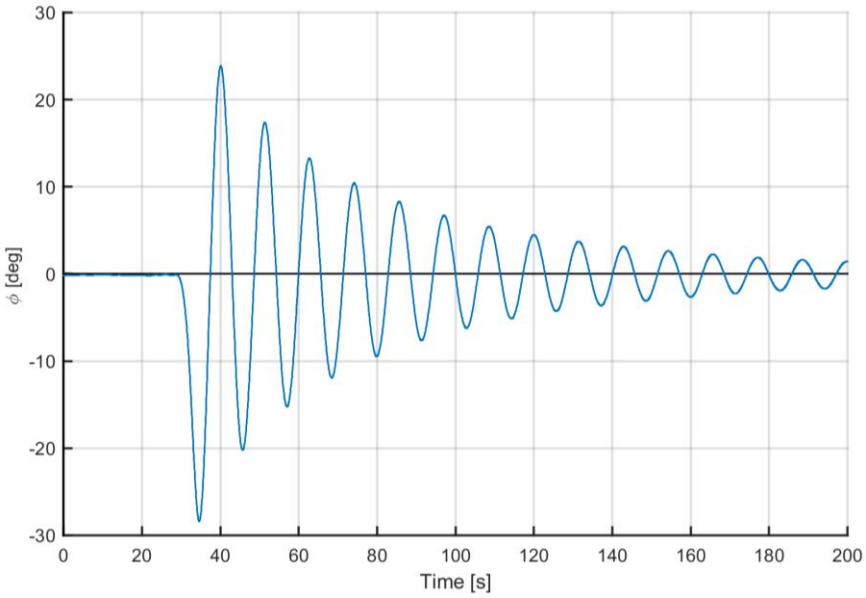

Time series of decaying roll signal

It is assumed that the decaying system can be accurately described by the following equation:

$$a\ddot{x} + b(\dot{x}) + cx = 0 \tag{1}$$

Where:

x	=	a motion signal (e.g. roll, pitch or heave)
$\dot{x}$	=	the first derivative of the motion signal (e.g. roll velocity)
$\ddot{x}$	=	the second derivative (e.g. roll acceleration)
a	=	the mass or inertia of the vessel (including added mass or added inertia)
c	=	the restoring term of the vessel
$b()$	=	the damping function

The damping function can have various terms. The following terms are implemented for analysis at MARIN:

$$b(\dot{x}) = B_1\dot{x} + B_2\dot{x}|\dot{x}| + B_3\dot{x}^3 \tag{2}$$

Where:

B_1	=	the linear damping coefficient
B_2	=	the quadratic damping coefficient
B_3	=	the cubic damping coefficient

Solving only for B_1 is called the “first order solution”, solving for B_1 and B_2 is called the “second order solution” and solving for B_1, B_2 and B_3 is called the “third order solution”. In very rare cases B_1 and B_3 can be determined while leaving B_2 zero. This is called the “13 order solution”. Usually the second order solution is used. Only when a damping test clearly shows cubic behaviour is the third term determined as well.

Analysis of a motion signal alone does not provide absolute damping coefficients; it only provides relative damping coefficients in the form B/c. An absolute value of c has to be provided before an absolute value of B can be found. As an example, c can be defined as $g\Delta GM$ for a roll decay.

The relative damping can be analysed by three methods. First, Equation 1 can be solved by inserting the measured motion, velocity and acceleration and solving in a least squared sense. This is called the “least squares fit”. Secondly, classic “PQ analysis” can be performed. PQ analysis sets out all individual crests and troughs as a function of amplitude and fits a polynomial through. The polynomial coefficients are denoted by P and Q (and R in the cubic damping case). Lastly, the motion signal itself can be fit in an optimal sense by varying the relative damping and natural period of the system until an optimum is found. This is called “motion optimised”.

All three methods determine the same relative damping values, but with different approaches to what is optimal. The classic PQ analysis works very well for lightly damped systems, but has difficulties to provide accurate values for highly damped systems (e.g. ships sailing at speed). The least squares fit and motion optimised methods are closely related. The motion optimised method actually removes the need for fitting velocity and acceleration in the system of equations, which sometimes caused irregularities in the fitting.

The decay analysis results can be verified using a PQ-diagram, a recalculation of the time series and via a plot of the damped period per oscillation.

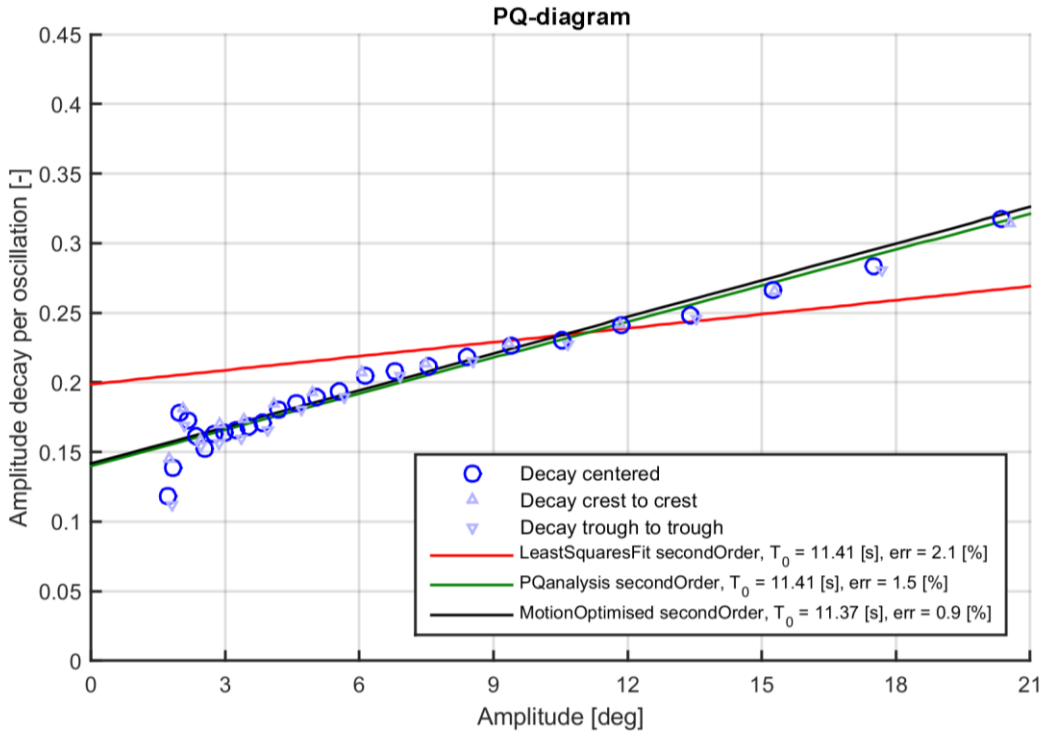

Example of a PQ-diagram showing all three methods

The PQ-diagram shows the decay of the crests and troughs in three ways. “Decay centred” shows the amplitude decay calculated as the difference between two consecutive crest-trough differences or trough-crest differences. This method is not sensitive to offsets in the signal. These values are also used in the PQ analysis method. The “crest to crest” and “trough to trough” decays are provided to indicate offsets and other irregularities in the signal. Ideally all three should coincide. In this case the second order results of all three fitting methods are indicated. Normally the best fitting method is used and the others are not shown.

The damping coefficients B_1, B_2, B_3 and P, Q, R values translate into one another as follows; see also “Slingergedrag van Schepen” door Ir J.J.W. van der Vegt, “KIVI-zeegangsdag”, March 1 1984:

$$\begin{aligned} \frac{B_1}{c} &= \frac{PT_0}{2\pi^2} \\ \frac{B_2}{c} &= \frac{3QT_0^2}{32\pi^2} \\ \frac{B_3}{c} &= \frac{RT_0^3}{6\pi^4} \end{aligned} \tag{3}$$

Where:

P, Q and R are the zeroth, first and second order polynomial components of the fit of crest and trough decay

T_0 is the natural or undamped period of the system

Ideally the natural period can be expressed as:

$$T_0 = 2\pi\sqrt{\frac{a}{c}} \tag{4}$$

The damped period T_d is the observed period and can change slightly with oscillation amplitude. In the case of an ideal linear damped system the damped and natural periods are related via:

$$\begin{aligned} T_0 &= T_d\sqrt{1-\zeta^2} \\ \zeta &= \frac{B_1}{2\sqrt{ac}} \end{aligned} \tag{5}$$

Where:

ζ = the damping ratio

T_d and hence T_0 is (initially) determined from the mean crossings of the signal; however, it is further optimised when the motion optimised method is used.

The error mentioned in the legend of the PQ-diagram is actually the error function used in the motion optimised method, which is the L2-norm of the difference between the measured motion and the recalculated motion after fitting. An example of the recalculation is shown in the next figure:

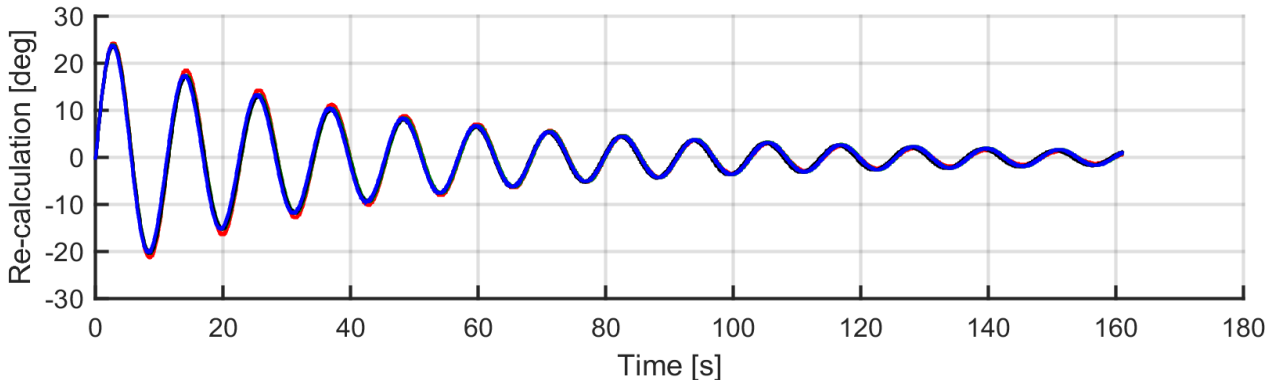

Example of a recalculation showing all three methods; the original signal is shown in blue

The recalculation diagram can be used to check whether the periods found and damping actually match with the measured signal. In this case the red line of the least square fit method shows too little damping at the beginning of the time series at large oscillation amplitudes and somewhat too much damping at the end of the time series. This was also indicated in the PQ-diagram. The other methods fit relatively accurate to the measured data.

The behaviour of the damped period is shown as a function of the number of oscillations as shown below:

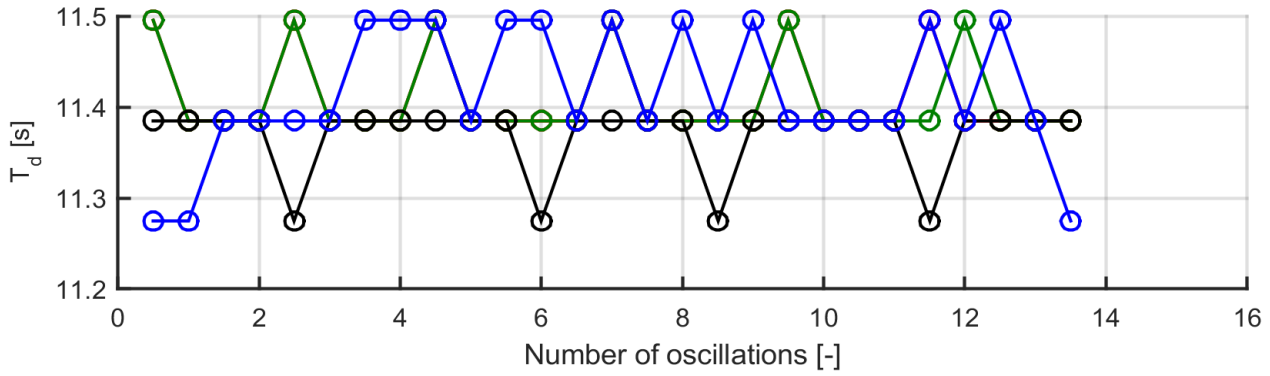

Example of a period overview; the original signal is shown in blue

This plot can be used to check for errors in the mean crossings (e.g. when a poorly conditioned signal has erratic mean crossings the average period estimate will be too small). In this case both the original signal and the three methods are in agreement and show a very constant damped period.

APPENDIX V

EXTRAPOLATION PROCEDURE

Extrapolation of resistance and propulsion test results according to the MARIN form factor method

This MARIN method of extrapolation of resistance and propulsion tests is based on the form factor concept. Accordingly the resistance is scaled under the assumption that the viscous resistance of the ship and its model is proportional to the frictional resistance of a flat plate of the same length and wetted surface area when towed at the same speed. Furthermore, it is assumed that the pressure resistance due to wave generation, stable separation and induced drag from non-streamlined or misaligned appendages is free of scale effects and follows Froude's similarity rule. The proportionality factor between the viscous resistance and the flat plate drag is called the form factor (1+k). This factor is supposed to be determined for each individual hull form from low speed resistance or propulsion measurements where the wave resistance components are supposed to vanish according to a certain rule:

$$1 + k = \lim_{F_n \to 0} \frac{R}{R_F}$$ (1+k from resistance test)

Or

$$1 + k = \lim_{F_n \to 0} \frac{F - T/(\partial T/\partial F)}{(F_{T=0}/R) R_F}$$ (1+k from propulsion test)

(For $(F_{T=0} / R)$ the average statistical value of 1.02 is generally used; $\partial T/\partial F$ is determined in a load variation test).

The form factor as determined from the low speed measurements can be used in the extrapolation only if scale independent pressure resistance is absent in this configuration (no immersed transom, flow oriented, slender appendages). Otherwise a lower 1+k value is chosen for extrapolation. The form factor is supposed to be independent of speed and scale in the extrapolation method. The method supposes appendages fitted to the ship model and assumes turbulent flow over the hull and appendage surfaces. The flat plate resistance is determined by the formula:

$$R_F = \tfrac{1}{2} \rho V^2 S C_F$$

where the coefficients of frictional resistance C_F are determined by one of the following two methods:

- the ITTC-1957 formula for model-ship correlation:
  $C_F = \frac{0.075}{(\log_{10} R_n - 2)^2}$

- Grigson's friction line (23rd ITTC 2002: propulsion committee):
  $C_{F-Grigson} = C_{F-ITTC'57} \times G$

The following values of G (the ratio of Grigson's friction line to that of the ITTC 1957) are used:

Reynolds number	G ($C_f/C_{f\text{-ITTC}}$)
1.0 E+06	0.92454
1.5 E+06	0.92836
2.0 E+06	0.93305
2.5 E+06	0.93777
3.0 E+06	0.94226
5.0 E+06	0.95725
1.0 E+07	0.98042
2.0 E+07	1.00256
5.0 E+07	1.02532
1.0 E+08	1.03685
2.0 E+08	1.04453
3.0 E+08	1.04780
5.0 E+08	1.05116
1.0 E+09	1.05497
2.0 E+09	1.05843
4.0 E+09	1.06168
6.0 E+09	1.06347

The scale effect on the resistance of the hull and appendages (F_D) is determined from:

$$F_D = {}^1\!/_2\ \rho_m\, V_m^2\, S_m((1+k)(C_{Fm} - C_{Fs}) - C_A)$$

where S is the total wetted surface area, C_F is the coefficient of frictional resistance according to the specific line, 1+k the form factor relative to this line and C_A is the incremental resistance coefficient for model-ship correlation.

The C_A-value mostly contains the following items:

- The empirical/statistical relation according to Holtrop-Mennen is often used as the basic C_A value in relation with the ITTC-1957 line with form factor:

  C_A-basic = $0.006\ (L+100)^{-0.16} - 0.00205$

  A similar relation is used for the basic C_A value in combination with the Grigson friction line:

  C_A-basic = $0.0058\ (L+100)^{-0.16} - 0.00196$

  It has to be noted that the difference in C_A-basic values between ITTC-1957 and Grigson, does not only reflect the difference in friction line, but also other elements in the extrapolation method that have been updated over time (such as propeller scale effects).
  This basic C_A value is valid for normal (conventional) displacement vessels at the design draught. This C_A value incorporates the still-air drag of the hull and superstructures of common type ships.

Additional allowances can be added for the following situations:

- for full hull forms at small ballast draughts.
- for appendages not present on model scale (e.g. bilge keels, bow thruster tunnels, etc.).
- for the additional air resistance of exceptional superstructure size and/or shape.
- for the presence (or absence) of deck load.
- for a hull roughness better/worse than standard (= 125-150 μm AHR).
- for specific experience with previous ships.
- for predictions for "contract" environmental circumstances other than (ideal) trial conditions.

Since the C_A value according to these rules reflects the true average, involving a 50 per cent probability that the actual ship's speed will be less than predicted, a small additional allowance is usually added to the C_A value to be at the conservative side.

The various ΔC_A components can be calculated by the following formula:

$\Delta C_A = R_{comp} / (½ \rho V^2 S)$

where R_{comp} is the (extra) resistance of each component at the speed of interest.

If complex propulsors are being tested additional scale effect contributions, which depend on the loading of the propulsor, may be accounted for. If relevant, these are explained in a separate appendix to this report.

The required full scale thrust is determined from:

$T_s = T_m \lambda^3 \rho_s / \rho_m$

thus assuming that there is no scale effect on the thrust deduction.
The measured relation between the thrust coefficient K_T and the apparent advance coefficient J_V is corrected for scale effects on the entrance velocity of the propeller(s) (wake) and for the scale effects on the propeller blade friction. These scale effects are accounted for in the following way:

$K_{Tm} = f_1 (J_V)_m$ (relation measured on model scale)

$K_{Ts} = f_1 (J_v * (Va/V_s / Va/V_m)) + \Delta K_T$ (ship)

Here $(V_A/V)_s / (V_A/V)_m$ is the scale effect on the entrance velocity of the propulsor and ΔK_T is the contribution of the scale effect on the propeller blade friction to the thrust coefficient.
The measured relation between the torque coefficient K_Q and the apparent advance coefficient J_V is corrected for the scale effects on the propeller blade friction:

$K_{Qm} = f_2 (J_V)_m$ (relation measured on model scale)

$K_{Qs} = f_2 (J_v * (Va/V_s / Va/V_m)) + \Delta K_Q$ (ship)

The scale effect corrections ΔK_T and ΔK_Q are determined by the Brard-Aucher-Lindgren method which has been incorporated in the ITTC-1978 method as well. Here the corrections are applied not to the open water test results, but to the K_T - K_Q - relation measured in the behind condition.
As to the scale effect on the entrance velocity (wake) $(V_A/V)_s / (V_A/V)_m$ statistical data are generally used, e.g. those according to Holtrop-Mennen.

Typical values for $(V_A/V)_s$ / $(V_A/V)_m$ are:

Type of ship	$(V_A/V)_s$ / $(V_A/V)_m$
Multiple screw ships	1.01
Slender single screw ships	1.03 - 1.08
Full single screw ships, loaded	1.10 - 1.25
Full single screw ships, ballast	1.15 - 1.35

By interpolation in the scaled-up relation between K_T, J_V and K_Q, using the required thrust from which $(K_T / J_V^2)_s$ is calculated, the propeller rotation rate and the full size delivered power are found for each speed. The required shaft power P_S is found from the delivered power P_D from:

$P_S = P_D / 0.99$

thus assuming a shafting efficiency of $\eta_S = 0.99$.

APPENDIX VI

FUNDAMENTALS OF A ROTOR SAIL

The Flettner rotor is a cylinder that is mechanically rotated continuously to induce the Magnus effect. In good circumstances, a relatively small amount of (electrical) energy is used in comparison to the delivered power due the aerodynamic thrust of the rotor.

Due to the rotation of the cylinder, the air flow in the boundary layer has a circumferential speed affecting the surrounding air flow around the cylinder. On one side, the rotation of the cylinder is in direction of the flow, and this results in a higher flow velocity on this side. The higher flow velocity causes a low pressure. Similarly, on the side the circumferential speed is opposite to the flow direction. This gives a lower relative speed compared to the free stream velocity, inducing a high pressure on this side. The overall flow is visualised in the figure below, which shows the relative velocity and streamlines of a 2D slice obtained from a 3D CFD calculation. It also shows the direction of the lift and drag vectors.

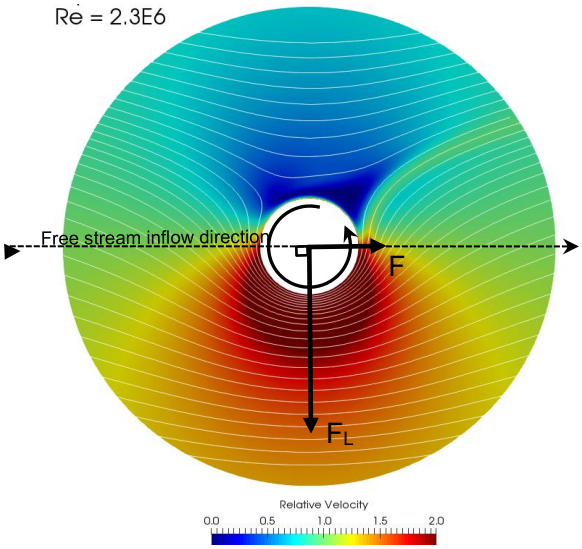

A two-dimensional view of the working mechanism showing the relative velocity and streamlines of a Flettner rotor and presenting the direction of lift and drag forces by vectors.

The Flettner rotor forces are calculated by a relation between spin ratio, CL and CD based on a stand-alone rotor without modelling interactions between the multiple rotors.

The lift is defined as the force perpendicular to the free stream flow, V_∞ or AWS. The drag is defined as the force parallel and in direction of the flow. It is common to express the lift and drag as non-dimensional parameters as defined in (A6-1) and (A6-2), respectively. In this way, the lift and drag of different type and size of wind propulsors can be compared and modelled.

$$C_L = \frac{F_L}{0.5 \cdot \rho V_\infty^2 A_{lat}} \quad \text{(A6-1)}$$

$$C_D = \frac{F_D}{0.5 \cdot \rho V_\infty^2 A_{lat}} \quad \text{(A6-2)}$$

The lift and drag forces can also be defined with respect to the yaw ship fixed reference system as F_X and F_Y, which describe respectively the “driving” and “side force”. The definition of F_X and F_Y is given in equations (A6-3) and (A6-4).

$$F_X = F_L \cdot sin(AWA) - F_D \cdot cos(AWA) \quad \text{(A6-3)}$$

$$F_Y = F_L \cdot cos(AWA) + F_D \cdot sin(AWA) \quad \text{(A6-4)}$$

The magnitude of the lift and drag force of the Flettner rotor depends on the spin ratio (SR). The spin ratio is defined in equation (A6-6).

$$SR = \frac{D \cdot \pi \cdot \left(\frac{n_{Flet}}{60}\right)}{V_\infty} \quad \text{(A6-6)}$$

Where $V_\infty$is the free stream velocity or the apparent wind speed and $n_{Flet}$is the rotation speed of the Flettner rotor (RPM).

APPENDIX VII

TEST FACILITY AND MEASUREMENTS

Test facility

The seakeeping tests have been conducted in the Seakeeping and Manoeuvring Basin (SMB), which measures 170 m by 40 m by 5 m in length, width, and depth, respectively. More information about the SMB can be found in the documentation sheet and on the MARIN website.

Test set-up

All tests were conducted with a self-propelled and (partially) free-running model. As tests were conducted with and without wind forces, the two following test set-ups were used:

- **Without wind forces**
  The model was connected to the carriage through power and measurement free hanging cables. Those cables entry point is located amidship of the vessel to limit their relative motion with respect to the vessel and a spring maintain them free hanging above the model. As such, these cables did not restrict the motions of the model.
- **With wind forces**
  During tests with wind forces, five wind winches were used to exert external loads on the model. The power and measurement cables used in the no wind test were also present in the wind mode.

Wind winches set-up

A combination of five winches was connected to the model through the wind mast where all the lines attached as shown in Figure A7-1. A schematised view of this experimental set up is shown in Figure A7-2 where the location of each winch is shown by winch number F1 to F5.
This wind mast is a tube carrying two attachments systems:

- A pivoting ring with low friction bearings. This ring functions as an attachment point where the lines of winches F1, F4 and F5 connect to the model, controlling the in-plane forces.
- A fixed wheel with two separates reels where winches F2 and F3 connect to the model. These winches allow to exert independently a yawing moment MZ and apply a transverse force.
- By combining winches F2, F3 and F5 a moment around the x-axis, MX can be generated to address roll and heel due to wind. In the data analysis, this moment is translated to the COG.

Forces were measured at the winches and additionally on the lines that connect the winches and the model.

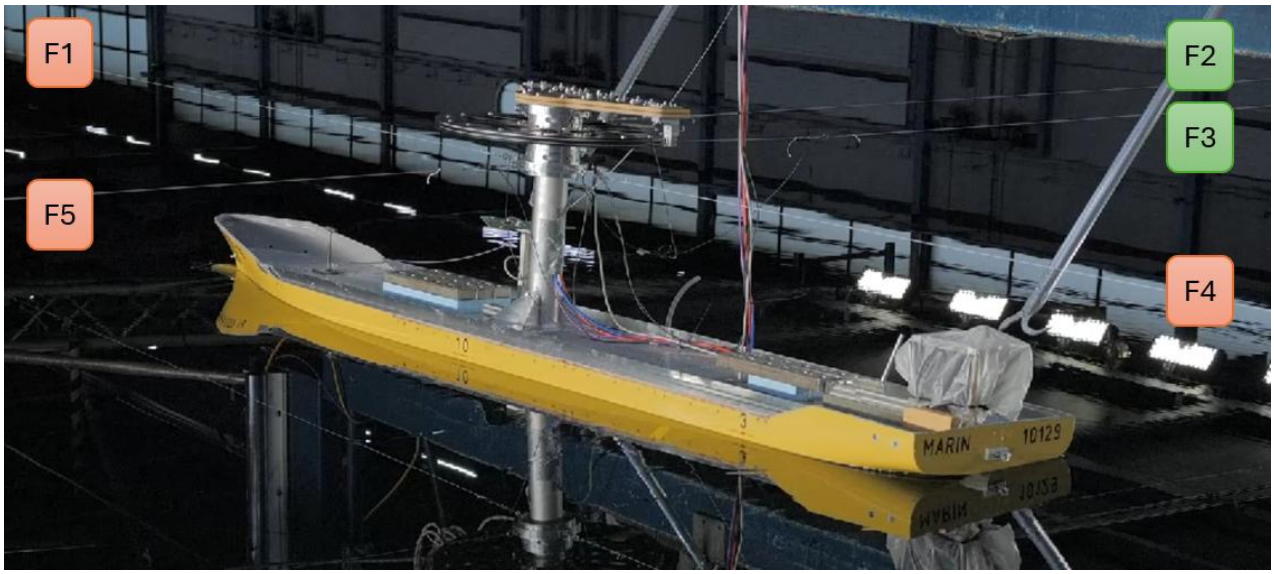

Figure A7-1: Wind winches set-up (F1 – F5) used to exert wind loads on the model.

Top view: winches F1, F4 and F5 are connected to the pivoting ring while F2 and F3 are connected to the fixed wheel.

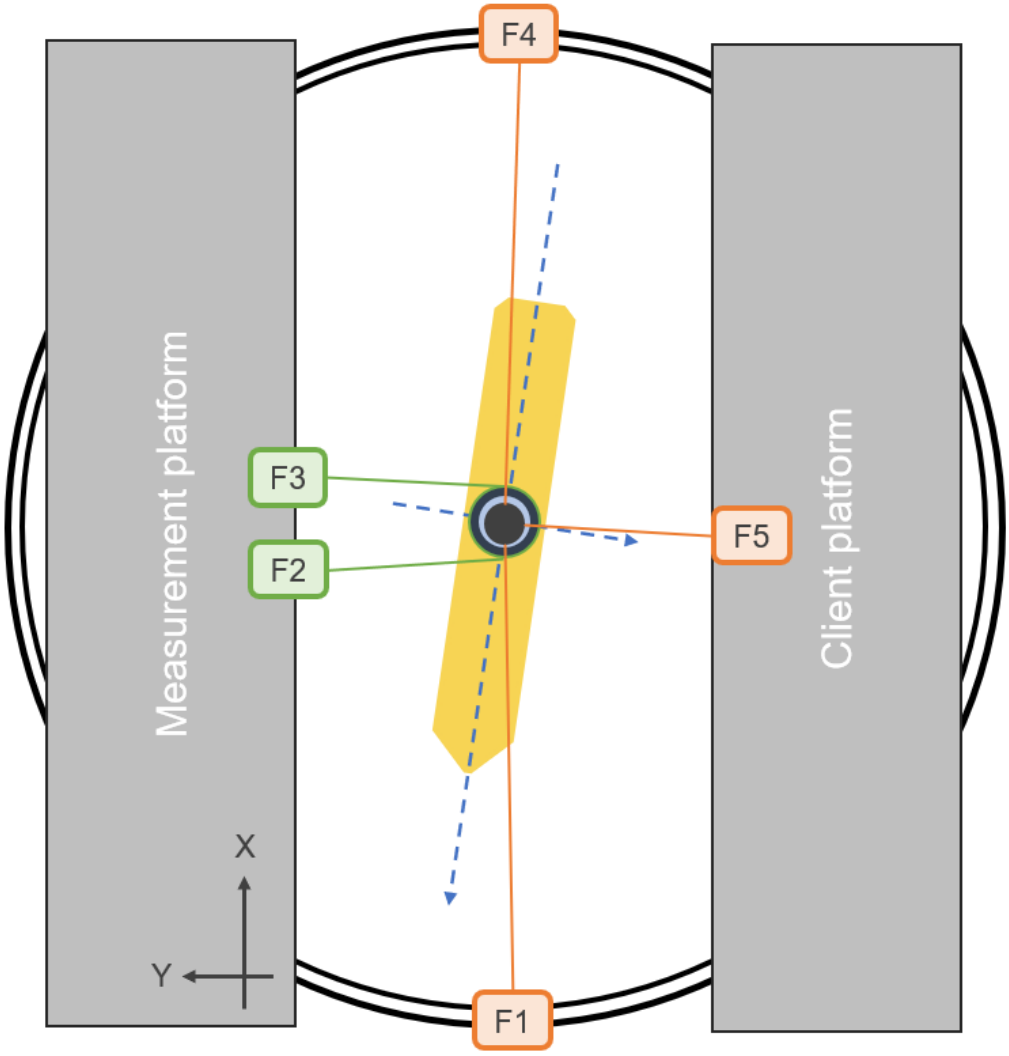

Front view: Cables supplying power and transmitting signals run through the wind mast.

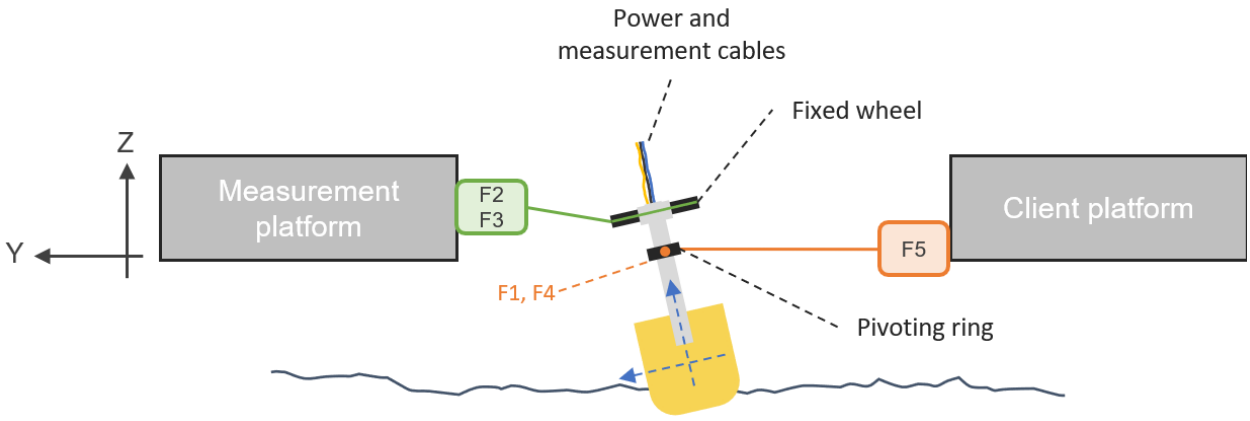

Figure A7-2: Schematic representation of the wind winches set-up.

Winch loads modelling

This desired winch loads consist of aerodynamic loads of the superstructure, rotor sails and the towing force to correct for Reynolds scale effects. These different load components are calculated alongside the test execution (software in the loop) by MARIN's time-domain software aNySIM XMF.

aNySIM XMF software in the loop

aNySIM XMF was used to perform fast-time manoeuvring and seakeeping simulations. Thanks to its modular architecture, aNySIM can simulate any ship type and any exterior loads through custom made mathematical models, including wind propulsion devices of any nature.

As it can be gathered from Figure A7-3, aNySIM XMF takes the instantaneous motions of the model as input and computes the associated forces. Then, the forces are allocated to the winches in order to be exerted on the model. The aNySIM XMF model was prepared before the tests to include the hydrodynamic reaction forces of the hull, the rudder and fin reaction forces and the loads of the wind propulsion devices.

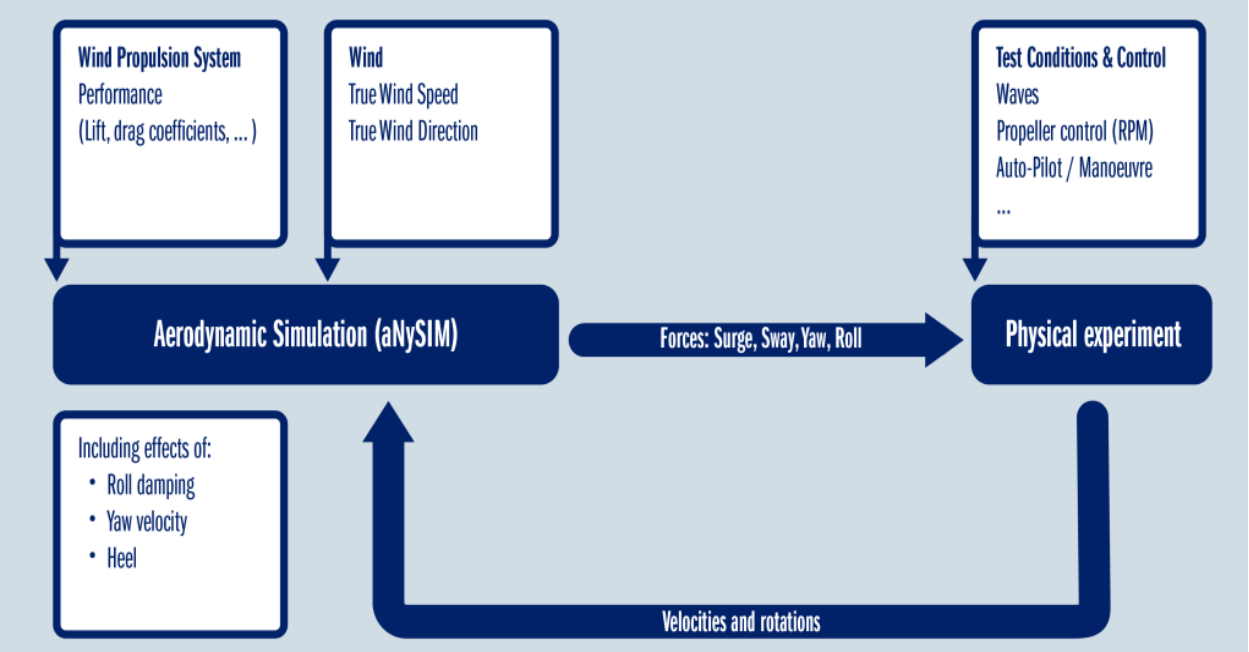

Figure A7-3: aNySIM XMF software in the loop scheme.

Simulation approach

The aNySIM XMF mathematical model is based on a time-domain representation of a system of coupled differential equations of motion. Its modular mathematical model computes the components of the forces separately (such as the hull reaction forces, propeller forces, rudder forces, Flettner rotor forces). Interactions are modelled distinctly.
The output is a time-trace of positions, angles, rudder, propeller and Flettner rotor data. The simulation results are presented as full-scale values with their nomenclature, sign definitions and units presented in the Tables T6 to T8.

Limitations

The mass and internal friction in the winch system is compensated using the winch control software. However, other similar projects have shown that a small change in damping and inertia is to be expected.

Windage coefficients for superstructure wind loads

In equations (7.2) – (7.5), the wind forces of the superstructure are calculated by means of windage coefficients $c_{X,SS}$, $c_{Y,SS}$ and $c_{K,SS}$, $c_{N,SS}$, frontal and lateral wind areas A_F and A_L, ship length, L_{PP}, reference height, H, and apparent wind speed AWS.

The wind coefficients depend on the apparent wind direction AWA, with 0° being wind from the bow and 90° wind from starboard. The apparent wind speed, AWS, is a vectorial summation of the true wind speed TWS and the ship speed.

$$X_{SS} = c_{X,SS}(AWA)\frac{1}{2}\rho_{air}A_F AWS^2 \quad (7.2)$$

$$Y_{SS} = c_{Y,SS}(AWA)\frac{1}{2}\rho_{air}A_L AWS^2 \quad (7.3)$$

$$K_{SS} = c_{K,SS}(AWA)\frac{1}{2}\rho_{air}A_L H \cdot AWS^2 \quad (7.4)$$

$$N_{SS} = c_{N,SS}(AWA)\frac{1}{2}\rho_{air}A_L L_{pp} AWS^2 \quad (7.5)$$

Here, these coefficients were obtained from a suitable reference vessel described in the literature[16].

Rotor sail loads

To model the forces of the Flettner rotors in aNySIM XMF, an aerodynamic assessment was carried out in order to derive an aerodynamic model that takes into account the rotor-rotor interaction and rotor-ship interaction effects. Summarised, the aerodynamic assessment combines information of different sources to create one aerodynamic model:

- CFD calculations that compute the aerodynamic loads with active rotors and the ship superstructure combined for a small selection of wind conditions.
- Lifting line calculations that compute the aerodynamic loads for a large variety of wind conditions.
- Supplier data from Norsepower for the performance of a standalone rotor, using the lift-drag-spin ratio relationship.

The software Equilibrium & Speed (E&S) was used to perform a performance assessment for the ship under consideration with wind propulsion. From this performance prediction, the optimal rotor rpm was calculated and used as input for the experiments.

To model these rotor sails forces in aNySIM XMF, a coupling between aNySIM XMF and E&S was made such that the aerodynamic model is the same for both the performance assessment as for the experiments.
Figure A7-4 presents the standalone rotor lift and drag curve for this particular rotor sail with an aspect ratio of 7. The curves are based on CFD calculations and supplier data from Norsepower and they are presented as function of the spin ratio. Only the supplier data is applied in the aerodynamic model. Using these dimensionless lift and drag coefficients, the rotor sail forces can be calculated for every combination of wind speed and ship speed.

[1616] 'Wind Loading of Ships', W. Blendermann, Institut fuer Schiffbau der Universitaet Hamburg, Germany, 1996

For more information about the fundamentals and working mechanism of a rotor sail, see Appendix VI.

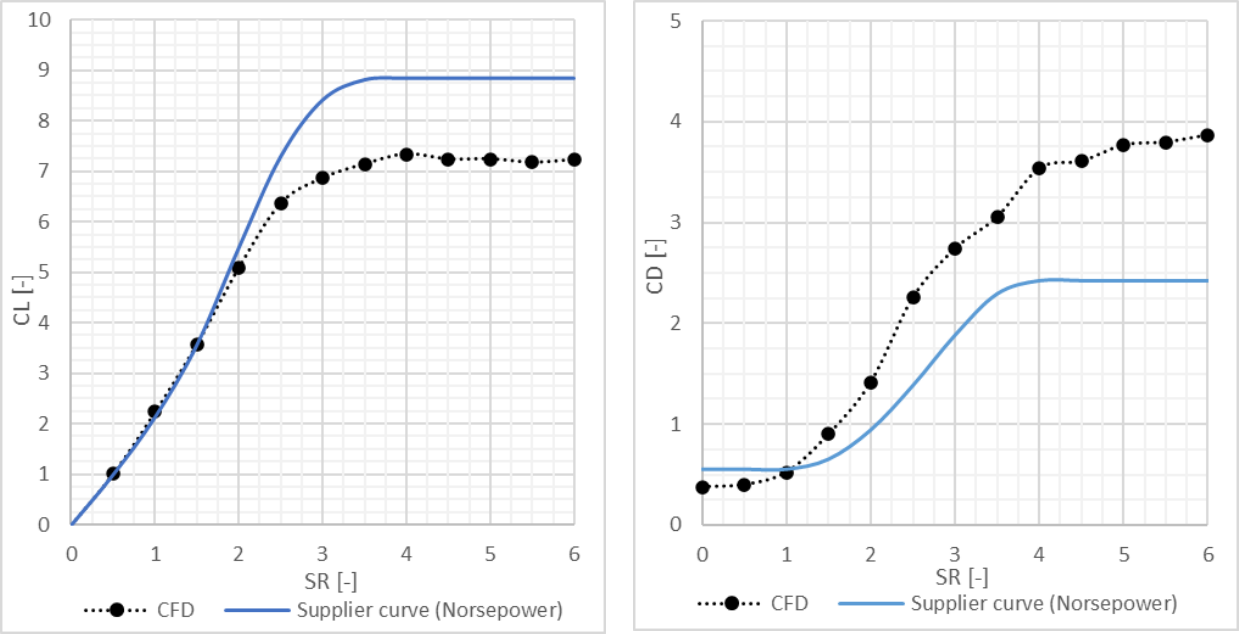

Figure A7-4: Lift (CL) and drag (CD) coefficient against spin ratio (SR) obtained for a standalone rotor sail calculated by CFD and compared to the used supplier curves (Norsepower).

Wind expose area

The exposed area of the vessel was calculated considering the chosen draught, superstructure, cargo on deck and rotor sails. Commercially available Norsepower rotor sails were assumed as reference case in the present study. The wind forces were calculated for application on the centroid above waterline. Table A7-2 shows the relevant parameters for wind exposure used in this study.

Table A7-2: Wind exposed area parameters of the vessel.

Designation	Value	Unit
Rotor foundation height	2.5	m
Rotor height	24	m
Rotor diameter	4	m
Total exposed area (frontal)	595	m^2
Total exposed area (lateral)	2659	m^2
Centroid above waterline (frontal)	13.6	m
Centroid above waterline (lateral)	7.6	m

Longitudinal towing force

The experimental setup allows to apply a correction on the resistance to correct for Reynolds scale effects. An additional towing force is applied to the model to sail at a more realistic propulsion point. Even though in standard seakeeping and manoeuvring tests this effect is neglected, the low propeller thrust required during wind assisted tests magnifies the Reynolds scale discrepancy. Modelling the additional towing force required to match the Reynolds scale effect (FD) becomes therefore more relevant.
The procedure to calculate FD is documented in Appendix V. Here, powering results from a comparable reference vessels were used for the correction.

Composite wind loads and allocation

The aNySIM XMF model computes the components of the wind loads and combines them. The resulting forces are then send to the allocation algorithm that computes the setpoints of each winch in the basin reference frame (BF), fulfilling a set of force and moment equations as is presented in Equations (7.6) to (7.8). In these equations, the manoeuvring coordinate system for forces and moments is applied. A line pre-tension load is also applied to ensure that the lines do not have slack.

The longitudinal and transverse force in a basin fixed reference frame are defined in equations (7.6) and (7.7) where the subscript w refers to the winch.

$$\Sigma FX_{BF} = -F1 + F4 = FX_{W,BF} \tag{7.6}$$

$$\Sigma FY_{BF} = -F2 - F3 + F5 = FY_{W,BF} \tag{7.7}$$

Under the assumption that the lines are perpendicular to the crew platform and the roll angle is zero, the yaw moment can be expressed in a yaw fixed (YF) reference system according to equation (7.8).

$$\Sigma \mathrm{MZ_{YF}} = F2 \cdot r - F3 \cdot r = MZ_{,W,YF} \tag{7.8}$$

In addition, depending on the sign of the desired forces, conditional equations as presented in equations (7.9) and (7.10) are required to fully solve equations (7.6) to (7.8) and obtain an expression for the modelled forces in every winch.

$$\begin{aligned}
&\text{If } \mathrm{FX}_{W,BF} \geq 0 \text{ then:} \\
&\quad \mathrm{F1} = \mathrm{F}_{pretension} \\
&\quad \mathrm{F4} = \mathrm{FX_{W,BF}} + \mathrm{F}_{pretension} \\
&\text{else if } \mathrm{FX}_{W,BF} < 0 \text{ then:} \\
&\quad \mathrm{F1} = -\mathrm{FX} + \mathrm{F_{pretension}} \\
&\quad \mathrm{F4} = \mathrm{F_{pretension}} \\
&end
\end{aligned} \tag{7.9}$$

$$\begin{aligned}
&\text{If } \mathrm{FY}_{W,BF} \geq 0 \text{ then and } \mathrm{MZ_{W,BF}} \geq 0\text{:} \\
&\quad \mathrm{F2} = -\frac{1}{2}\mathrm{FY_{W,BF}} + \frac{\mathrm{MZ_{W,BF}}}{r} + \mathrm{F}_{pretension} \\
&\quad \mathrm{F3} = -\frac{1}{2}\mathrm{FY_{W,BF}} + \mathrm{F}_{pretension} \\
&\quad \mathrm{F5} = 2 \cdot \mathrm{F}_{pretension} \\
&\text{If } \mathrm{FY}_{W,BF} \geq 0 \text{ then and } \mathrm{MZ_{W,BF}} < 0\text{:} \\
&\quad \mathrm{F2} = -\frac{1}{2}\mathrm{FY_{W,BF}} + \mathrm{F}_{pretension} \\
&\quad \mathrm{F3} = -\frac{1}{2}\mathrm{FY_{W,BF}} - \frac{\mathrm{MZ_{W,BF}}}{r} + \mathrm{F}_{pretension} \\
&\quad \mathrm{F5} = 2 \cdot \mathrm{F}_{pretension} \\
&\text{elseif } \mathrm{FY}_{W,BF} < 0 \text{ and } \mathrm{MZ} \geq 0 \text{ then:} \\
&\quad \mathrm{F2} = \frac{\mathrm{MZ_{W,BF}}}{r} + \mathrm{F}_{pretension} \\
&\quad \mathrm{F3} = \mathrm{F}_{pretension} \\
&\text{elseif } \mathrm{FY}_{W,BF} < 0 \text{ and } \mathrm{MZ} < 0 \text{ then:} \\
&\quad \mathrm{F2} = \mathrm{F}_{pretension} \\
&\quad \mathrm{F3} = -\frac{\mathrm{MZ_{W,BF}}}{r} + \mathrm{F}_{pretension} \\
&\quad \mathrm{F5} = \mathrm{FY}_{W,BF} + 2 \cdot \mathrm{F_{pretension}} \\
&\text{end}
\end{aligned} \tag{7.10}$$

Although the connection points are kept constant during these tests, the allocation software is already prepared to also apply the correct roll moment. For that purpose the calculations for the roll moment are

performed in real time. To determine the roll moment, the $FX_{W,CALC\_BF}$ and $FY_{W,CALC\_BF}$ forces are translated from a basin fixed reference frame to a ship fixed (SF) reference frame based on measured, current ship orientation, such that an expression for the roll moment can be obtained. The roll moment is calculated by multiplication of the transverse force in a ship fixed reference frame, $FY_{WINCH,SF}$ with the height of the mast to where the force is applied, h_F, as shown in equation (7.11).

$$\Sigma MX_{SF} = FY_{,WINCH,SF} \cdot h_F \quad = MX_{W,SF} \tag{7.11}$$

All winches' forces and moments signals that are presented in this report are translated to a yaw-fixed reference frame and are given with respect to the centre of gravity. Here, yaw-fixed refers to the coordinate system rotating with the ship's yaw motion, but not with roll motion, see Figure A7-5 and Figure A7-6. The calculated measured moments at the COG will be referred to as M_{WIND} and the calculated values obtained from XMF as M_{XMF}.

As the force transducers are instrumented to measures the tension in each line, the total measured winch loads that are applied on the ship model can be reconstructed by solving the force and moments equations (7.6) to (7.8). For total wind loads measured on the lines connecting winches and model, an additional subscript "LINE" is added to the signal name. Figure A7-5 and Figure A7-6 show sketches of the applied forces and moments as detailed above.

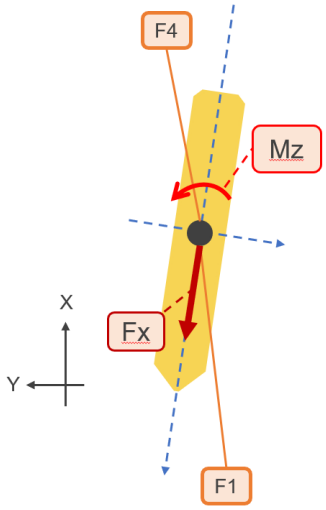

Figure A7-5: Measured and calculated forces and moments Fx and Mz, top view

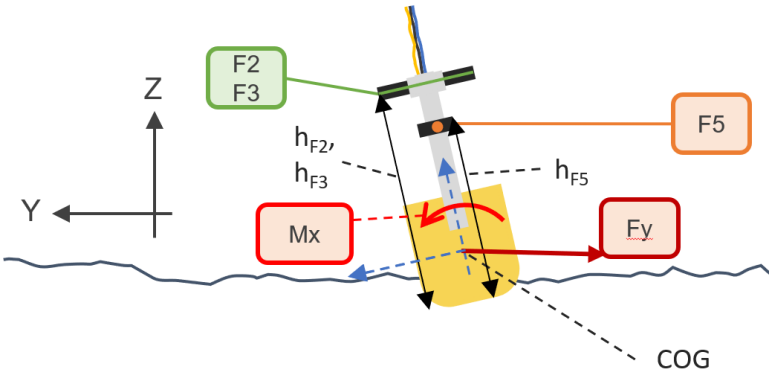

Figure A7-6: Measured and calculated forces and moments Fy and Mx, front view.

Test execution

Decay tests

Decay tests were performed at zero-speed and forward speed to capture the roll decay evolution with speed. The model was manually heeled to around 10 deg angle, without inducing any other motion, and suddenly released. The decaying roll motion was measured.

Tests in transit

To maintain the target wave heading with lowest possible drift angle, the model is kept on course by an autopilot. The autopilot reacts on course deviation and rate of turn (see Table T3 for rudder control settings). This makes the model sail a diagonal trajectory through the basin, with a sideways drift that depends on the sea state, wave heading and sailing speed.

Tests at zero speed

At zero speed, the model was free drifting and the heading was corrected with the winch system or, if necessary, manually using poles. Care was taken not to influence the vessel motions significantly during correction. The goal was to keep the yaw below 15 deg.

Waves
Waves were not calibrated before the test. Instead, their amplitude was monitored during the tests to ensure that the amplitude, period, and spectral characteristics are correct.

MEASUREMENTS, DEFINITIONS AND NOTATIONS

Throughout this report, SI units are used unless indicated otherwise.

Measurements

MARIN's Measurement System is used to record the measurements. After being subject to an anti-aliasing filter, the signals are digitised and stored on disc for further analysis. The following quantities are measured during all tests.

Table A7-3: Basic measurement signals.

Signal	Sampling rate (model scale)[17]	Description
Ship six degrees of freedom motions	100 Hz	Measured using an optical tracking system; from these measurements, the rigid-body motions at the ship CoG are derived.
Incident waves	50 Hz	Using acoustic wave probes, the incoming waves are measured at two location up-wind of the model.
Ship accelerations	200 Hz	Accelerations are measured by a set of four accelerometers in suitable position on the model (mounted to rigid beams whose positions are known with precision). From accelerations of the model as a rigid body, local accelerations at designated locations are computed latter on.
Torque, thrust and rotation rate of the propeller	200 Hz	Thrust and torque are measured in the shaft housing right before the propeller to ensure that no additional mechanical loses are affecting the measurement. Revolutions are measured at the engine output shaft by a numerical encoder.
Rudder angle	200 Hz	The angle of the rudder is measured by the numerical encoders build in the servo rotating them.
Relative wave elevations	200 Hz	Relative wave elevation is measured by resistive probes.
Winch forces and moments	200 Hz	X, Y and Z forces in addition to the yaw and roll moments. Measured at winches and additionally on the lines connecting the winches and model.

[17] Model scale sampling rate, for full scale sampling rates divide by the square root of the model scale

Derived signals

Several signals are derived from the measured signals by means of filtering or by means of a sample-by-sample construction (see Table A7-4):

Table A7-4: Derived signals.

Signal	Sampling rate (model scale)	Description
Vessel speed	100 Hz	The vessel speed is derived from the measured velocity of the carriage in combination with the position of the model with respect to the carriage.
Low-frequency and wave-frequency motions	100 Hz	For waves from forward and transverse directions, the motions in the horizontal plane are split into a “wave-frequency” and a “low-frequency” component. The first may be regarded as the reaction to an individual wave; the second is caused by low-frequency variations from the wave “drift” forces and non-linear aspects of manoeuvring.
Local motions and acceleration at reference locations	200 Hz	From the rigid body motion and accelerations, the local motions and accelerations are derived at designated positions.
AWA **AWS** **Wind forces and moments due to wind on superstructure, rotor sails and total**	200 Hz	Computed by XMF in the loop.

Wave heading convention

The coordinate system and related sign conventions follow ITTC standards. The heading (μ) of the vessel is given in a ship co-ordinate system; it is defined as the angle between the direction of wave propagation and the direction of the vessel's bow. The following sign convention for the heading and reference system for positions applies:

Table A7-5: Heading convention and reference system.

Ship heading convention	
180 deg	Head seas
135 deg	Bow-quartering seas over starboard
90 deg	Beam seas over starboard
45 deg	Stern-quartering seas over starboard
0 deg	Following seas

Reference system	
X=0	at aft perpendicular and positive forward
Y=0	at centreline and positive to portside
Z=0	at base line and positive upward

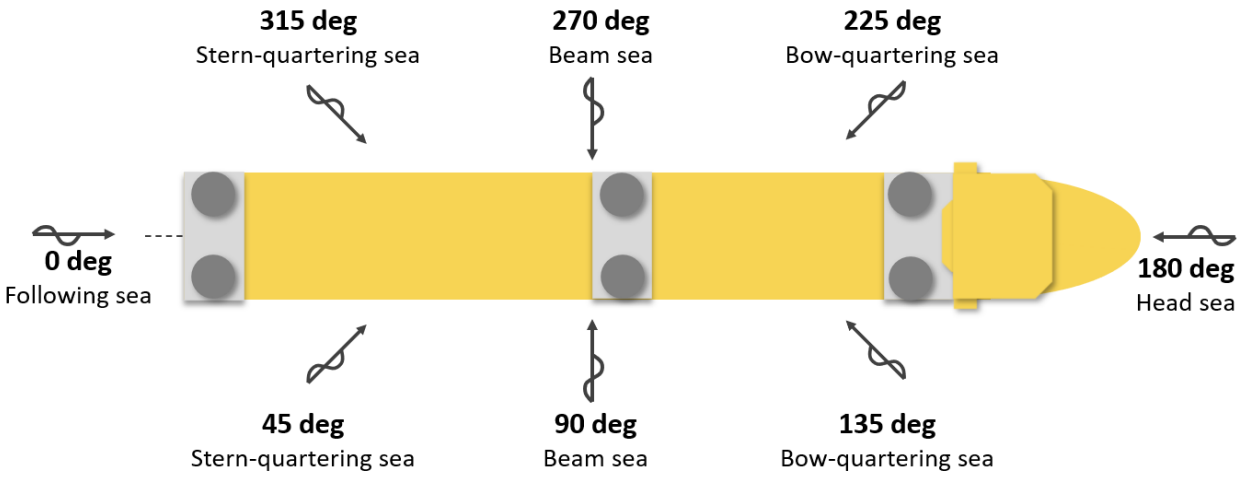

Figure A7-7: Wave heading convention (ITTC standard).

Wind direction conventions

The conventional description of TWA are shown in Figure A7-8, with a modification to avoid confusion and stay consistent with the conventional description of wave directions: wind from bow is noted 180 deg, wind from starboard is 90 deg and wind from astern is 0 deg. As the vessel sails two distinct wind vectors emerge: the true wind (TW) is the wind measured in a stationary and earth fixed reference frame while the apparent wind (AW) is the wind experienced by the vessel sailing.

The AW is the vectorial summation of the TW minus the vessel speed (Vs). The main difference between the true wind angle (TWA) and the apparent wind angle (AWA) is that whereas the TWA is taken from the vessel track, the AWA is taken from the vessel heading.

The apparent and true winds breakdown and their respective angular definitions are gathered in the Figure A7-8 while the relations between TWS, TWA and AWS, AWA are shown in equations (7.14) and (7.15).

$$V_{x\,AWS} = -TWS\,cos(TWA - \beta) - V_s\,cos(\beta) \quad (7.12)$$

$$V_{y\,AWS} = TWS\,sin(TWA - \beta) - V_s\,sin(\beta) \quad (7.13)$$

$$AWS = \sqrt{{V_{x\,AWS}}^2 + {V_{y\,AWS}}^2} \quad (7.14)$$

$$AWA = atan2\left(\frac{V_{y\,AWS}}{-V_{x\,AWS}}\right) \quad (7.15)$$

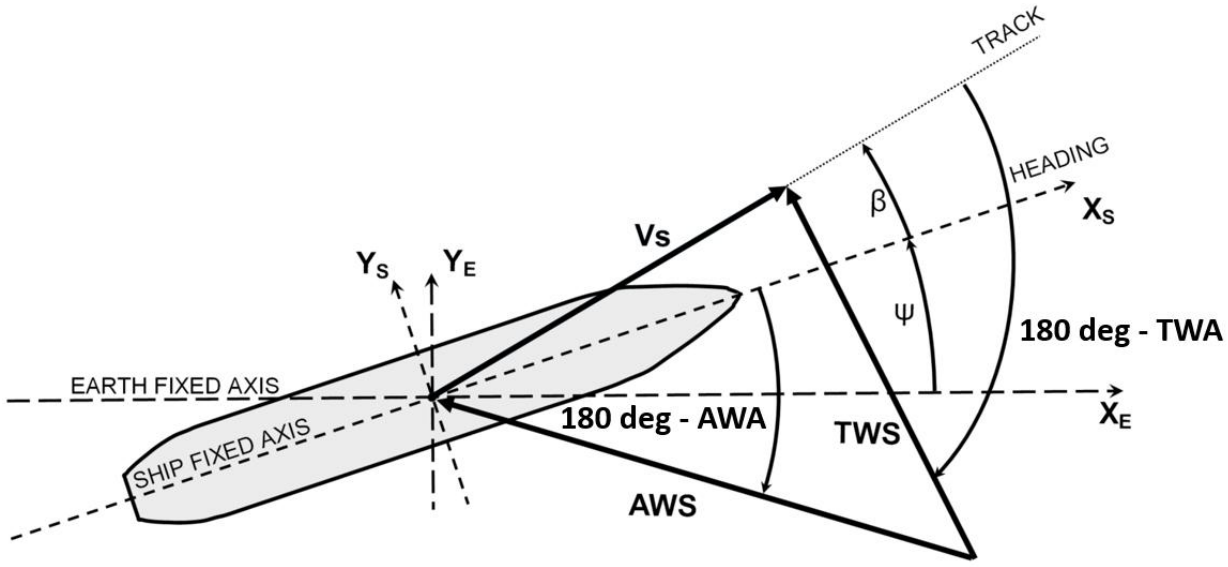

Figure A7-8 Illustration of wind definitions, ship speed, drift, yaw and longitudinal and transverse forces.

DOCUMENTATION SHEET

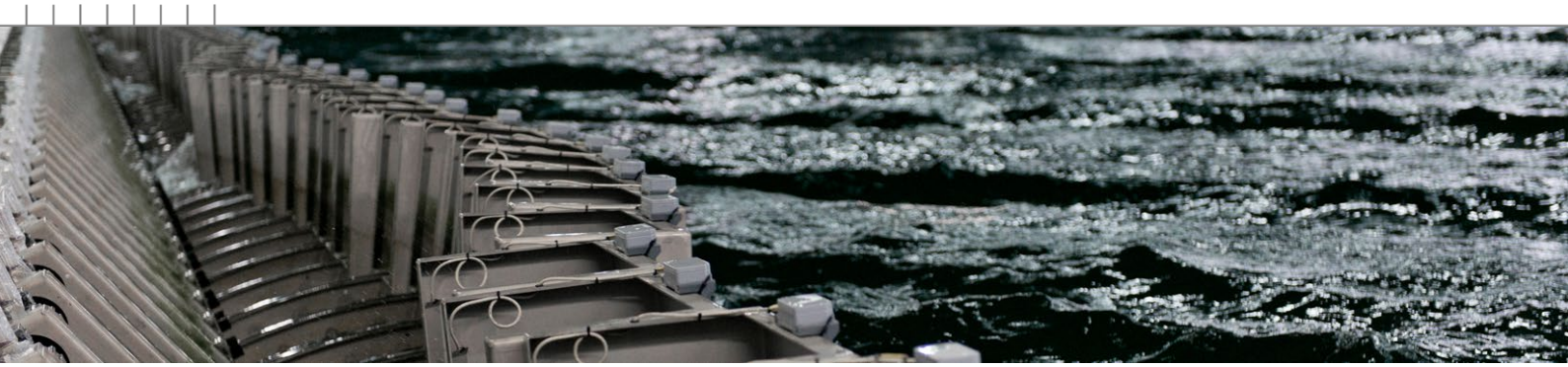

Seakeeping and Manoeuvring Basin

To simulate and test the behaviour of ships at sea as closely as possible, we use free sailing models for most seakeeping and manoeuvring test campaigns. To ensure accurate test results by using adequately large models, a sufficiently wide and long basin is required. The Seakeeping and Manoeuvring Basin (SMB) with its 170 m x 40 m x 5 m is perfectly fit. The basin is fitted with flap-type wave makers on two adjacent sides and adjustable beaches on the opposite sides. This allows for free sailing ship models to sail in regular and irregular waves from any direction and for free sailing manoeuvring tests such as zig-zag and turning circles at the design speed of the ship.

Tests in the SMB:

- Seakeeping tests in regular and irregular waves.
- Free sailing manoeuvring tests in calm water and waves
- Captive (CPMC) manoeuvring tests
- Tests on (floating) offshore structures to determine the motions and load due to waves.
- Tests for wind assisted ships
- Wireless controlled models at high speeds.
- Underwater manoeuvring.
- Side by side operations.

Basin capabilities

Model size

Although ship models can vary between 0.3 and 11 metre of length, the typical length of free sailing models is between 4 and 6 metre. Scale depends on required speed, wave conditions, model outfitting and measurement requirements. For floating (offshore) structures the model size is also determined by water depth and required wave conditions.

Model instrumentation

Ship models are fitted with all relevant appendages, including propulsion lines, steering gear, stabilising fins, ESD's and anti-roll tanks. All appendages are fully functional, adapted to work at model scale and with a realistic control based on the ship motions. Model tests for side by side operations and launch and recovery tests with multiple models can be performed as well. DP systems and control is available using an in-house developed control system.

Carriage

The carriage runs over the total length of the basin with a maximum speed of 6 m/s and consists of a main frame and sub frame. The main frame spans the full width of the basin, the sub frame can move along this main frame over the entire width of the basin at a maximum speed of 4 m/s. The carriage can follow all movements of a model that is sailing freely by itself under auto pilot control or it can follow a prescribed track with a ship model mounted to the carriage. The latter case is used for Computerized Planar Motion Carriage (CPMC) tests.

For each specific need MARIN has test facilities available:

- Offshore Basin
- Concept Basin
- Shallow Water Basin
- Deep Water Basin
- Depressurised Wave Basin
- Cavitation Tunnel
- Multi Phase Wave Lab

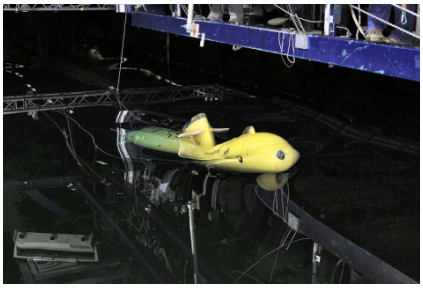

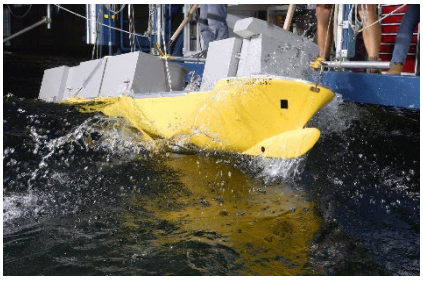

For more information contact MARIN;
department Ships
T + 31 317 49 34 72
E ships@marin.nl

Waves

Waves can be generated with peak periods ranging from 0.8 to 4.2 seconds and, depending on the peak period, up to a significant wave height of 0.45 m. At two adjacent sides of the basin, segmented wave generators are installed, consisting of 320 hinged flaps of 60 cm wide. Each flap is controlled separately by a servo motor. The wave generator can be used to produce regular and irregular, long and short crested waves from arbitrary directions. Opposite the wave generator passive sinkable wave absorbers are installed. To further dampen the waves, the wave generators are equipped with an active reflection compensation.

Wind

Wind forces can be modelled using portable wind fans or by attaching lines with controlled tension winches.

Measurement and observations

Models are tracked by a 6 degree of freedom position measurement system. Instrumentation of propellers rudders and accelerations, pressured, loads are well possible. Typical registration is with 200 Hz, but for high frequent phenomena, higher measurements rates are being used. Default close-up video recordings are made for allowing registration of important phenomena. To measure captive forces and moments on the complete model, a turn table and force measurement frame can be fitted between the model and carriage to also force yaw motions and to determine the current or manoeuvring forces.

Expertise and experience

Over the years MARIN has gained a vast experience in performing a wide range of tests for all kind of ships and offshore structures, varying from small fast craft, 400 m container vessels to autonomous submarines.
Besides ship motions, seakeeping tests can focus on any behaviour in waves. This includes added resistance in waves, optimisation of anti-roll devices and non-linear behaviour such as parametric roll, broaching and slamming. In addition, we perform IMO tests on a regular basis, for weather criterion, safe return to port and ships with an open top notations. Manoeuvring tests are often carried out to verify and improve the performance as required by IMO manoeuvring regulations (zig-zag and turning circles tests). Many custom manoeuvres are performed to verify market-specific performance criteria, such as for naval ships, towed FPSO's, tugs and submarines. CPMC tests are performed to compose mathematical models to perform fast time or real time simulations.

Publications

- Dallinga, R.P.: 'The New Seakeeping and Manoeuvring Basin of MARIN, Japanese workshop on waves', 1999.
- Quadvlieg, H.H.A.: 'A New Combined Seakeeping and Manoeuvring Basin for the Third Millennium Maritime Research', MARSIM 2000.
- ITTC leaflet: https://ittc.info/media/7879/seakeeping-and-manoeuvring-basin.pdf.

M A R I N
P.O. Box 28

6700 AA Wageningen
The Netherlands

T +31 317 49 39 11
E info@marin.nl

I www.marin.nl